BUREAU OF RECLAMATION

Appendix B

Development of Future Climate and Hydrology Scenarios

American River Basin Study
Interior Region 10 – California-Great Basin

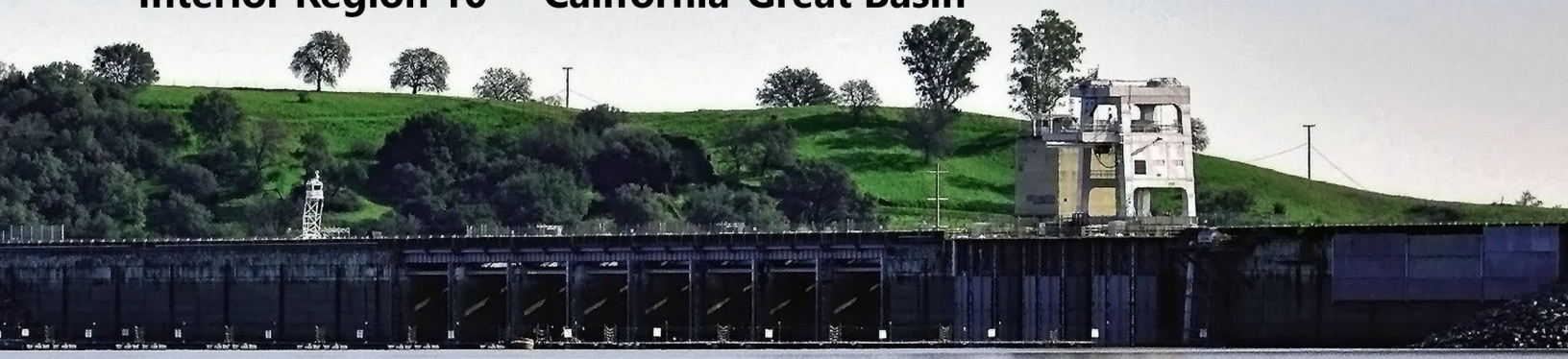

Note: This appendix is a record of analysis for the ongoing study (2018 - 2022).
The main report may have updated information that is not reflected in this appendix.

U.S. Department of the Interior

March 2022

BUREAU OF RECLAMATION

Technical Memorandum No. ENV-2020-067

American River Basin Study:
Development of Future Climate and Hydrology Scenarios

U.S. Department of the Interior **August 2020**

Mission Statements

The U.S. Department of the Interior protects and manages the Nation's natural resources and cultural heritage; provides scientific and other information about those resources; and honors its trust responsibilities or special commitments to American Indians, Alaska Natives, and affiliated Island Communities.

The mission of the Bureau of Reclamation is to manage, develop, and protect water and related resources in an environmentally and economically sound manner in the interest of the American public.

Technical Memorandum No. ENV-2020-067

American River Basin Study:
Development of Future Climate and Hydrology Scenarios

prepared by

Water Resources Engineering and Management (86-68210)

Ian Ferguson, Hydrologic Engineer

Kristin Mikkelson, Civil Engineer

peer reviewed by

Alan Harrison, Environmental Engineer

Jamie Anderson, Senior Engineer, California Department of Water Resources

Contents

page

Tables

No. *page*

Figures

No. *page*

Acronyms

°C	degrees Celsius
°F	degrees Fahrenheit
%	percent
ARB	American River Basin
ARBS	American River Basin Study
BCSD	Bias Correction Spatial Disaggregation
CDF	Cumulative Distribution Function
CMIP	Coupled Model Intercomparison Project (CMIP1, CMIP2, CMIP3, and CMIP5 refer to CMIP Phases 1, 2, 3, and 5, respectively)
CPC	Climate Prediction Center
CT	Central Tendency Climate Scenario
CVP	Central Valley Project
CWC	California Water Commission
Delta	Delta method of developing climate scenarios
DTR	Diurnal Temperature Range
DWR	California Department of Water Resources
GCM	Global Climate Model
GHCN-Daily	Global Historical Climate Network – Daily
HD	Hot-Dry Climate Scenario
HDe	Ensemble-informed hybrid-delta method of developing climate scenarios
HUC	Hydrologic Unit Code
HW	Hot-Wet Climate Scenario
LOCA	Localized Constructed Analogs
NCDC	National Climatic Data Center
NCEI	National Center for Environmental Information
NOAA	National Oceanic and Atmospheric Administration
NWS	National Weather Service
RCP	Representative Concentration Pathway
SWP	State Water Project

TAF	Thousand Acre-Feet
WBA	Water Budget Area
WD	Warm-Dry Climate Scenario
WW	Warm-Wet Climate Scenario

1 Introduction

Water managers in the American River Basin are experiencing a growing imbalance between water supplies and water demands due to variety of factors, including population growth; increasing regulatory requirements and constraints; changes in Central Valley Project (CVP) operations; and inadequate water resources infrastructure. Water managers are also struggling to address emerging climate change conditions, including increases in the frequency and intensity of extreme events such as droughts and floods.

The American River Basin Study (ARBS) is a collaborative effort by the Bureau of Reclamation and six non-Federal partners to address current and projected imbalances between water supplies and water demands in the American River Basin. The six non-Federal partners are: Placer County Water Agency (PCWA), City of Roseville (Roseville), City of Sacramento (Sacramento), El Dorado County Water Agency (EDCWA), City of Folsom (Folsom), and Regional Water Authority (RWA). A key objective of the ARBS is to develop a more detailed understanding of current and future water supplies and demands in the American River Basin and to evaluate potential imbalances between supplies and demands under a range of potential future conditions.

Numerous studies have shown that global and regional climate conditions are changing, that climate change will continue and likely accelerate over the 21st century, and that climate change will significantly affect local and regional water supplies, demands, and management (IPCC 2014 [AR5 Synthesis]; IPCC 2014 [AR5 Impacts], USGCRP 2018, Bedsworth et al. 2018). To facilitate analysis of future water supplies and demands in the American River Basin, a suite of future climate and hydrology scenarios was developed to represent the projected range of future climate conditions over the study area. Climate scenarios were developed from an ensemble of bias-corrected and downscaled climate projections using the ensemble-informed hybrid-delta (HDe) scenario methodology. Hydrology scenarios were subsequently developed by using the Variable Infiltration Capacity (VIC) hydrology model to simulate hydrologic conditions under each climate scenario. These climate and hydrology scenarios were subsequently used as the basis for evaluating future water supplies and demands.

The American River Basin is a major tributary to the Sacramento River, and water supplies and management in the American River Basin are strongly affected by operation of the Central Valley Project and State Water Project (CVP-SWP) systems. The ARBS therefore used the CalSim3 water resources planning model (DWR 2019 [CalSim3]) to evaluate current and future water supplies, demands, and management. Climate and hydrology scenarios developed for the ARBS encompass all watersheds represented in the CalSim3 model. The area

encompassed the watersheds represented in CalSim3 is illustrated in Figure 1 and is referred to here as the CalSim3 domain.

This technical memorandum describes the climate and hydrology scenarios developed for the ARBS. Sections 2 and 3 describe observed historical climate conditions and projected future climate conditions over the study region, respectively. Section 4 describes the suite of climate scenarios developed for the ARBS, and Section 5 describes the corresponding suite of hydrology scenarios. Section 6 describes how these hydrology scenarios were used to adjust inputs to CalSim3 to simulate effects of climate scenarios on water supplies, demands, and operations within the CVP-SWP system.

Figure 1. ARBS study area and CalSim3 domain.

2 Observed Historical Climate

The term *weather* is generally used to describe the state of the atmosphere at a specific place and time, including characteristics such as temperature, precipitation, wind speed, and humidity. *Weather* thus refers to the day-today conditions directly experienced by people and the environment, including rainstorms and heat waves. The term *climate*, on the other hand, is generally used to describe the long-term average weather conditions over a given region. *Climate* thus describes "normal" or "average" conditions for a given place averaged over a given period.

Most of California is characterized as having a Mediterranean climate, with generally mild, wet winters and hot, dry summers (Bedsworth et al. 2018, DWR 2019 [Climate Change Basics]). In addition to this distinct seasonal variability, California also experiences significant climate variability on interannual to decadal timescales. California also experiences large differences in climate between different parts of the state. Most notably, the northwestern part of the state and the Sierra Nevada and Cascade mountains receive significantly more precipitation than the central and southern portion of the state. These seasonal, interannual, and regional variations in climate conditions affect water supplies, demands, and management throughout the state.

This section describes historical observed climate conditions over the ARBS study area and CalSim3 domain (Figure 1). Observational datasets used to characterize historical climate conditions are described in Section 2.1. Observed historical climate variability and climate trends are described in Section 2.2.

2.1 Observational Datasets

A combination of weather station records and gridded observational datasets were used to characterize historical climate variability over the CalSim3 domain.

Weather station records generally constitute the best-available information on weather and climate conditions at the station location and its immediate vicinity. However, weather station records often have missing values due to instrument malfunction, delays or gaps in manual readings, and other operations and maintenance challenges. In addition, weather stations typically provide relatively sparse spatial coverage: many watersheds may contain just a few weather stations, and weather conditions at those station locations may not be representative of the entire watershed due to the effects of topography, land cover, and other factors on local-scale weather conditions. Using weather station records to characterize climate variability and trends over a region of interest is often challenging due to limited data coverage in both time and space (Livneh et al. 2013, Livneh et al. 2015).

Gridded observational datasets, by contrast, provide a temporally and spatially complete record of climate conditions over a given area. Gridded observational

datasets are typically developed from weather station records. Station data are interpolated onto a rectilinear grid using sophisticated interpolation procedures combined with scaling or adjustment to account for the influence of topography on local-scale weather conditions. Gridded observational datasets also utilize statistical techniques to minimize inconsistencies in weather station records over time, including effects of weather stations coming online or going offline, being relocated, or being affected by changes in site conditions or surrounding landscape. Gridded observational datasets allow for analysis of spatio-temporal characteristics of weather and climate variability; provide a consistent input dataset for use with spatially-distributed hydrologic models; and provide a basis for evaluating, downscaling, and bias-correcting climate projections from global climate models (GCMs).

Analysis of historical climate conditions for the ARBS is based primarily on the gridded observational dataset developed by Dr. Ben Livneh (Livneh 2016 [Pers. Comm.]). The Livneh gridded historical climate dataset is consistent with the data used in California's Fourth Climate Change Assessment (Pierce et al. 2018).

Three versions of the Livneh dataset were merged to develop a spatially and temporally complete record covering the CalSim3 domain for the period 1915-2015:

- *Livneh et al. 2013 (L2013)*
  Period of Record: 1915-2011
  Spatial Extent: Continental US, Mexico, and Southern Canada

- *Livneh et al. 2015 (L2015)*
  Period of Record: 1950-2013
  Spatial Extent: Continental US, Mexico, and Southern Canada

- *Livneh 2016 (L2016)*
  Period of Record: 1915-2015
  Spatial Extent: Continental US, Mexico, and Southern Canada

All three versions of the Livneh observational dataset were developed from ground-based weather station records. Station data were interpolated to a 1/16° rectilinear grid using the SYMAP algorithm (Shepard 1984) followed by orographic scaling to account for the effects of topography (Livneh et al. 2013, Livneh et al. 2015). All three datasets share the same 1/16° grid. The three datasets were compared over their overlapping period of record (1950-2011). Differences were found to be generally minor.

The merged dataset used in this study was developed as follows. The L2015 dataset was selected as the primary dataset for the period 1950-2013. The L2015 dataset was selected as the primary dataset because it served as the observational basis for downscaling and bias correction in developing the LOCA downscaled climate projections (Pierce et al. 2014; see Section 3). The L2016 dataset was

used to extend the period of record to include 1915-1949 and 2014-2015. The L2016 dataset was selected to extend the L2015 period of record as it represents the most recent version of the Livneh dataset and because it includes recent years that are not included in other versions (2014-2015) (Livneh 2016 [Pers. Comm.]). The L2013 dataset was then used to fill a small number of missing values from the L2015 and L2016 datasets. Lastly, spatial interpolation between neighboring grid cells was used to fill remaining values that were missing from all three datasets.

The resulting merged dataset was compared to available weather station records from the Global Historical Climatology Network–Daily (GHCN-Daily) dataset to ensure that the gridded dataset was consistent with available station records (NOAA 2019 [GHCN-Daily]). GHCN-Daily is an integrated database of daily climate summaries from more than 80,000 ground-based weather stations around the globe (Menne et al. 2012). Data are compiled by the National Oceanic and Atmospheric Administration (NOAA) National Centers for Environmental Information (NCEI; formerly the National Climatic Data Center) from numerous sources, including more than a dozen separate weather station networks and databases within the United States as well as international datasets shared by national meteorological and hydrological services and by personal communication between NOAA NCEI and international agencies. All station records are subjected to routine quality assurance checks prior to being integrated into the GHCN-Daily database.

GHCN-Daily stations from within CalSim3 domain (see Figure 1) were identified and station records were compiled for precipitation, daily maximum air temperature, daily minimum air temperature, and daily mean air temperature. Station records were reviewed and screened based on the available period of record (start and end dates of station record) and completeness of record (frequency of missing values). Stations with fewer than 20 years of data values (7,300 daily values) or with more than 50 percent missing values over their period of record were excluded from analysis. The merged Livneh dataset developed for the ARBS was ultimately compared to records from 262 GHCND stations for precipitation, 251 stations for daily maximum air temperature, 250 stations for daily minimum air temperature, and 94 stations for daily mean air temperature.

In general, precipitation from the merged Livneh dataset exhibits good agreement with GHCND station data, with larger biases in precipitation data occurring prior to 1950 than after. For example, monthly precipitation at the GHCND station located near the Bush Creek Ranger Station in Plumas National Forest (GHCND Station ID USC00041130[1]) correspond well to the L2015 data from the overlying cell after 1950 (Figure 2 and Figure 4). However, prior to 1950 the L2015 dataset underestimates precipitation compared to the GHCND dataset, with the largest

[1] GHCND Station USC00041130 is located near the Brush Creek Ranger Station in Plumas National Forest. The station is approximately 13.5 miles northeast of Oroville Dam on the western slope of the Sierra Nevada foothills at approximately 3,560 feet above mean sea level. The station is in a clearing surrounded by forest.

biases occurring during the wetter months (Figure 3 and Figure 5). This pre-1950 bias in the merged Livneh dataset compared to GHCND station data is more pronounced in wetter areas and not as apparent in the dry areas. For example, the GHCND station near Alturas, California (GHCND Station ID USC00040161[2]) exhibits good agreement with the merged dataset for the entire climatological record (Figure 6 and Figure 7).

Similar to precipitation, temperatures from the merged dataset generally agree well with the GHCND station data. The largest biases in temperature tend to occur in grid cells that contain varied terrain. For example, the merged dataset tends to underestimate maximum temperatures in the grid cell overlying the GHCND station at Canyon Dam (GHCND Station ID USC00041497[3]; Figure 8). This is because the grid cell encompasses a portion of the Sierra Nevada foothills surrounding Lake Almanor. The GHCND station is located adjacent to Lake Almanor, which is at the lowest elevation within the corresponding grid cell. The gridded temperature value represents the average over the cell, which includes areas at higher elevations that are typically cooler.

The merged Livneh gridded observation dataset accurately reflects interannual fluctuations in sub-area-averaged annual precipitation (Figure 9) and temperature (Figure 10 and Figure 11) as compared to available station data within each sub-area. The magnitude of sub-area-averaged precipitation is generally within the range of individual stations, and interannual variability in sub-area-averaged precipitation is highly correlated with individual stations within each sub-area. The magnitude of the ARBS study area averaged maximum and minimum temperatures is generally cooler than most stations as most stations are found in the lower elevation part of the ARBS study area and therefore do not fully represent the cooler temperatures found in the mountainous areas.

Overall, the areal averages from the merged Livneh dataset are consistent with climatic trends observed in individual station data and thus imparting historically consistent trends and variability onto future projections.

[2] GHCND Station USC00040161 is located in the city of Alturas, California. The station is approximately 20 miles south-southeast of Goose Lake, in a broad flat valley in the North Fork Pit River watershed at approximately 4,380 feet above mean sea level. The station is located in an large open area away from buildings, trees, and other structures.

[3] GHCND Station USC00041497 is located at Canyon Dam (Lake Almanor). The station is approximately 50 miles northeast of Chico California and 30 miles south-southeast of Lassen Volcanic National Park. The station is in the North Fork Feature River watershed at approximately 4,400 feet above mean sea level. The station is located in a clearing surrounded by forest.

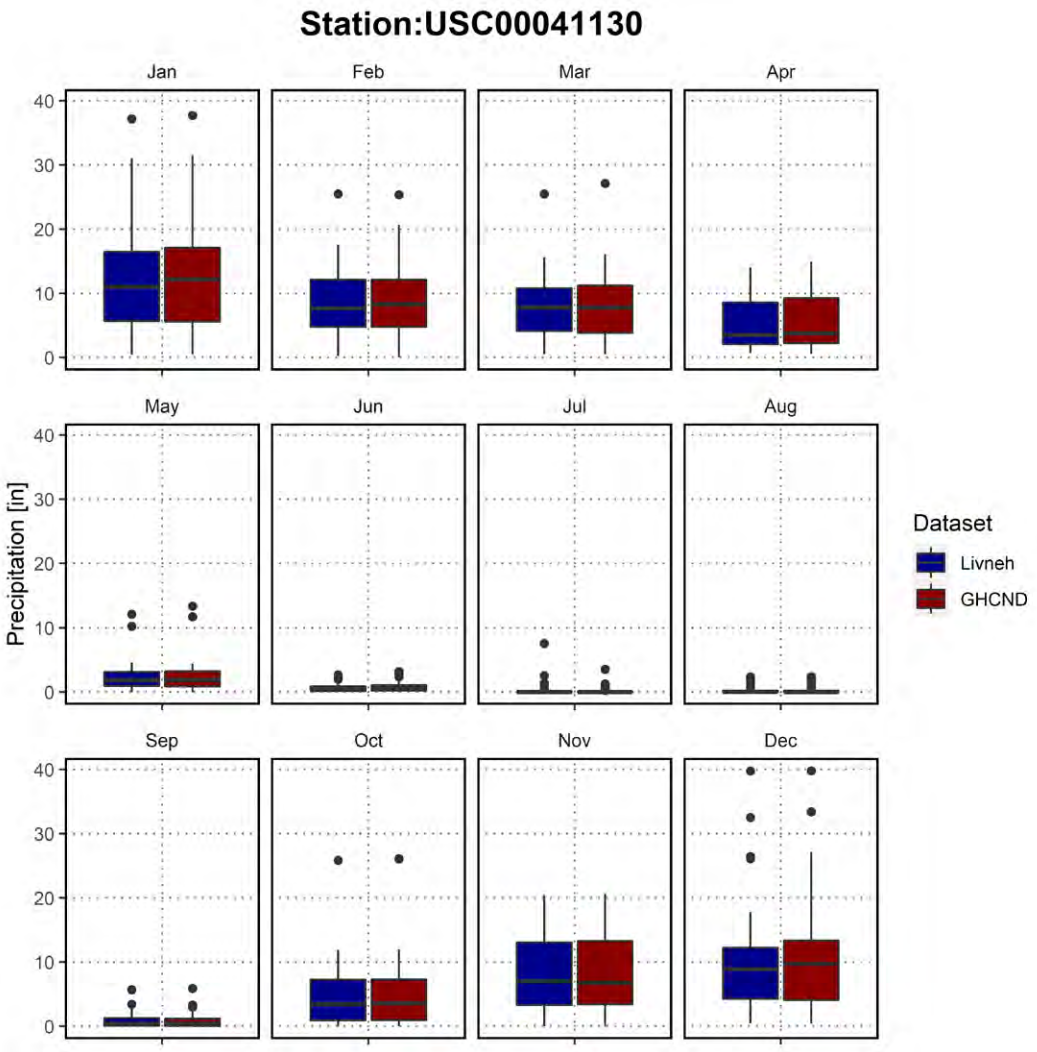

Figure 2. Boxplots of monthly precipitation for the period 1950-2015 for the GHCND station located near the Bush Creek Ranger Station in Plumas National Forest (GHCND Station ID USC00041130; NOAA) and the corresponding grid cell from the gridded historical observed dataset developed for this study (Livneh).

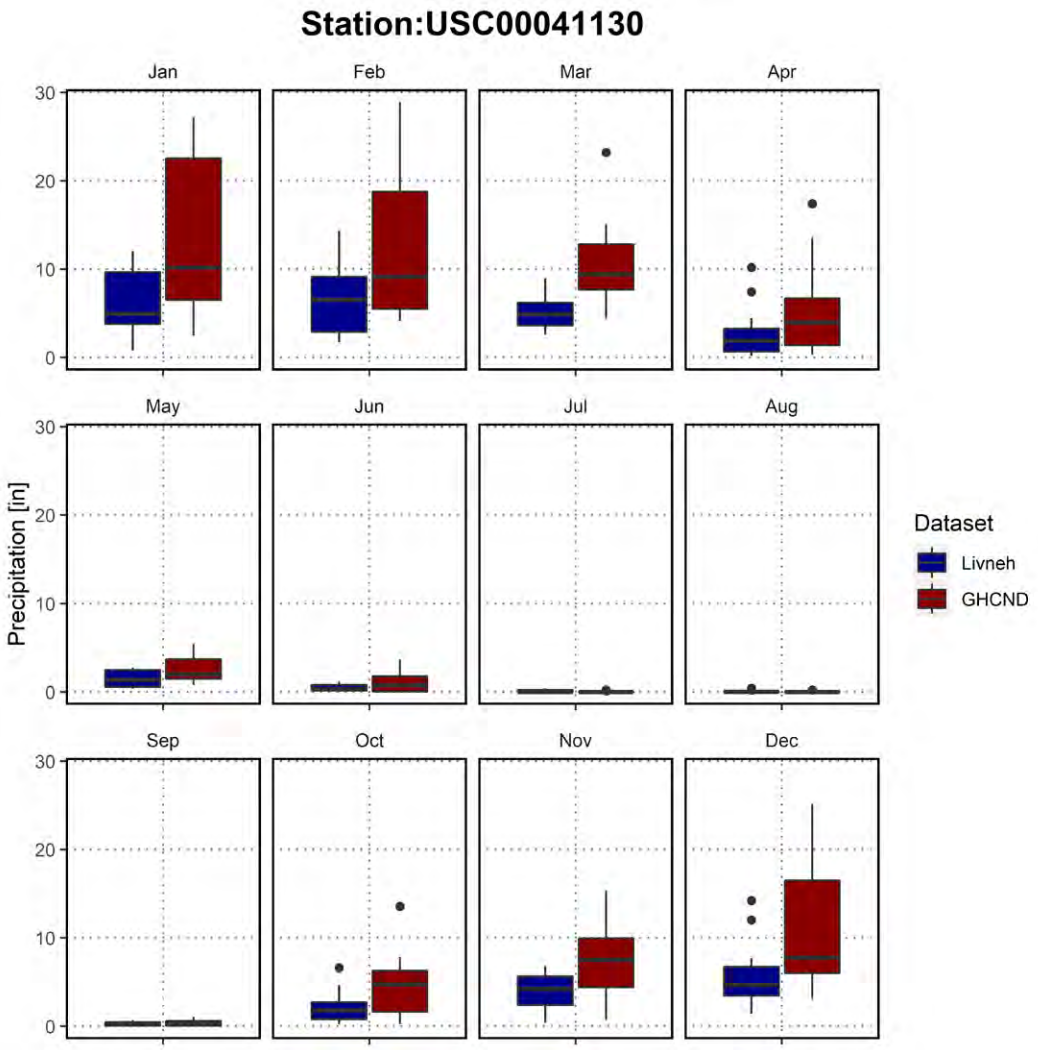

Figure 3. Boxplots of monthly precipitation for the period 1937-1949 for the GHCND station located near the Bush Creek Ranger Station in Plumas National Forest (GHCND Station ID USC00041130; NOAA) and the corresponding grid cell from the gridded historical observed dataset developed for this study (Livneh).

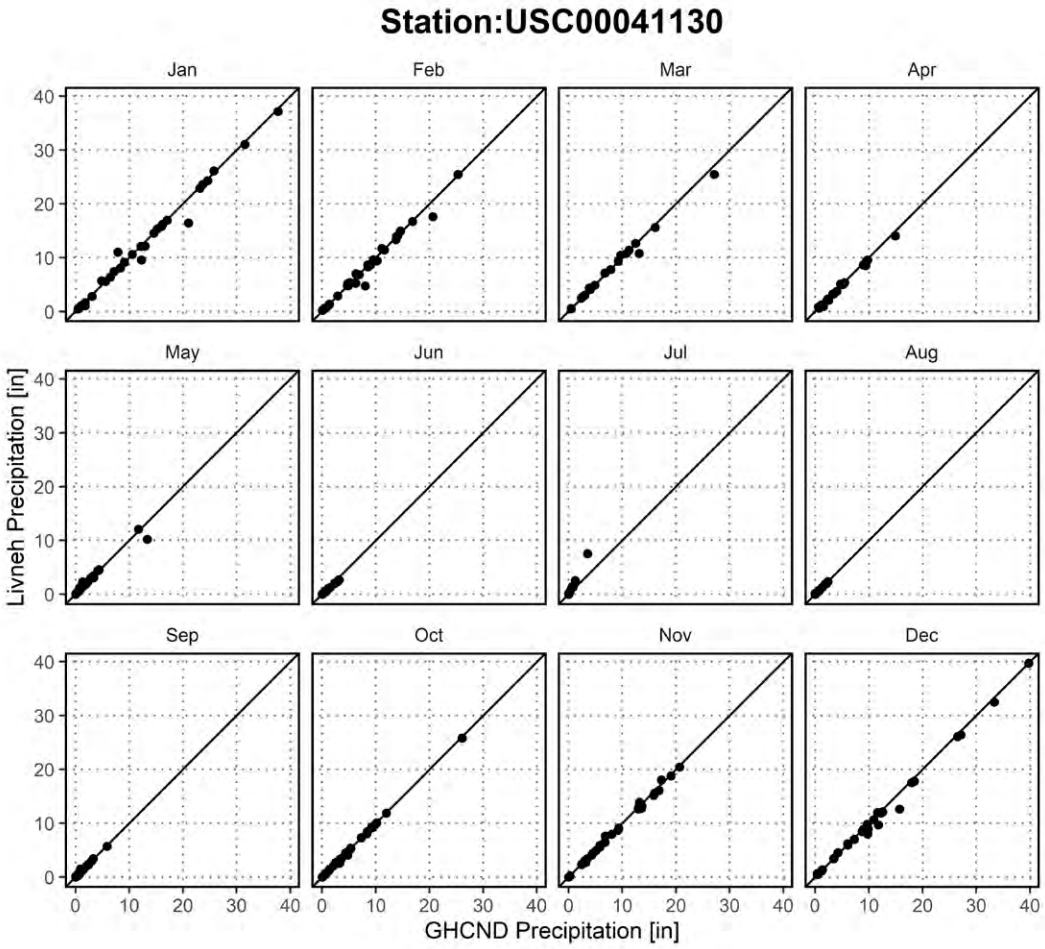

Figure 4. Scatterplots comparing monthly precipitation for the period 1950-2015 for the GHCND station located near the Bush Creek Ranger Station in Plumas National Forest (GHCND Station ID USC00041130; NOAA) and the corresponding grid cell from the gridded historical observed dataset developed for this study (Livneh).

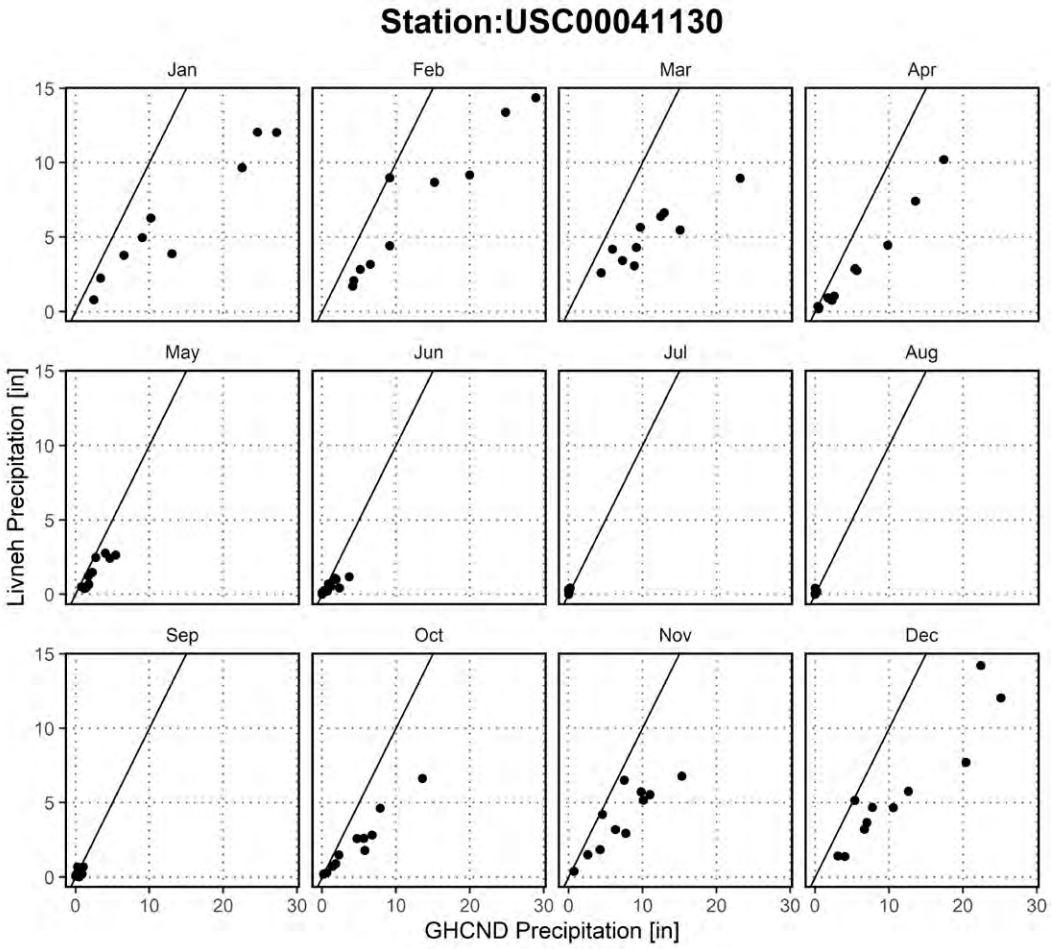

Figure 5. Scatterplots comparing monthly precipitation for the period 1937-1949 for the GHCND station located near the Bush Creek Ranger Station in Plumas National Forest (GHCND Station ID USC00041130; NOAA) and the corresponding grid cell from the gridded historical observed dataset developed for this study (Livneh).

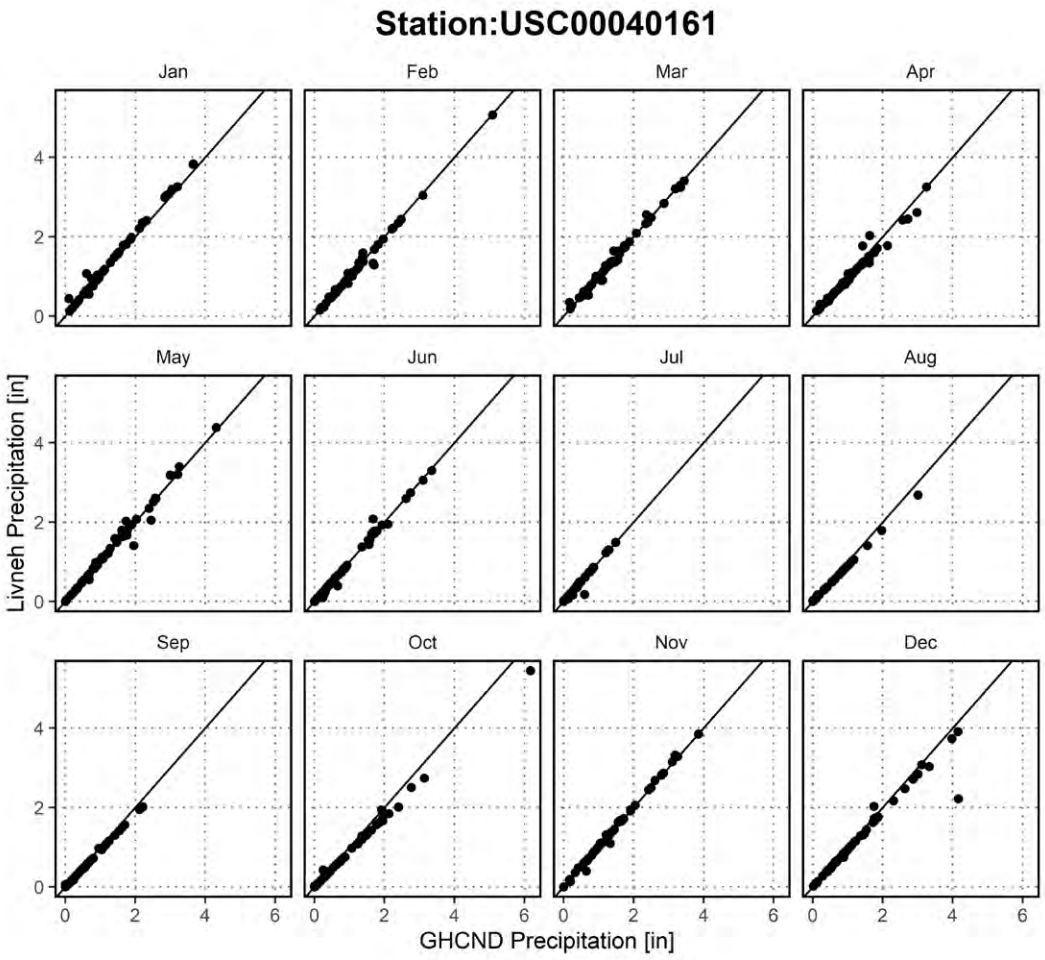

Figure 6. Scatterplots comparing monthly precipitation for the period 1950-2015 for the GHCND station located in Alturas, California (GHCND Station ID USC00040161; NOAA) and the corresponding grid cell from the gridded historical observed dataset developed for this study (Livneh).

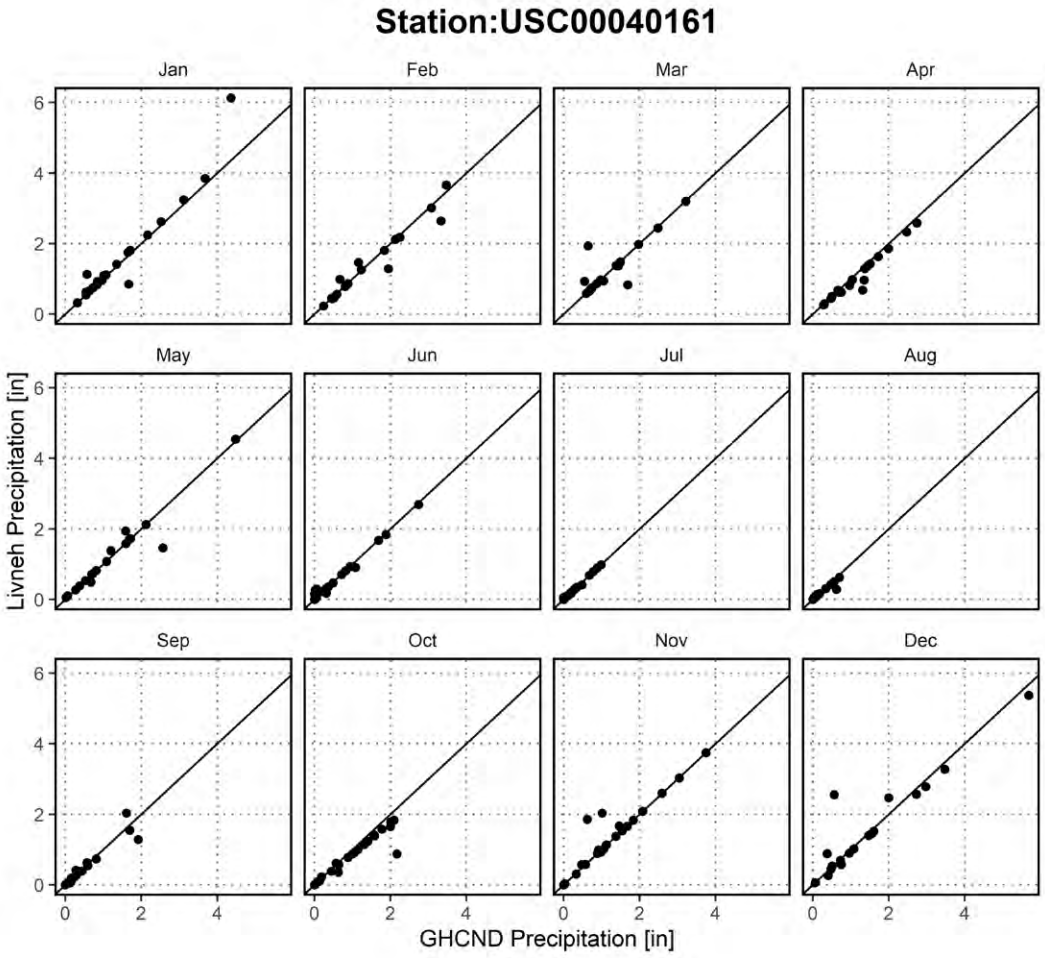

Figure 7. Scatterplots comparing monthly precipitation for the period 1915-1949 for the GHCND station located in Alturas, California (GHCND Station ID USC00040161; NOAA) and the corresponding grid cell from the gridded historical observed dataset developed for this study (Livneh).

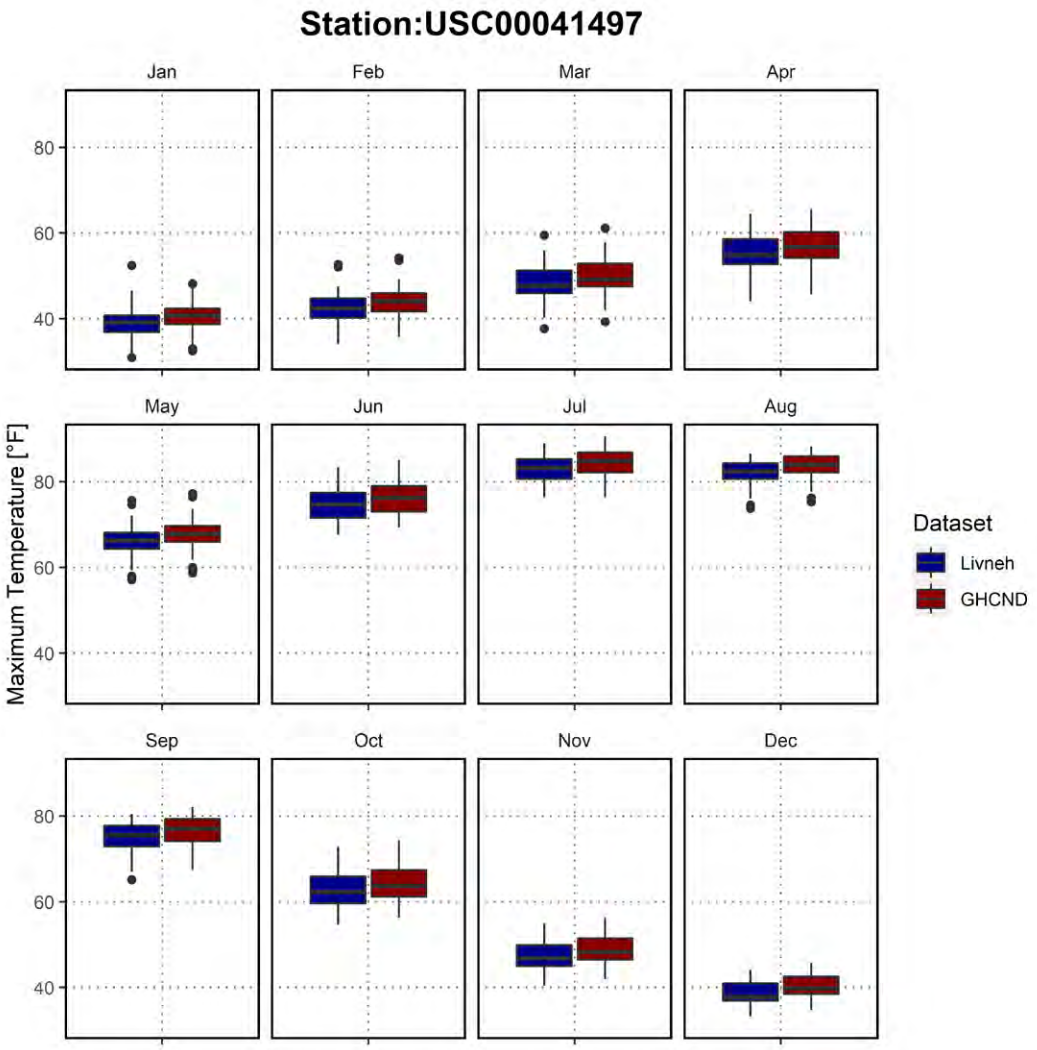

Figure 8. Boxplots of monthly mean maximum temperature for the period 1950-2015 for the GHCND station located near Canyon Dam (GHCND Station ID USC00041497; NOAA) and the corresponding grid cell from the gridded historical observed dataset developed for this study (Livneh).

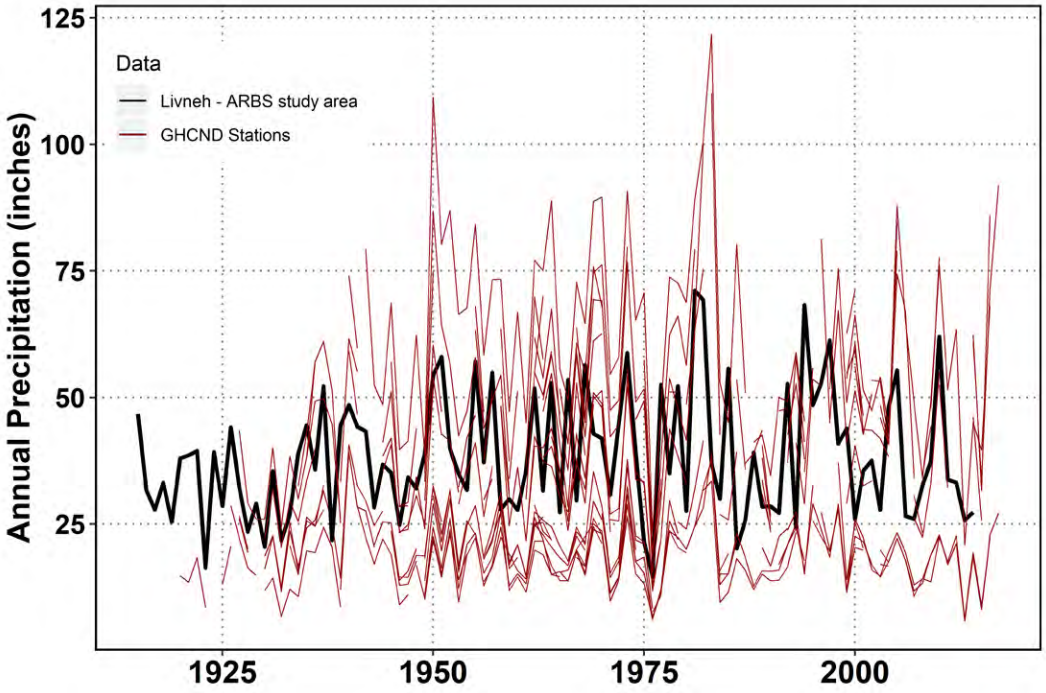

Figure 9. Annual historical precipitation observations. Observations include individual GHCND stations (red) and the area-average from the L2015 dataset for the ARBS study area (black).

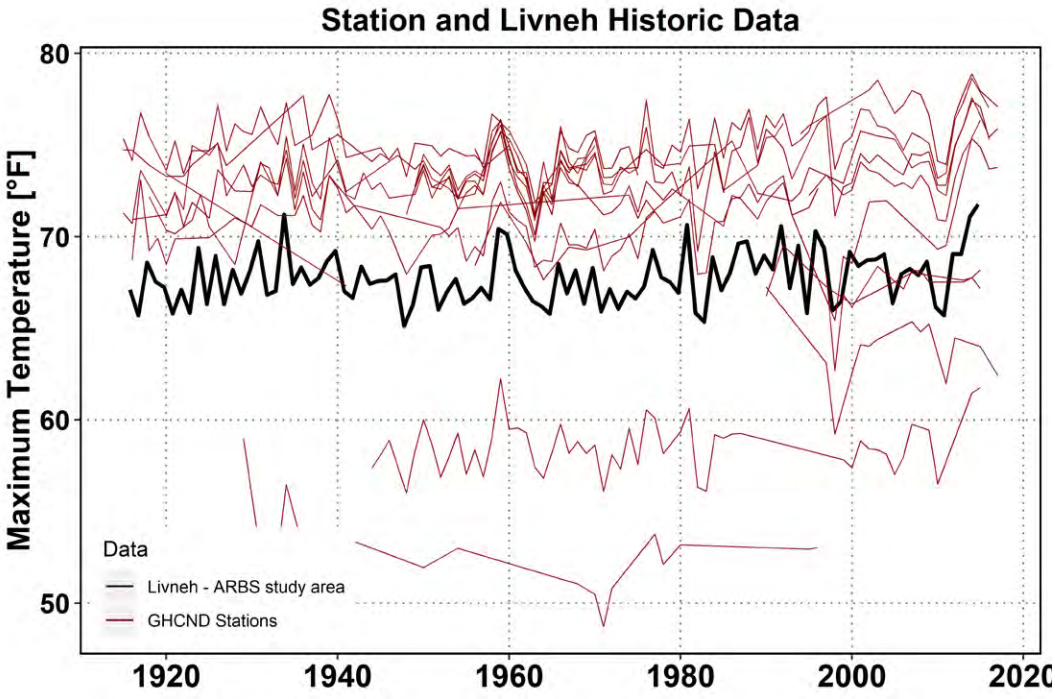

Figure 10. Annual historical maximum temperature observations. Observations include individual GHCND stations (red) and the area-average from the L2015 dataset for the ARBS study area (black).

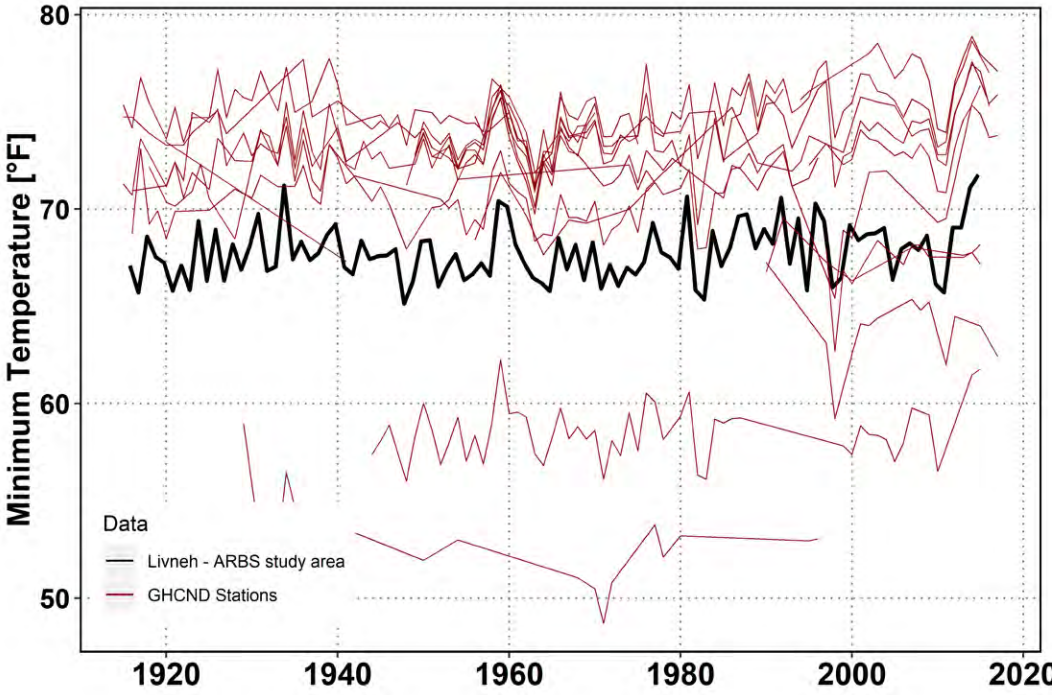

Figure 11. Annual historical minimum temperature observations. Observations include individual GHCND stations (red) and the area-average from the L2015 dataset for the ARBS study area (black).

2.2 Observed Historical Climate Conditions

Observed historical climate conditions were evaluated and characterized based on the gridded dataset described in Section 2.1 . Climate conditions were evaluated on a 1/16th degree grid and averaged over the ARBS study area, the CalSim3 domain, and selected basins.

Selected basins considered in evaluating historical climate conditions are illustrated in Figure 12. Selected basins include the eight major tributary basins to the Sacramento-San Joaquin Rivers:

- Sacramento River basin above Bend Bridge near Red Bluff, CA

- Yuba River basin above Smartville, CA
- American River basin above Folsom, CA
- Stanislaus River basin above Goodwin Dam near Oakdale, CA
- Tuolumne River basin above La Grange Dam near La Grange, CA
- Merced River basin above Merced Falls, CA
- San Joaquin River basin above Friant Dam near Friant, CA

In addition, selected basins include the two subbasins of the Sacramento Valley Groundwater Basin located within the ARBS study area:

- North American Subbasin (Subbasin 5-021.64)
- South American Subbasin (Subbasin 5-021.65)

2.2.1 Observed Temperature

Historical temperatures exhibit significant spatial and temporal variability across the ARBS study area and the CalSim3 domain. Spatial variability in annual average temperature over the period 1980-2009 is shown in Figure 13; annual average temperatures were computed by averaging the daily average temperature at each grid cell over each water year (October 1 to September 30).[4] The median (50^{th} percentile) annual average temperature ranges from less than 35°F in the higher elevation mountain regions of the Sierra Nevada to more than 65°F in the low elevation regions of the Central Valley. The fifth percentile annual average temperature is up to 5°F cooler than the median, and the ninety-fifth percentile is up to 3°F warmer than the median.

Temperatures throughout the region also exhibit strong seasonality. Spatial variability in seasonal average temperatures over the period 1980-2009 are shown in Figure 14; seasonal temperatures were computed by averaging daily average temperature over each season. As expected, the coldest temperatures typically occurring in winter (January, February and March) and the warmest temperatures in summer (July, August and September). Seasonal temperatures can range from less than 20°F during the winter in the mountains to more than 80°F during the summer in the Central Valley.

Boxplots of basin-averaged monthly temperature over the period 1980-2009 are shown in Figure 15 for the ARBS study area, CalSim3 domain, eight major tributary basins[5] to the CVP-SWP system, and two groundwater subbasins within the ARBS study area. January is typically the coldest month and July and August are typically the warmest months. The American River basin is the warmest of the eight major tributary basins with average monthly temperatures reaching above 70°F during the summer and dropping below 35°F in the winter. The San Joaquin River basin is the coldest of the eight major tributary basins with average monthly summer temperatures around 60°F and average monthly winter temperatures dropping close to 30°F.

While there is considerable interannual variability in annual and seasonal mean temperatures, spatial variability across basins is much greater than interannual variability within a given basin. Timeseries of basin-average annual temperatures

[4] For purposes of the ARBS, a water year is defined as the period from October 1 to September 30. For example, water year 2000 is from October 1, 1999 to September 30, 2000.

[5] The eight major tributaries include the Sacramento River at Bend Bridge; Feather River at Oroville; Yuba River near Smartville; American River at Folsom; Stanislaus River at Goodwin; Tuolumne River near La Grange Dam; Merced River at Merced Falls; and San Joaquin River below Friatn Dam.

are shown in Figure 16. The range of variability across basins exceeds the range of variability over time for any given basins.

Despite the large spatial variability across basins, however, interannual variability of annual temperatures is highly correlated between basins. The pattern of above average and below average years is generally consistent across all parts of the study area; there are few if any years where above normal temperatures in one basin coincide with below normal temperatures in another basin.

Long-term trends in basin-average annual temperatures are listed in Table 1 and shown in Figure 17. Trends in basin-average temperature were evaluated over the period 1915-2015 for daily maximum temperature, daily minimum temperature, and daily average temperature. Trends were evaluated using the Mann-Kendall Test with a significance threshold of 0.05 (95% confidence); blue shading in Table 1 indicates a statistically significant trend in precipitation and red shading indicates a statistically significant trend in temperature. Analysis reveals statistically significant positive trends in minimum temperature for all but one of the basins evaluated, indicating widespread warming of minimum temperatures throughout the region over the last century. Similarly, trends in average temperature are positive over all but one of the basins considered and are statistically significant over all but three basins. In contrast, trends in annual maximum temperature exhibit considerable variability. Trends in maximum temperature are positive over half of the basins evaluated and negative over the other half, and statistically significant positive trends occur in only two of the basins evaluated. Out of the 70 Hydrologic Unit Code (HUC) watersheds[6], 47 have significant increases in annual average temperature (Table A1 and Figure A1) and out of the 40 CalSim3 water budget areas (WBA), 35 have significant increases in annual average temperature (Table A2 and Figure A2).

[6] Eight-digit hydrologic unit code (HUC) watersheds for the Basin Study area were obtained from the USGS Watershed Boundary Dataset (USGS et al. 2013)

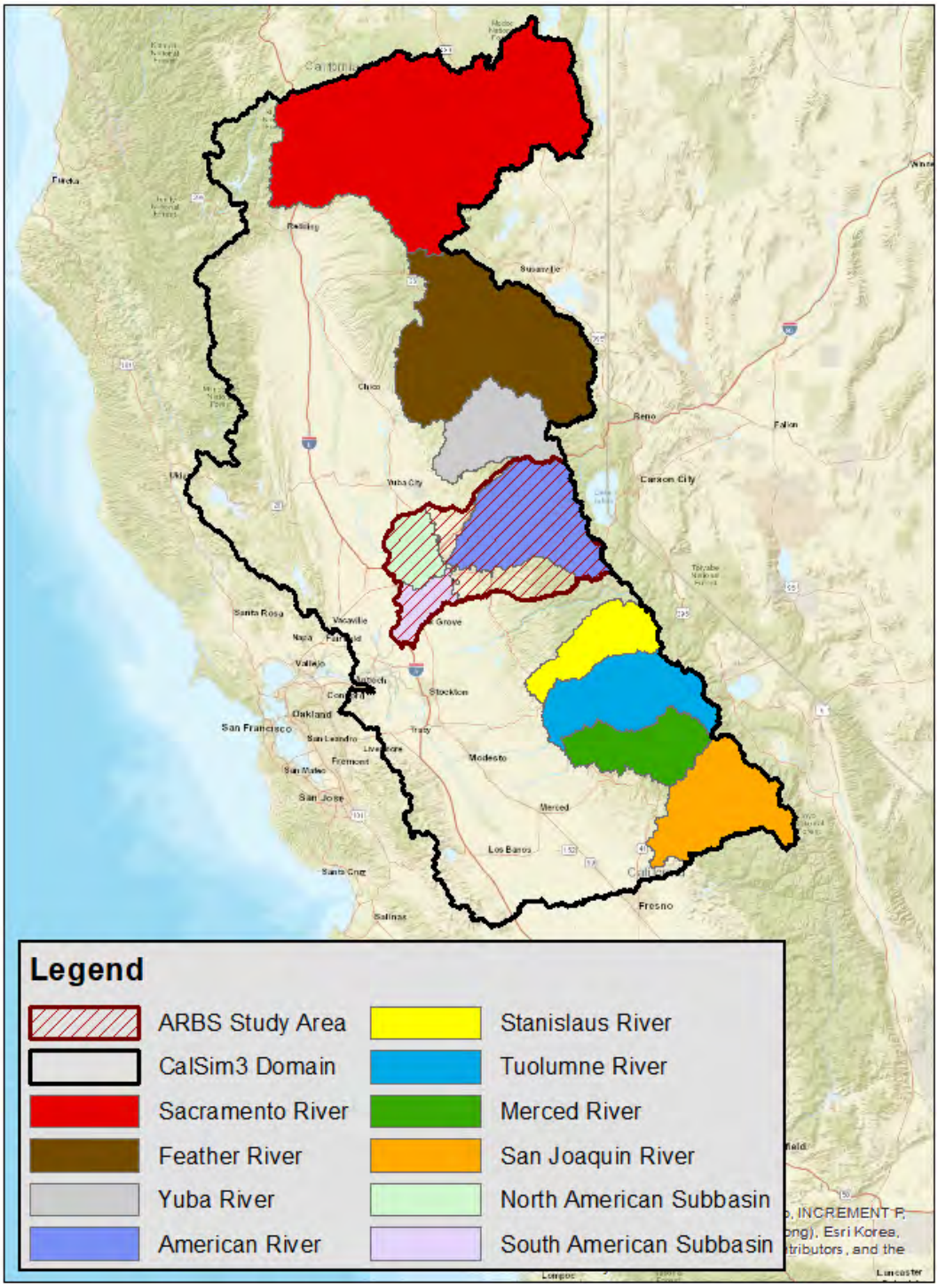

Figure 12: Basins considered in evaluating observed historical climate conditions.

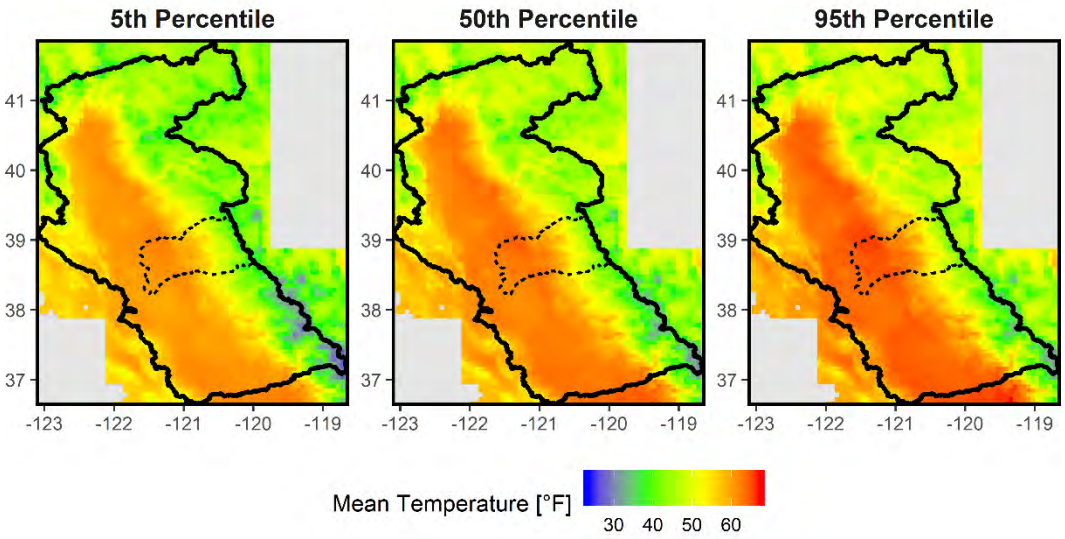

Figure 13. Spatial distribution of the 5th, 50th and 95th percentiles of annual average temperature from 1980–2009. The CalSim3 domain is delineated by the solid black line and the ARBS study area is delineated by the black dashed line.

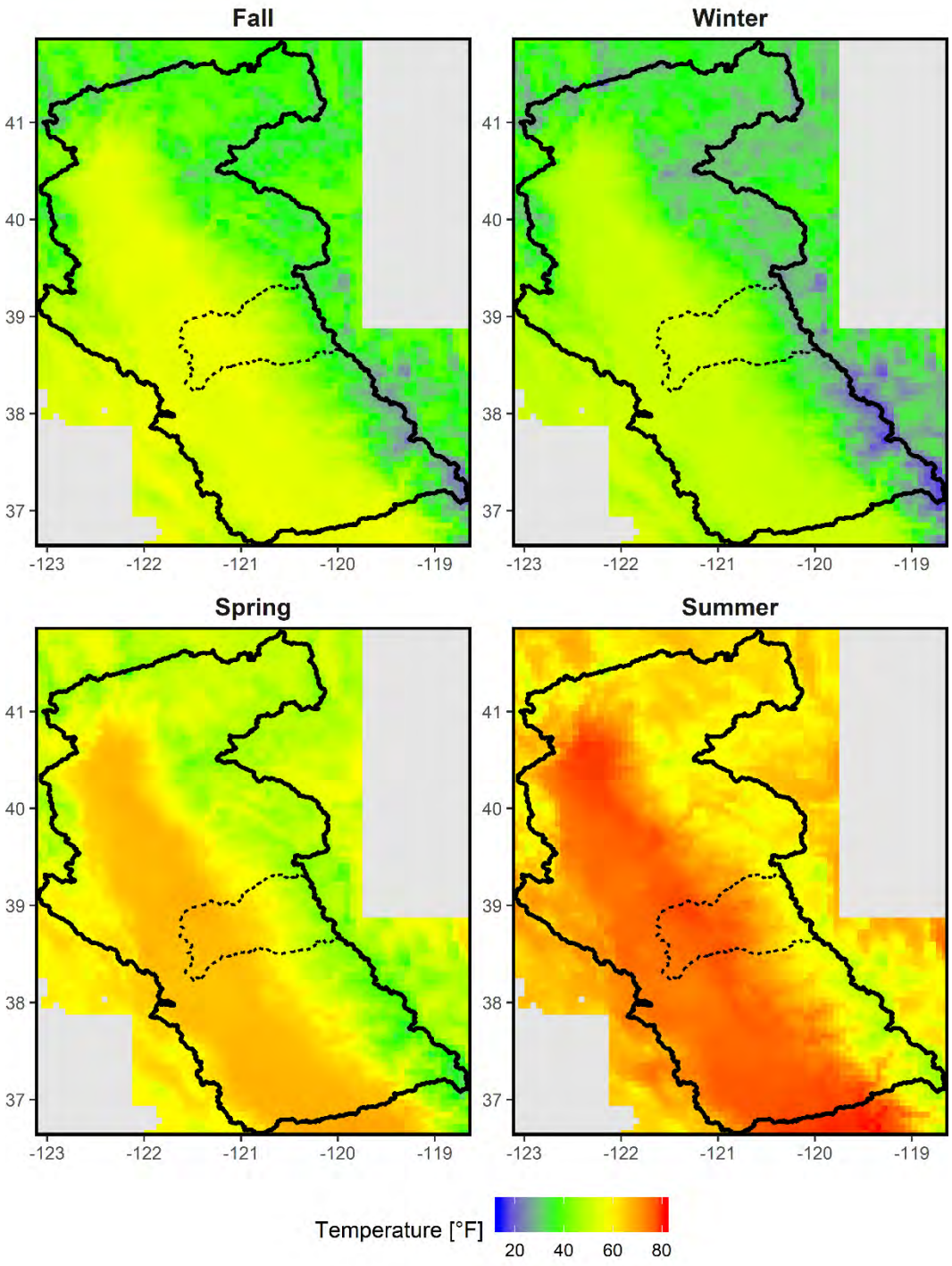

Figure 14. Spatial distribution of seasonal average temperature. Seasonal average temperature is computed for fall (October-November-December), winter (January-February-March), spring (April-May-June), and summer (July-August-September) for the period 1980-2009. The CalSim3 domain is delineated by the solid black line and the ARBS study area is delineated by the black dashed line.

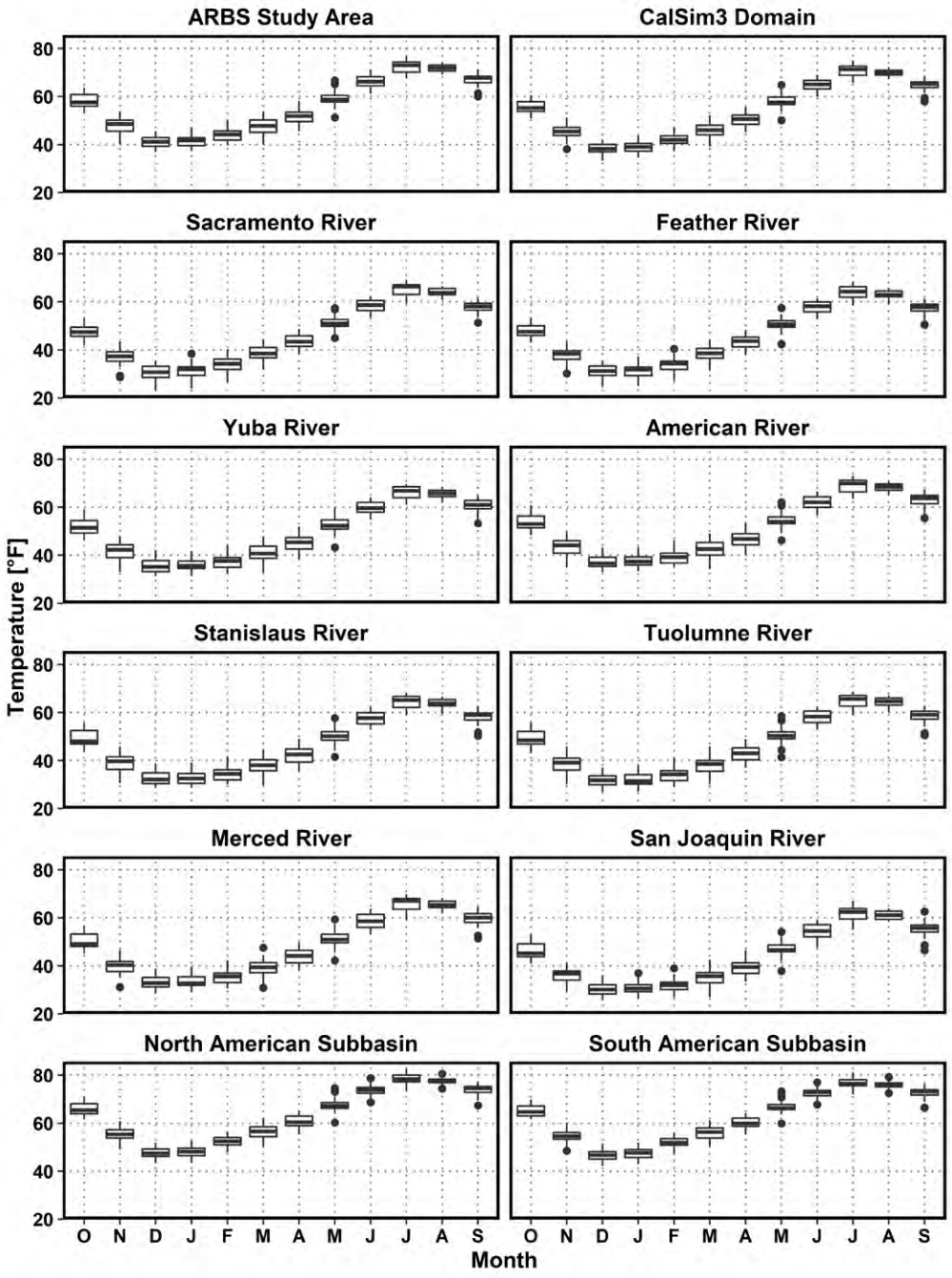

Figure 15. Boxplots of monthly average temperature averaged over the CalSim3 domain, the ARBS study area and select basins. Basins are illustrated in Figure 12. Monthly averages are computed for the period 1980-2009. Box limits represent the 25th and 75th quartiles; solid lines within each box represent the median; whiskers represent values extending from the 25th and 75th quartiles to values within ± 1.5*(Interquartile Range); and outliers are represented by solid black circles. X-axis labels represent: O = October, N = November, D = December, J = January, F = February, M = March, A = April, M = May, J = June, J = July, A = August and S = September.

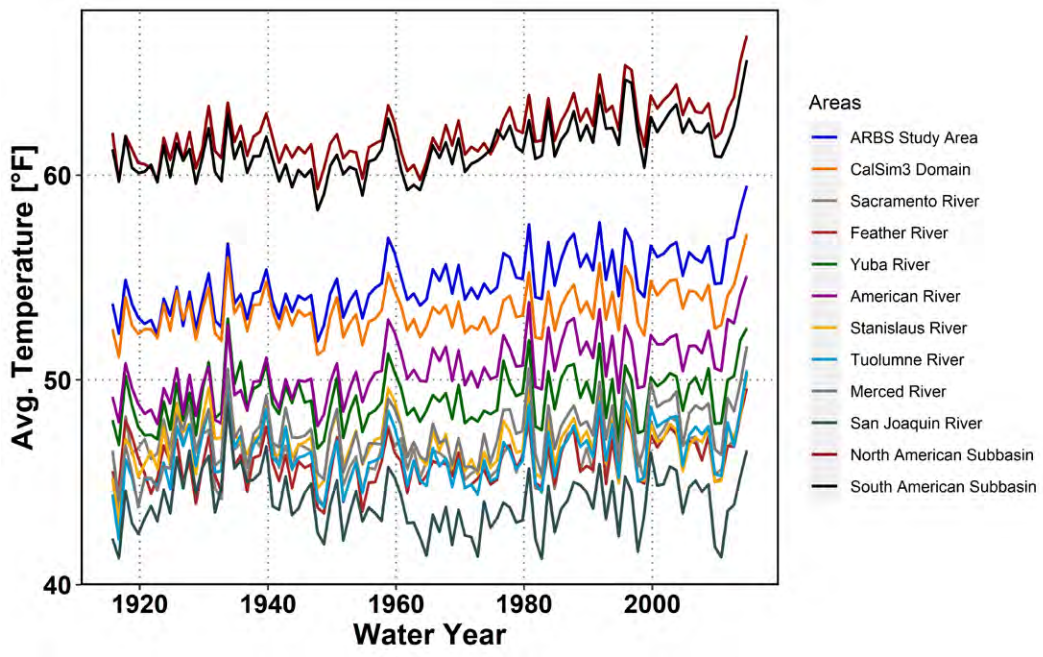

Figure 16. Timeseries of basin-average annual average temperature.

Table 1. Observed trends in basin-average historical precipitation and temperature over the period 1915–2015.

Basin	Precip (in)	Tavg (°F)	Tmax (°F)	Tmin (°F)
ARBS Study Area	3.5	**3.5**	**1.2**	**5.9**
Sacramento River	**16.0**	0.3	-0.2	**1.2**
Feather River	6.1	**1.1**	-0.4	**2.9**
Yuba River	10.8	**1.5**	-0.1	**3.0**
American River	3.5	**3.6**	1.0	**6.0**
Stanislaus River	**10.4**	0.3	**-1.2**	**1.9**
Tuolumne River	2.1	**1.7**	0.5	**3.1**
Merced River	2.5	**2.4**	-0.7	**5.6**
San Joaquin River	5.0	0.0	-0.1	-0.3
North American Subbasin	0.6	**3.0**	**1.0**	**4.9**
South American Subbasin	2.4	**2.6**	**1.8**	**3.2**
CalSim3 Domain	**6.1**	**1.5**	0.3	**2.8**

Notes:

- *Precip = annual precipitation, Tavg = annual mean of daily average temperature, Tmin = annual mean of daily minimum temperature, Tmax = annual mean of daily maximum temperature.*
- *Values are observed trends in precipitation and temperature over the period 1915-2015*
- *Values are given as change per century, in inches per 100 years for precipitation and degrees Fahrenheit per century for temperature*
- *Change per century was calculated using Sen's slope (Hirsch et al. 1991).*
- *Bold and shaded values indicate a statistically significant increase or decrease over the period 1915-2015. Blue shading indicates a statistically significant change in precipitation and red shading indicates a statistically significant change in temperature. Statistical significance was determined using the Mann-Kendall Test ($p < 0.05$).*

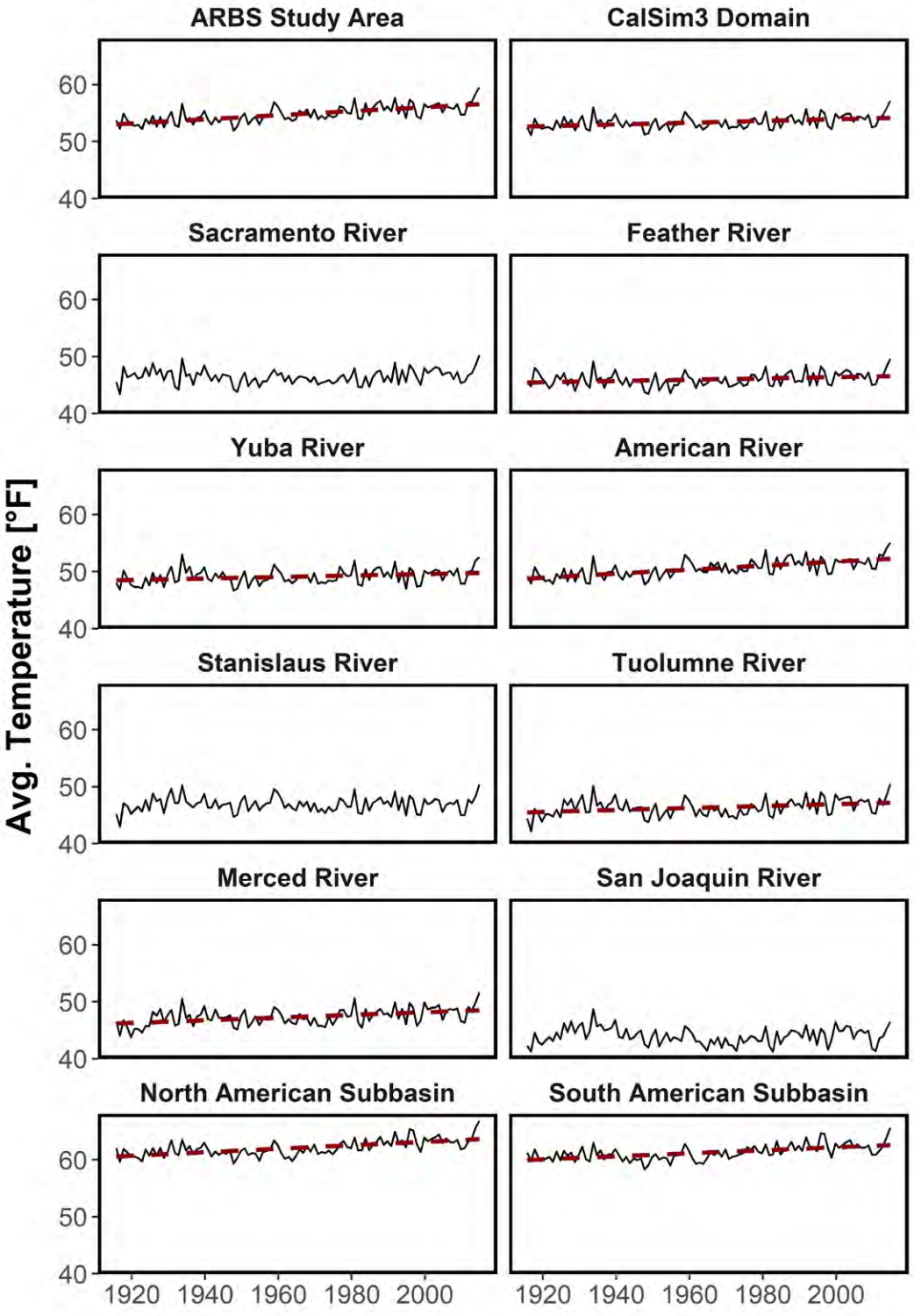

Figure 17. Timeseries of observed basin-average annual mean temperature. Solid black line indicates water year averages; red dashed line indicates the trend over period 1915-2015; red lines are only shown if the trend is statistically significant.

2.2.2 Observed Precipitation

Similar to observed historic temperatures, there is considerable spatial variability in observed precipitation across the CalSim3 domain. Spatial variability in annual precipitation over the period 1980-2009 is shown in Figure 13; annual precipitation was computed by summing the daily precipitation at each grid cell over each water year. The majority of precipitation over the region falls in the mountains, particularly the western slopes of the northern Sierra Nevada and southern Cascade mountains where the 50th percentile (median) annual precipitation exceeds 75 inches in some areas. The Central Valley receives the lowest annual precipitation, with a median annual precipitation of about 20 inches. The difference in annual precipitation between very wet years (95th percentile) and very dry years (5th percentile) is as little as 7 inches in the Central Valley and as much as 100 inches in some areas of the northern Sierra Nevada mountains.

Consistent with a typical Mediterranean climate, precipitation throughout the region is highly seasonal. Seasonal mean precipitation over the period 1980-2009 is shown in Figure 19. On average, winter (January, February, and March) is the wettest season, followed by fall (October, November, and December), spring (April, May, and June) and then summer (July, August, and September).

Boxplots of basin-average monthly mean precipitation over the period 1980-2009 are shown in Figure 20. January and February are typically the wettest months and July and August are the driest. The large range of the boxes and whiskers in Figure 20 are indicative of the large interannual variability in precipitation over most basins, and the circles in Figure 20 reflect the high frequency of wet outliers. The Yuba River basin is the wettest of the major tributary basins, with median monthly precipitation exceeding 10 inches in January and February and outliers exceeding 30 inches. The Sacramento River basin is the driest of the major tributary basins, with median monthly precipitation barely exceeding 5 inches in winter and no outliers above 20 inches per month. The North American and South American groundwater subbasins are the driest basins considered. These basins are located on the eastern edge of the Central Valley and receive much less precipitation than the foothill and mountain areas.

In addition to seasonality, precipitation exhibits significant interannual variability. Timeseries of basin-average annual precipitation are shown in Figure 21. Basin-average annual precipitation over the CalSim3 domain ranges from less than 15 inches to more than 60 inches. Wet years are typically followed by dry years and vice versa; occurrence of consecutive wet or dry years are rare.

The standard deviation and coefficient of variation of seasonal precipitation over the period 1980-2009 are shown in Figure 22 and Figure 23, respectively. Comparison of Figure 19 and Figure 22 indicates that variability of seasonal

precipitation generally aligns with the magnitude of seasonal mean precipitation – i.e., areas with higher seasonal mean precipitation tend to exhibit greater interannual variability. Interannual variability is thus greatest during the wet fall and winter seasons and in the wetter mountain regions. However, as shown in Figure 23, the magnitude of interannual variability relative to the annual mean (the coefficient of variation) is greatest in drier areas and drier seasons.

Despite the substantial range in annual mean precipitation across the region, interannual variability in precipitation is highly correlated between basins. Figure 21 indicates that the year-to-year pattern of wet and dry years is largely consistent across all parts of the study area and there are few if any years when anomalously wet conditions in one basin coincide with anomalously dry conditions in another basin. This correlation of wet and dry years across the region has important implications for regional water supplies and management.

Long-term trends in basin-average annual precipitation are listed in Table 1 and shown in Figure 24. Trends in basin-average precipitation were evaluated over the period 1915-2015. Overall, trends in precipitation indicate a statistically significant increase in annual precipitation across the study area. Interestingly, when analyzing these trends individually across the eight basins, only two of the relatively drier basins—i.e., the Sacramento River and Stanislaus River—exhibit significant trends. Trend analysis indicates that annual mean precipitation has increased on average by 1.6 inches per decade in the Sacramento River basin and 1.0 inches per decade in the Stanislaus River basin over the past century. Out of the 70 HUC watersheds within the CalSim3 domain, 4 have significant decreases in annual precipitation and 22 have significant increases in annual precipitation (Table A.1 and Figure A.3). Out of the 40 WBA areas, 7 have significant decreases in annual precipitation and 8 have significant increases in annual precipitation (Table A.2 and Figure A.4).

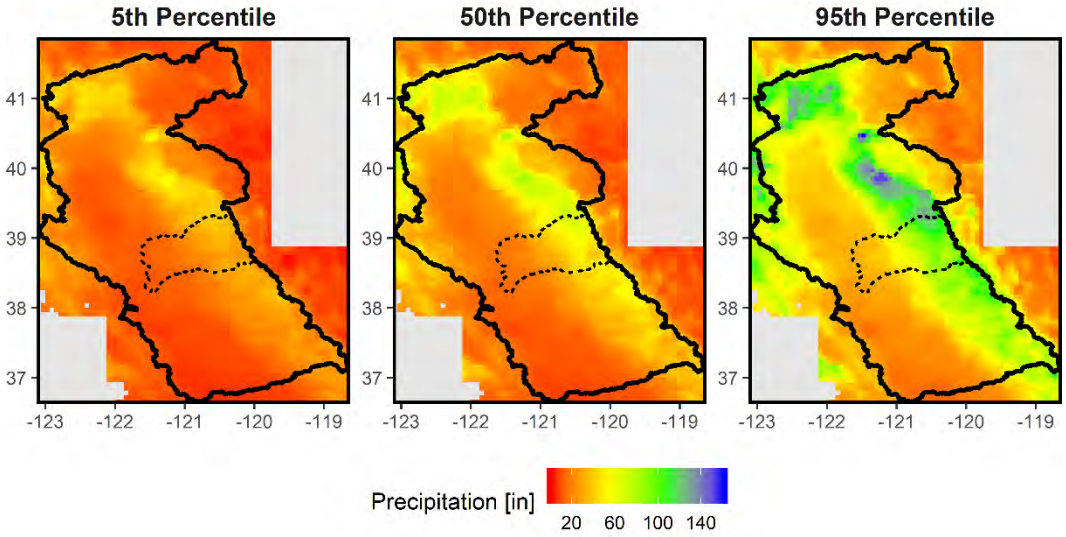

Figure 18. Spatial distribution of the 5th, 50th and 95th percentiles of annual precipitation from 1980–2009. The CalSim3 domain is delineated by the solid black line and the ARBS study area is delineated by the black dashed line.

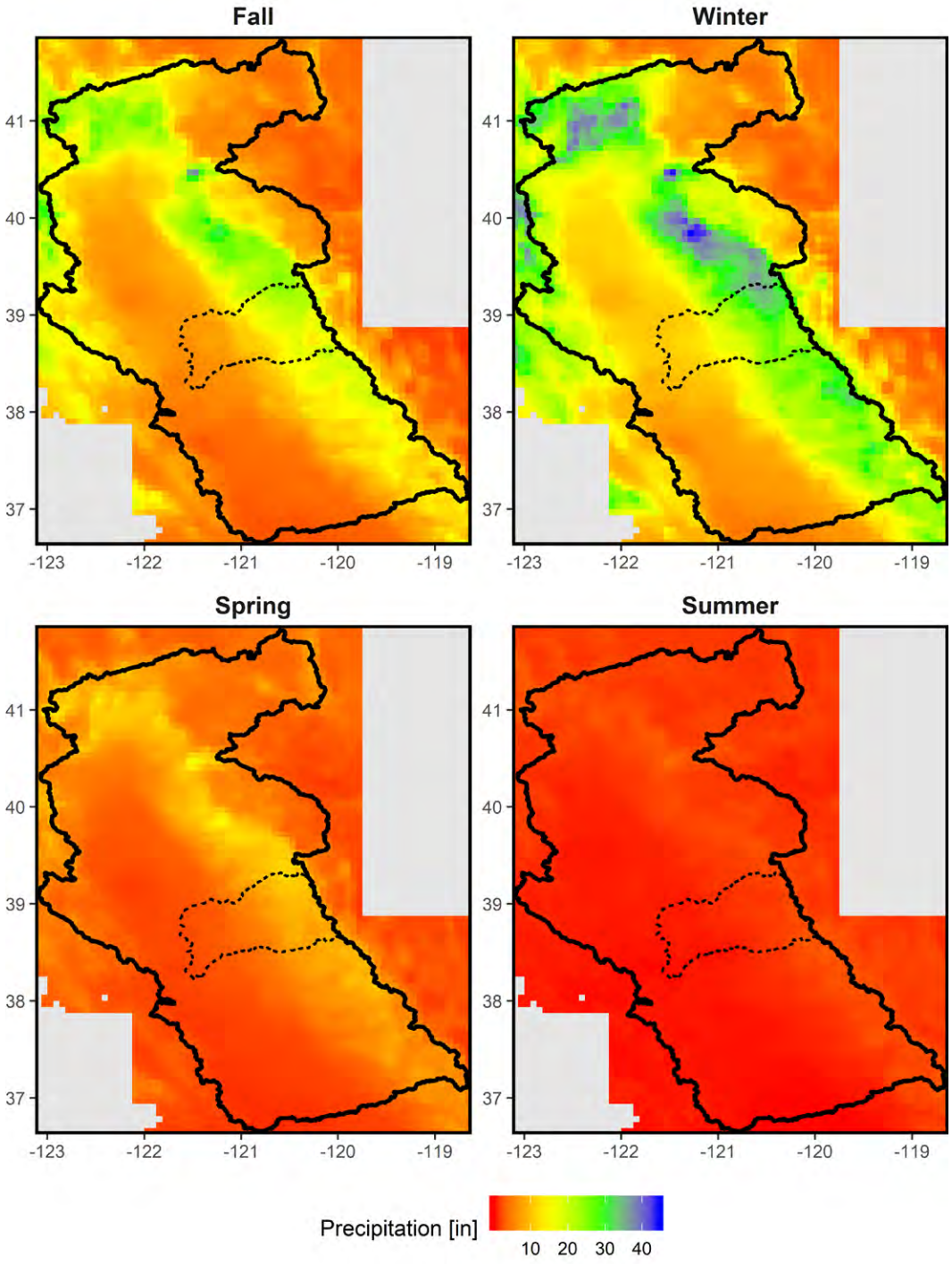

Figure 19. Seasonal distribution of seasonal average precipitation across the CalSim3 domain. Seasonal means are computed for fall (October-November-December), winter (January-February-March), spring (April-May-June), and summer (July-August-September) for the period 1980-2009. Axes are latitudinal and longitudinal coordinates. The color scale indicates the magnitude of cumulative precipitation, with red representing lower magnitude and blue representing higher magnitude. The CalSim3 domain is delineated by the solid black line and the ARBS study area is delineated by the dashed black line.

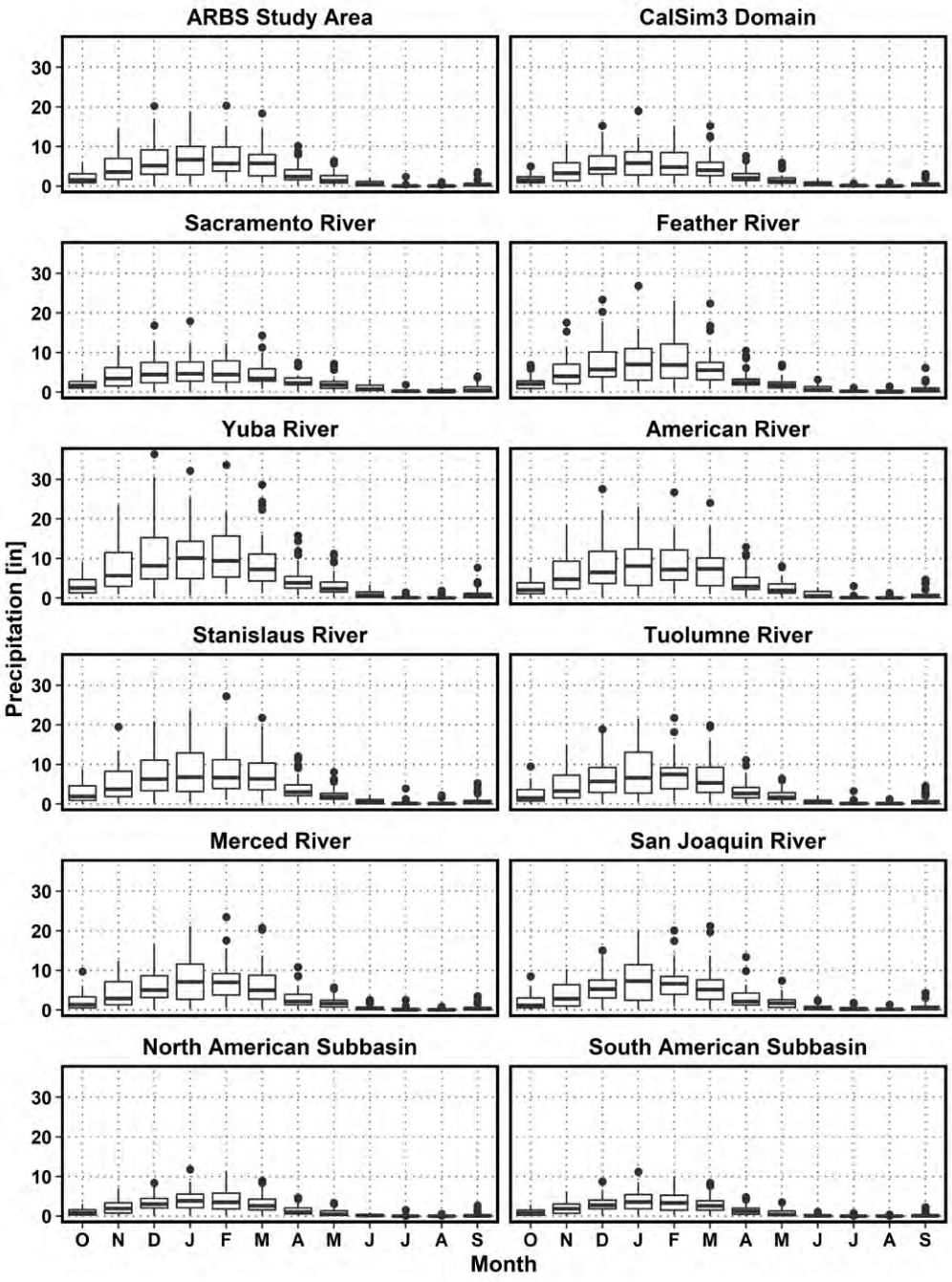

Figure 20. Boxplots of monthly precipitation averaged over the CalSim3 domain, and selected basins. Basins are illustrated in Figure 12. Monthly precipitation is computed for the period 1980-2009. Box limits represent the 25th and 75th quartiles; solid lines within each box represent the median; whiskers represent values extending from the 25th and 75th quartiles to values within ± 1.5*(Interquartile Range); and outliers are represented by solid black circles. X-axis labels represent: O = October, N = November, D = December, J = January, F = February, M = March, A = April, M = May, J = June, J = July, A = August and S = September.

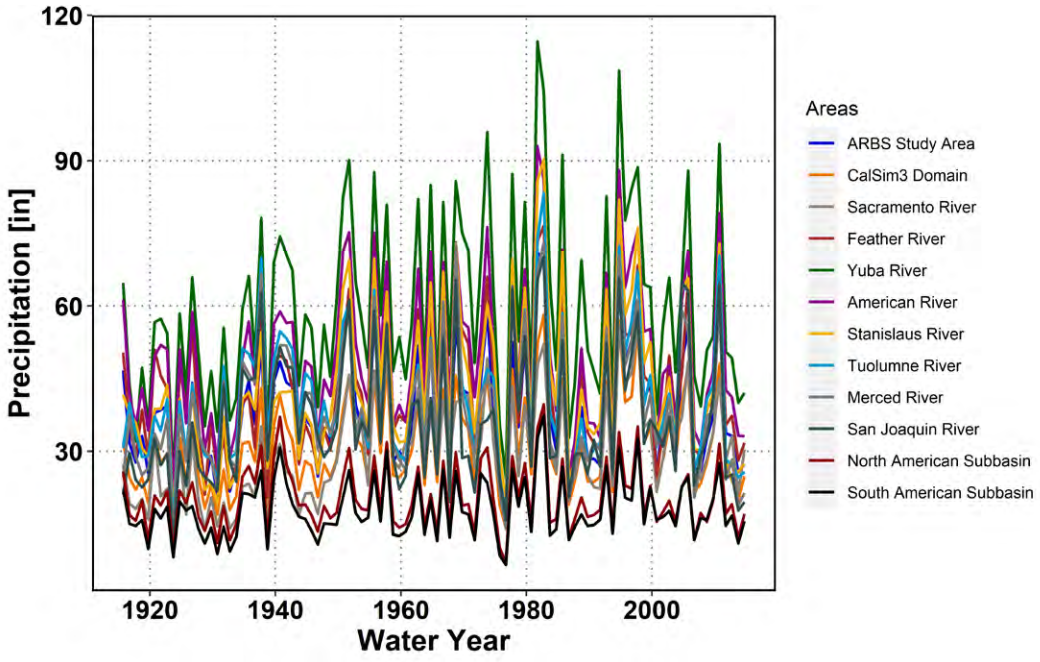

Figure 21. Timeseries of basin-average annual precipitation over the CalSim3 domain, the ARBS Study Area, the two bulletin 118 groundwater basins and the 8 subbasins.

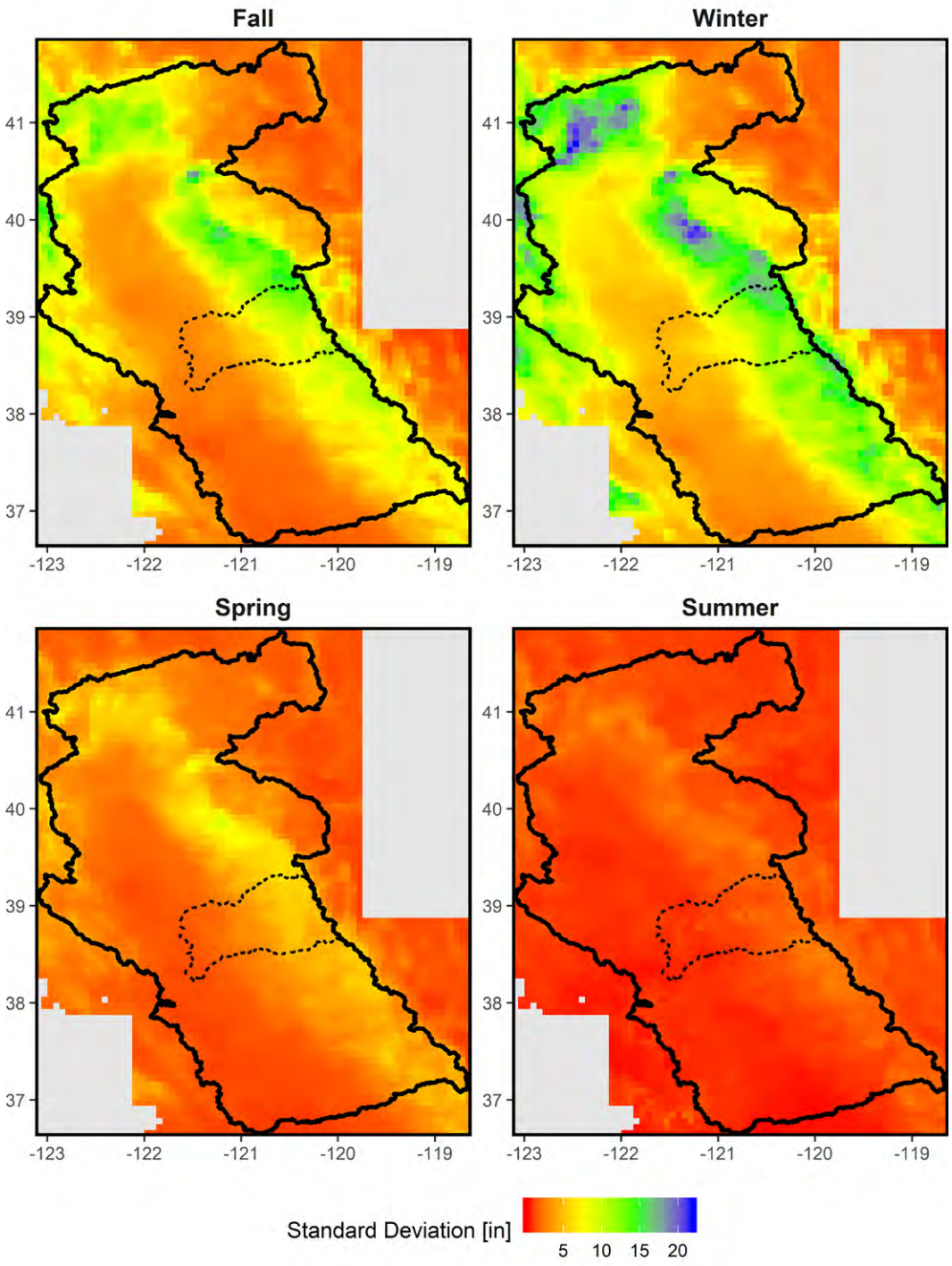

Figure 22. Spatial distribution of the standard deviation of seasonal precipitation across the CalSim3 domain. Standard deviations are computed for fall (October-November-December), winter (January-February-March), spring (April-May-June), and summer (July-August-September) for the period 1980-2009. The CalSim3 domain is delineated by the grey dashed line and the ARBS Study area is delineated by the solid black line.

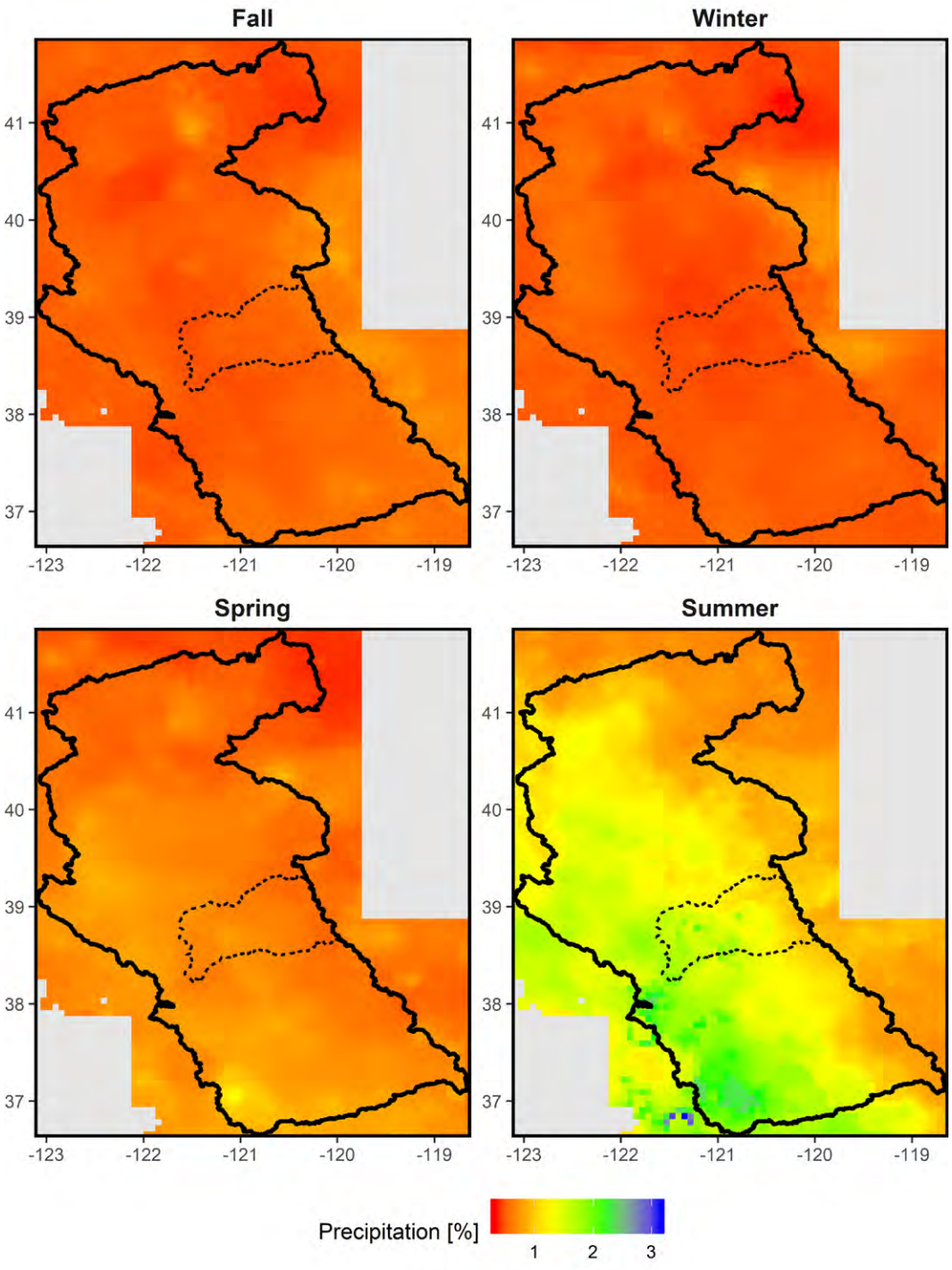

Figure 23. Spatial distribution of the coefficient of variation (mean / standard deviation) of seasonal precipitation across the CalSim3 domain. Coefficient of variation are computed for fall (October-November-December), winter (January-February-March), spring (April-May-June), and summer (July-August-September) for the period 1980-2009. The CalSim3 domain is delineated by the grey dashed line and the ARBS Study area is delineated by the solid black line.

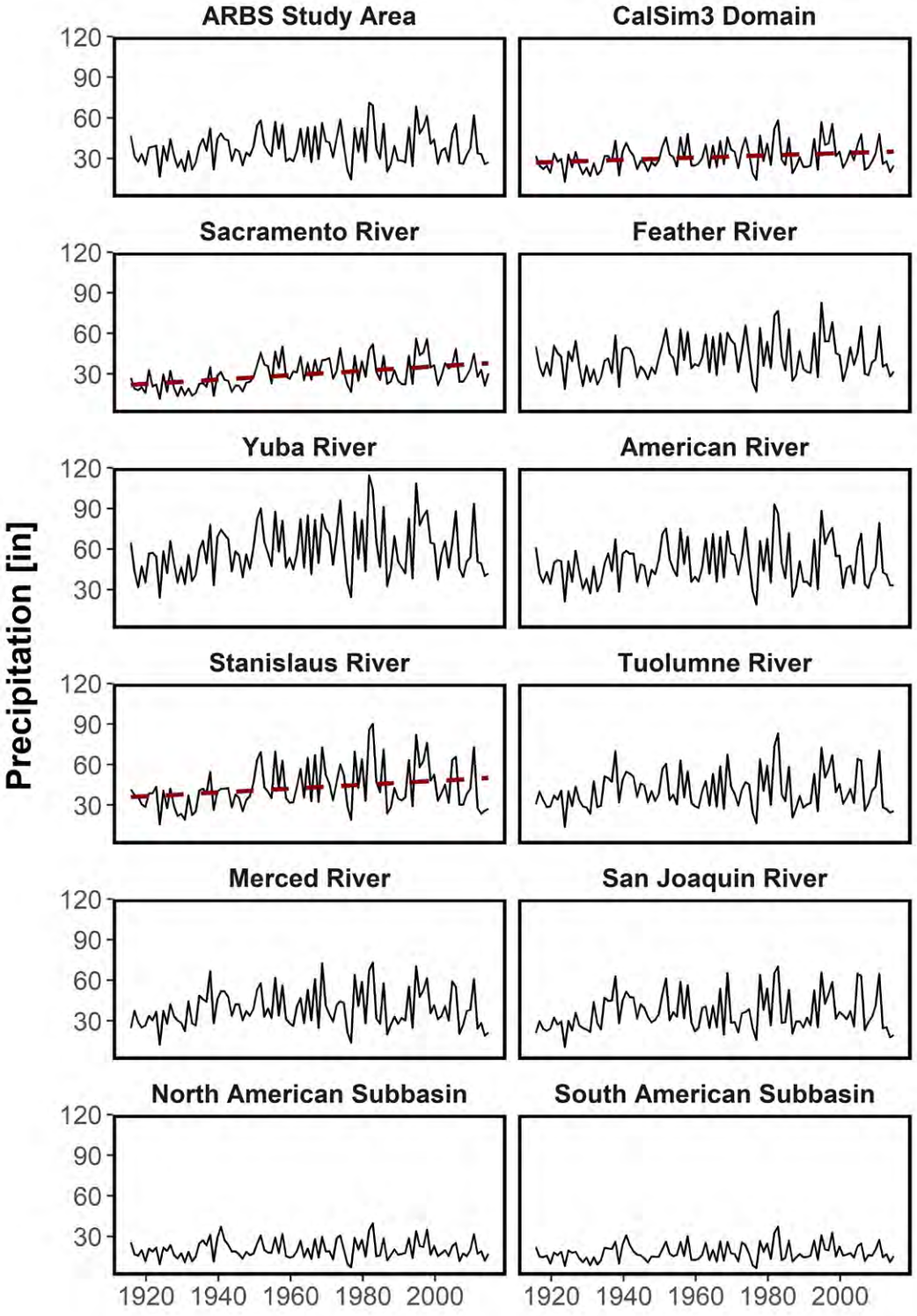

Figure 24. Timeseries of observed basin-average annual mean precipitation. Solid black line indicates water year totals; red dashed line indicate trends over the period 1915-2015; red lines are shown only if the trend is statistically significant.

3 Future Climate Projections

Climate change is driven by changes in atmospheric composition, namely increasing concentrations of greenhouse gasses and aerosols. Changes in atmospheric composition affect the earths energy balance—e.g., the reflection or absorption of energy from the sun, re-radiation of energy from the earth surface to the atmosphere, and movement of energy within the earth system—which in turn affect weather and climate at global, regional, and local scales (Lindsey 2009, IPCC 2013 [Physical Basis]).

Climate is a key driver of water supply and water demand. Precipitation, for example, drives runoff and infiltration, which in turn drive streamflow (surface water supply) and groundwater recharge (groundwater supply), respectively. Temperature, humidity, and wind speed also influence evapotranspiration (ET) from vegetation and evaporation from bare soil and open water. ET is a major driver of water demands in the Basin Study area, including water demands for irrigated agriculture and landscape irrigation in urban and residential areas. Temperature also affects whether precipitation falls as rain or snow and the timing of snowpack accumulation and melting, which in turn affects the amount and timing of snowmelt runoff. Snowmelt runoff is a critical source of water to the Central Valley Project and State Water Project. In addition to influencing water supplies and demands, weather and climate extremes also influence water management actions, such as flood control operations and drought response.

Because weather and climate conditions directly affect water supplies and demands, climate change directly affects the assumptions underlying water resources planning and decision making (Reclamation 2016 [Climate Projections]).

This section describes projections of future climate conditions in the ARBS study area and CalSim3 domain (see Figure 1). The climate projection dataset evaluated in this study is described in Section 3.1 and projected future climate conditions are described in Section 3.2.

3.1 Climate Projection Dataset

Analysis of projected future climate conditions in the American River Basin and development of climate scenarios for the ARBS are based on an ensemble of bias-corrected and spatially-downscaled climate projections. Global climate projections from the Coupled Model Intercomparison Project Phase 5 (CMIP5; Tayler et al 2009, Tayler et al 2012) were bias corrected and downscaled over the continental United States, southern Canada, and northern Mexico using the Localized Constructed Analogs (LOCA) method (Pierce et al. 2015). Bias-corrected and downscaled projections over the study region were obtained from the Downscaled CMIP3 and CMIP5 Climate and Hydrology Projections archive (Reclamation et al. 2018) hosted on the Lawrence Livermore National Laboratory Green Data Oasis (LLNL 2019). A

total of 64 bias-corrected and downscaled climate projections were used in the ARBS, including projections from 32 different global climate models (GCM) under two future climate scenarios.

Climate projections are typically developed by using global climate models[7] (GCM) to simulate changes in the earth's energy balance, and corresponding changes in weather and climate conditions, in response to projected changes in atmospheric composition. The NOAA National Weather Service (NWS) defines climate models as "mathematical model[s] for quantitatively describing, simulating, and analyzing the interactions between the atmosphere and underlying surface (e.g., ocean, land, and ice)" (NWS 2015). The NOAA Climate Prediction Center (CPC) further describes GCMs as computer models capable of reproducing the earth's weather patterns and that can be used to predict and analyze changes in global weather and climate (CPC 2015).

The World Climate Research Programme (WCRP) initiated CMIP in 1995 to coordinate international climate modeling efforts focused on better understanding the global climate system, including projected climate changes resulting from changes in atmospheric composition (WCRP 2015). A key focus of CMIP is facilitating the development, analysis, and application of global climate projections. To this end, CMIP has developed standards and guidelines to facilitate comparison of GCM results from scientists and research groups around the world. The U.S. Department of Energy's Program for Climate Model Diagnostics and Intercomparison (PCMDI) works closely with CMIP to compile GCM datasets from modeling centers around the globe and make them freely available to the scientific community (PCMDI 2015). The multi-model datasets developed by each phase of CMIP constitute the primary source of climate projections used by the international climate science community to evaluate climate change and its potential impacts (IPCC 2013 [Physical Basis]).

At the time this of this study, the CMIP5 Multi-Model Dataset was the best-available source of global climate projections for the 21st century.[8] The multi-model dataset includes climate projections from a total of 61 GCMs from 27 modeling centers representing 15 countries around the world (PCMDI 2015). CMIP5 projections of 21st century climate are based on two primary scenarios of future greenhouse gas and aerosol emissions, referred to as representative concentration pathways (RCP) 4.5 and 8.5. RCP 8.5 represents a "business as usual" future emissions trajectory where greenhouse gas concentrations continue to rise unchecked. RCP 4.5 represents a medium-level future emissions trajectory where greenhouse gas emissions peak around 2040 and decline thereafter. RCPs 4.5 and 8.5 have been widely used to evaluate climate change and its impacts around the globe. RCPs do not represent forecasts or projections of future atmospheric composition; rather, RCPs represent plausible future trajectories of atmospheric composition under various assumption of

[7] Throughout this technical memorandum, the term *global climate model* and acronym *GCM* are used generally to refer to numerical models of the global climate system, including general circulation models, global climate models, earth system models, and related classes of models.
[8] Initial climate projections from Phase 6 of the Climate Model Intercomparison Project (CMIP6) became available in January 2019. At the time of writing, climate projections for CMIP6 are still being completed.

population growth, economic growth, technology development, and governmental policies regarding greenhouse gas emissions.

The spatial (grid) resolutions of GCM-based climate projections from the CMIP5 multi-model dataset is typically on the order of one to two degrees latitude by one to two degrees longitude, or roughly 110-220 kilometers (km) by 110-220 km over mid-latitudes. Local weather and climate conditions, by contrast, vary significantly across a degree of latitude or longitude due to variations in topography, land cover, and many other factors that affect local climate. In addition, GCM-based projections generally exhibit biases in simulated climate conditions that stem largely from the coarse spatial resolution of GCMs and the use of simplified parameterizations to represent physical processes that cannot be explicitly represented at the GCM grid scale. Coarse spatial resolution and biases limit the direct application of GCM-based climate projections to local and basin-scale analyses.

A broad range of methods have thus been developed to bias-correct and downscale GCM-based climate projections to support local and basin-scale analyses, planning, and decision making. Climate projections selected for the ARBS were downscaled using the Localized Constructed Analogs (LOCA) downscaling procedure. The LOCA procedure uses an the L2015 grid observational dataset to develop relationships between large-scale and local-scale weather and climate conditions. These relationships are then used "downscale" coarse-resolution GCM projections onto a finer resolution grid—i.e., observed relationships between large-scale and local-scale weather and climate are used to estimate projected climate conditions on a finer-resolution grid from coarser-resolution GCM projections (Pierce et al. 2015).

The LOCA procedure was used to downscale GCM projections to a finer resolution of 1/16 degree latitude by 1/16 degree longitude (approximately six kilometers by six kilometers). The LOCA procedure was applied at a daily timestep. Compared to other downscaling methods, the LOCA procedure has been shown to preserve regional patterns of projected changes in precipitation and temperature. In addition, the LOCA procedure better preserves extreme hot days and heavy precipitation events, which are often damped by other downscaling methods.

An ensemble of LOCA projections is available from Dr. David Pierce at the Scripps Institution of Oceanography. The LOCA ensemble includes bias-corrected and downscaled projections of daily precipitation, daily minimum temperature, and daily maximum temperature for the period 1950-2099. LOCA data over the period 1950-2005 reflect GCM simulations driven with historical atmospheric conditions, including estimate historical greenhouse gas and aerosol concentrations. LOCA data over the period 2006-2099 reflect GCM simulations driven with atmospheric conditions from two future emissions scenarios (RCP 4.5 and RCP 8.5). Projections are provided at a spatial resolution of 1/16 degree latitude by 1/16 degree longitude and cover the continental United States and portions of Mexico and Canada. The LOCA ensemble includes climate projections from 32 GCMs under the RCP4.5 and RCP8.5 emissions scenarios for a total of 64 climate projections. The LOCA ensemble has been used by the California Water Commission (CWC) and California Department of Water Resources (DWR) as the primary source of climate projection information in several recent studies, including the Water Storage

Investment Program (WSIP) and California's Fourth Climate Change Assessment (CWC 2016, Pierce et al. 2018).

3.2 Projected Future Climate Conditions

Projected future climate conditions were evaluated and characterized based on the LOCA ensemble of downscaled climate projections described above in Section 3.1 . Similar to observed historical climate conditions, projected future climate conditions were evaluated on a 1/16th degree grid and averaged over the ARBS study area, the CalSim3 domain, and selected basins. Selected basins considered in evaluating projected climate conditions are illustrated in Figure 12.

3.2.1 Future Temperature

All LOCA projections indicate a significant increase in annual and seasonal average temperatures over the ARBS study area and CalSim3 domain by the end of the 21st century. The range of projected seasonal and annual average temperature are shown in Figure 25. The ensemble median of 64 LOCA projections suggest that increases in temperature over the ARBS study area are greatest during the summer months, with summer temperature increasing by approximately 7.2°F by the end of the 21st century (Table 2). Projected warming is least for winter months, with a median projected increase of 4.9°F by the end of the century. Projections of daily maximum and minimum temperatures suggest similar seasonal trends, with the most warming occurring during summer and the least during winter. Maximum temperatures are projected to increase more than minimum temperatures during all seasons, with the largest projected increase of 7.3 °F during the summer months.

All LOCA projections indicate that warming will be largely consistent throughout the region. The spatial distribution of projected change in annual average temperature over the 21st century from each of the 64 LOCA projections is shown in Figure 26. Several projections indicate slightly greater warming over the Sierra Nevada mountains along the eastern border of the CalSim3 domain, and two projections showing greater warming over the southeaster portion of the region. However, most projections indicate that warming will be nearly uniform over the region.

While all 64 projections indicate generally uniform warming over the region, Figure 26 shows considerable variability in the magnitude of projected warming between individual projections. Projected warming by the end of the 21st century ranges from approximately 2°F to 10°F. The range of projected warming reflects uncertainties in future atmospheric composition (i.e., differences between RCP4.5 and RCP8.5) as well as uncertainties how global, regional, and local climate will respond to future changes in atmospheric composition.

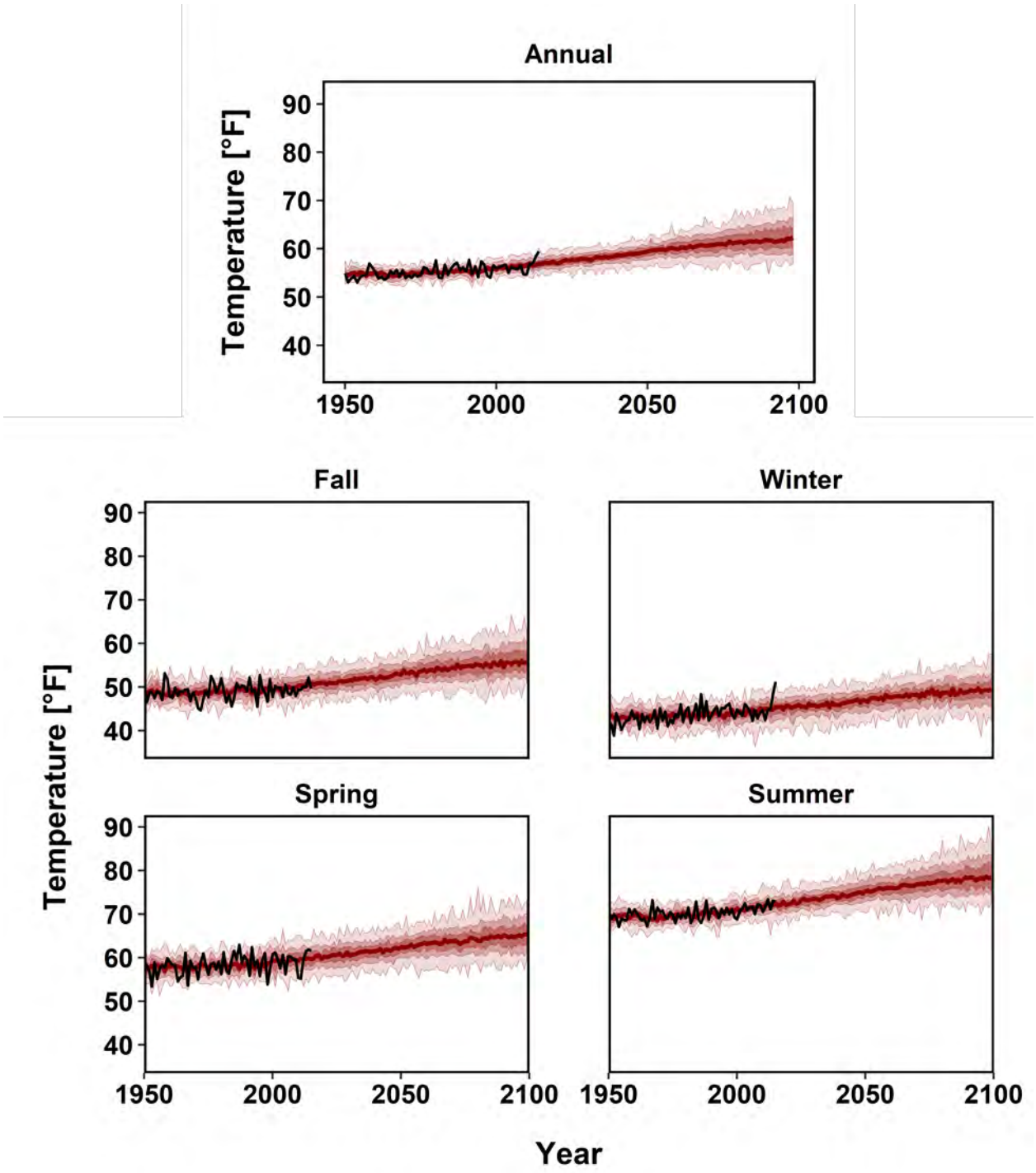

Figure 25. Timeseries of basin-average annual and seasonal average temperature [°F] over the ARBS study area for the period 1950-2099. The dark red line shows the ensemble median; dark red shading indicates the range between ensemble 25th and 75th percentile values; medium red shading indicates the range between ensemble 10th and 90th percentile values; light red shading indicates the ensemble maximum and minimum values; black line shows observed historical values.

Table 2. Ensemble median projected change in basin-average precipitation and temperature over the ARBS Study Area from 1980-2009 to 2070-2099

	Precip		Tavg	Tmax	Tmin
	(in)	(%)	(°F)	(°F)	(°F)
Fall	-0.78	-6.0	+5.8	+6.1	+5.5
Winter	+0.92	+4.7	+4.9	+5.0	+4.8
Spring	-0.62	-11.9	+5.8	+6.3	+5.1
Summer	+0.07	+10.4	+7.2	+7.3	+7.0

Notes:

- *Precip = seasonal precipitation, Tavg = seasonal mean of daily average temperature, Tmin = seasonal mean of daily minimum temperature, Tmax = seasonal mean of daily maximum temperature.*
- *Projected change was calculated by comparing the basin-average ensemble-median projection for the ARBS study area between the historical period 1980-2009 and future period 2070-2099.*
- *Values for precipitation are given as the absolute change in inches and the percent change; values for temperature are given as absolute change in degrees Fahrenheit (°F)*

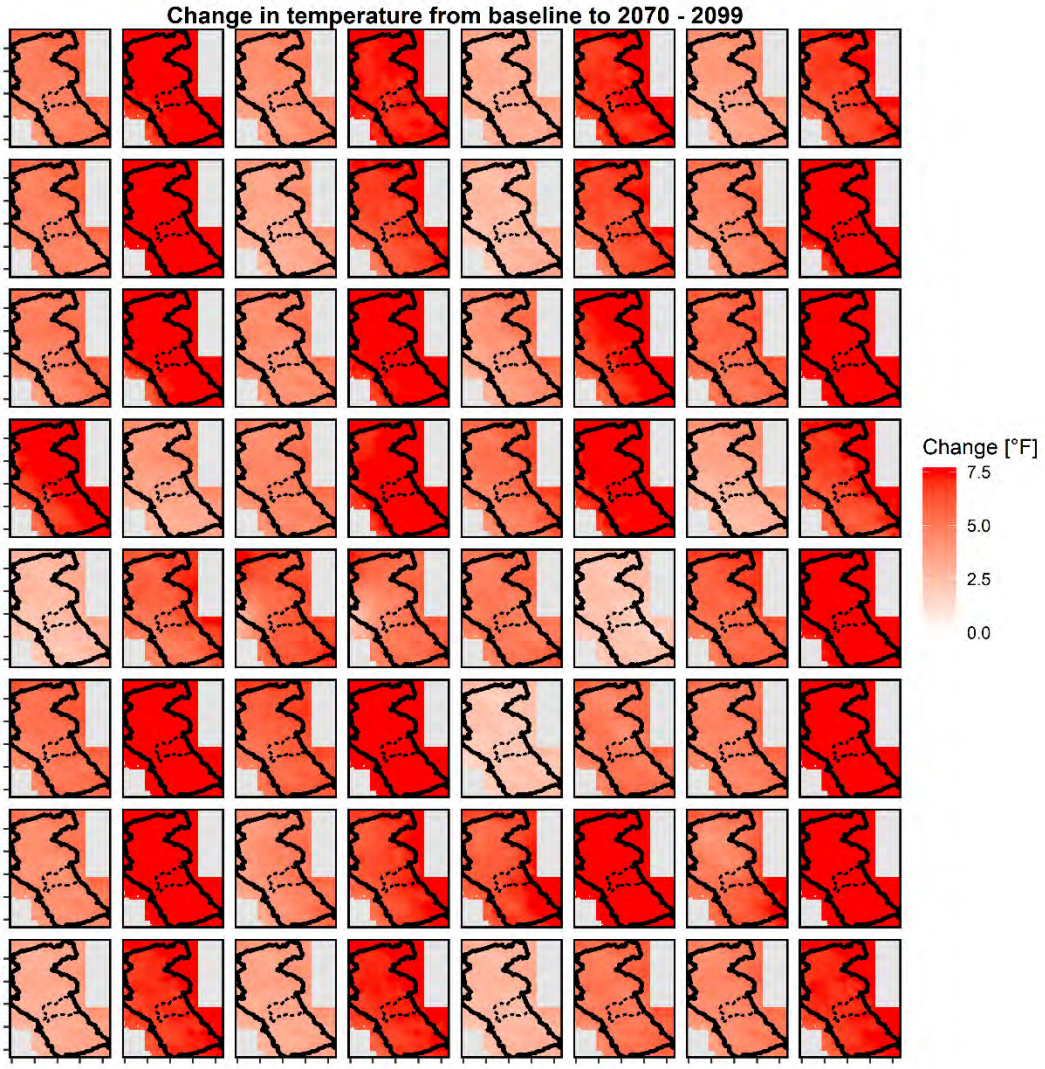

Figure 26. Spatial distribution of projected change in annual average temperature between historical (1980–2009) and future (2070–2099) period for each LOCA projection. The CalSim3 domain is delineated by the black solid line and the ARBS study area is delineated by the black dashed line. Names for each individual projection can be found in Appendix Table A.3.

3.2.2 Future Precipitation

In contrast to projected temperature, there is no clear trend in projected precipitation over the ARBS study area or the CalSim3 domain. Projections of basin-average annual and seasonal precipitation over the ARBS study area are shown in Figure 27. Approximately half of the LOCA projections indicate an increase in annual precipitation and half indicate a decrease. The ensemble median exhibits no trend in projected annual precipitation over the 21st century. The lack of consistency in projected annual precipitation highlights the large uncertainty in future precipitation over this region.

The large uncertainty in projected annual precipitation is further illustrated in Figure 28, which shows the spatial distribution of projected change in annual precipitation over the 21st century from each of the 64 LOCA projections. Several projections indicate increases or decreases in annual precipitation of more than 25% over portions of the region. In addition, some projections indicate a projected increase over some parts of the region and a projected decrease over other parts. The large uncertainty in projected precipitation changes suggests that using multiple climate projections or scenarios is required to represent the potential impacts of climate change on water supplies within the study region. This is consistent with recommendations from the California DWR Climate Change Technical Advisory Group and California's Fourth Climate Change Assessment to consider multiple climate projections or scenarios to reflect uncertainties in future climate projections (DWR 2015 [CCTAG]; Pierce et al. 2018).

Despite the lack of clear trend in projected annual precipitation, trends in projected seasonal precipitation are more apparent (Figure 27 and Table 2). By the end of the 21st century, the ensemble median indicates average fall precipitation will decrease by approximately 6% while average winter precipitation increases by approximately 5%. The ensemble median indicates larger relative changes for the drier seasons, with projected spring precipitation decreasing by approximately 12% and projected summer precipitation increasing by approximately 10%. Overall, these opposing seasonal projected trends culminate in little projected change in annual precipitation over the ARBS study area. However, it should be noted that while projected changes in spring and summer precipitation are large relative to seasonal means (larger percent change), precipitation during spring and summer is generally low. Projected changes in spring and summer precipitation therefore do not have a substantial impact on water supplies or demands within the study area. Projected changes in fall and winter precipitation, while small relative to seasonal means, have a much greater impact on water resources within the study area.

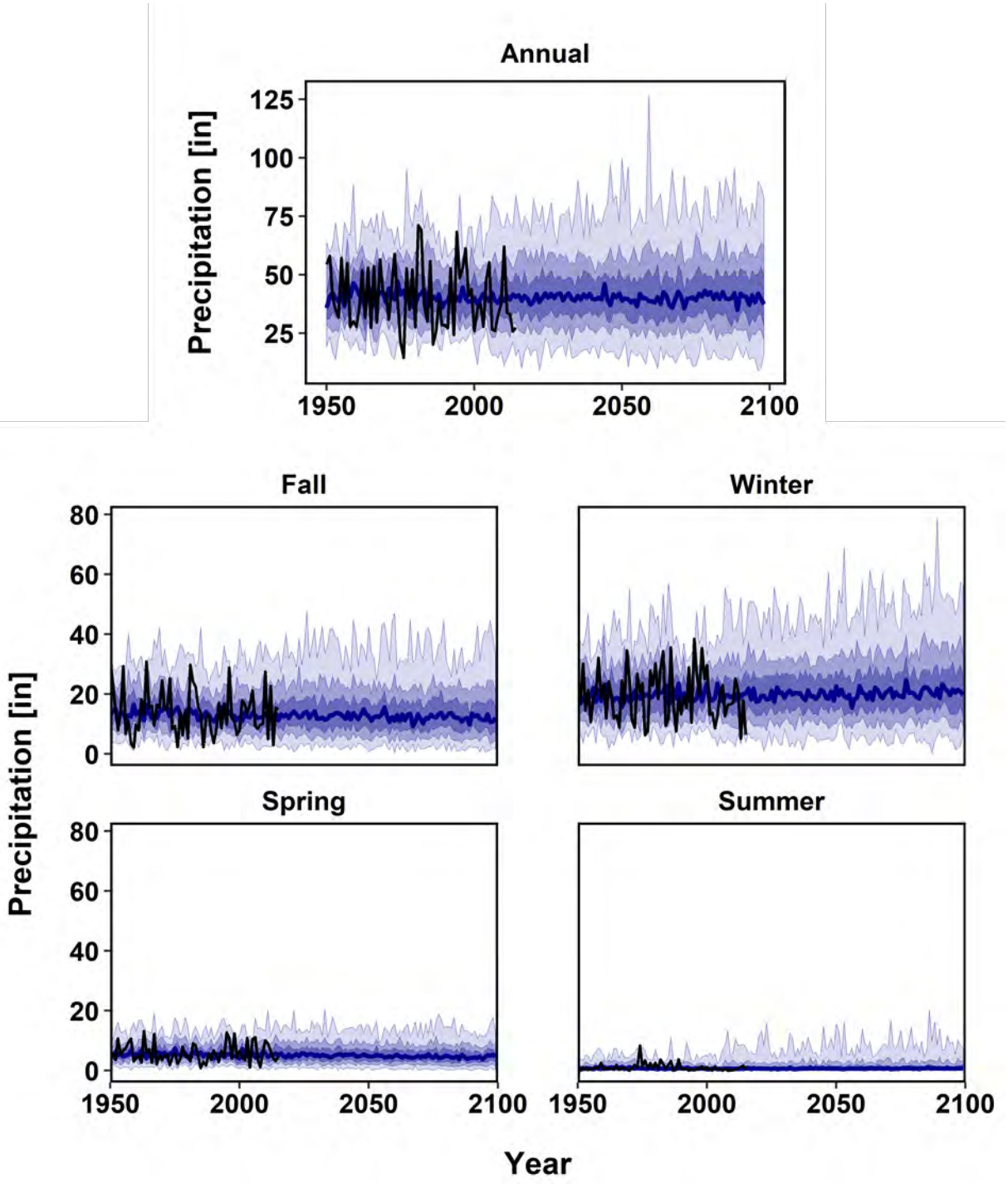

Figure 27. Timeseries of area-weighted, basin-average seasonal and annual average surface temperature over the ARBS Basin Study area for the period 1950-2099. Dark blue line shows the ensemble median; dark blue shading indicates the range between ensemble 25th and 75th percentile values; medium blue shading indicates the range between ensemble 10th and 90th percentile values; light blue shading indicates the maximum and minimum ensemble values; black line shows observed Livneh historical values.

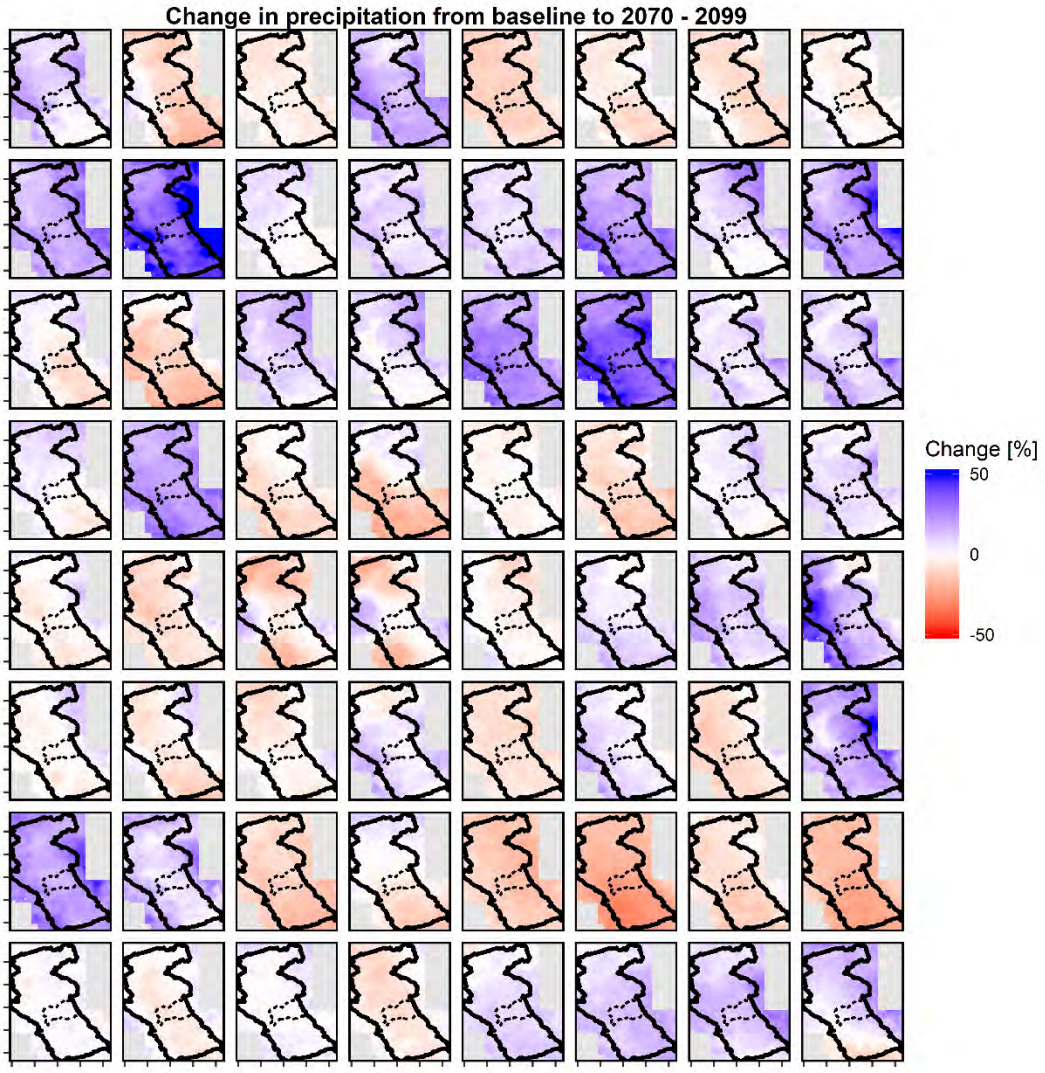

Figure 28. Spatial distribution of the change in annual precipitation between historical (1980 – 2009) and future (2070 – 2099) time periods for each individual LOCA projection. Axes are longitudinal and latitudinal coordinates. The CalSim3 domain is delineated by the black solid line and the ARBS study area is delineated by the black dashed line. Names for each individual projection can be found in Appendix Table A.3.

4 ARBS Climate Scenarios

A baseline climate scenario and a suite of future climate scenarios were developed as the basis for analyzing future water supplies, demands, and management in the ARBS. Climate scenarios were developed using the ensemble-informed hybrid-delta method (HDe; Reclamation 2010). The HDe scenario methodology is consistent with several previous studies carried out by Reclamation and the State of California (e.g., Reclamation et al. 2016 [Niabrara], Reclamation et al. 2016 [Republican], Reclamation et al. 2016 [Klamath]).

In the context of water resources planning, climate scenarios provide several advantages compared to direct use of downscaled climate projections. Climate scenarios distill the range of uncertainty across a large ensemble of GCM-based climate projections into a relatively small number of scenarios for detailed analysis. Climate scenarios thus allow for consideration of uncertainty in future climate conditions while significantly reducing the number of future conditions that must be modeled and analyzed. Climate scenarios can also be developed to align with specific planning horizons of interest, such as defined levels of development or build-out conditions. Lastly, the HDe methodology retains the sequencing of observed historical climate variability—e.g., droughts and pluvials—but with climate conditions adjusted to reflect projected future climate conditions. Retaining historical climate variability facilitates comparison of drought and surplus conditions between historical climate and future climate scenarios. In addition, retaining historical climate variability reduces potential biases in GCM-simulated interannual and decadal variability, which is not explicitly addressed in downscaling and bias correction procedures.

The ARBS climate scenarios were developed based on the merged Livneh dataset (Section 2.1) and the LOCA ensemble of downscaled climate projections (Section 3.1). The baseline scenario was developed by removing observed trends in precipitation and temperature from the merged Livneh dataset such that monthly and annual mean precipitation and temperature over the full period of the baseline scenario (1915-2015) are consistent with observed historical means over specified historical reference period (1980-2009). Future climate scenarios were then developed by adjusting the baseline scenario to reflect projected changes in precipitation and temperature between the historical reference period (1980-2009) and three future periods: 2040-2069, 2055-2084, 2070-2099. For each future period, a suite of five climate scenarios was developed to reflect the uncertainty in projected climate change across the ensemble of 64 LOCA projections analyzed in the ARBS (see Section 3). The five climate scenarios for each future time period include warm-wet (WW), warm-dry (WD), hot-wet (HW), hot-dry (HD), and central tendency (CT) scenarios.

The baseline scenario represents a 101-year record of observed historical climate variability that is consistent with monthly and annual mean climate conditions over the historical reference period (1980-2009). Similarly, each future climate

scenario represents a 101-year record of climate variability that reflects projected changes in monthly and annual mean climate conditions between the historical reference period and a given future period.

This section describes the climate scenarios developed to represent projected future climate conditions over the ARBS study area and surrounding region. Climate scenarios are used as the basis for developing hydrology scenarios, which in turn are used to analyze future water supplies, demands, and management in the ARBS. The HDe climate scenario methodology is described in Section 4.1 and the resulting climate scenarios are characterized in Section 4.2.

4.1 Climate Scenario Methodology

The ensemble-informed hybrid-delta (HDe) climate scenario methodology was developed by Reclamation (2010) as a basis for evaluating the impacts of projected climate change on water supplies, demands, and management. The HDe methodology has since been applied in numerous studies, including several Impact Assessments and Basin Studies carried out under the WaterSMART Program (e.g., Reclamation et al. 2016 [Niabrara], Reclamation et al. 2016 [Republican], Reclamation et al. 2016 [Klamath]).

The HDe methodology involves adjusting a dataset of observed historical precipitation and temperature to remove historical trends, then adjusting this de-trended dataset to reflect projected climate changes between a historical reference period and a selected future period. The de-trended observed historical dataset is referred to as the baseline scenario. The baseline scenario reflects observed historical climate variability over the period 1915-2015, adjusted such that monthly and annual mean climate conditions are consistent with the historical reference period (1980-2009). Each future scenario is based on projected climate change derived from a subset (or sub-ensemble) of climate projections. Precipitation and temperature from the baseline scenario are adjusted by applying quantile-based climate change factors that represent projected changes in the probability distributions of precipitation and temperature between the historical and future time periods. Similar to the baseline scenario, future climate scenarios reflect historical climate variability over the period 1915-2015. However, future scenarios are adjusted such that monthly and annual mean climate conditions reflect projected climate conditions during a selected future period (2040-2069, 2055-2084, or 2070-2099).

The HDe methodology consists of three primary steps: selection of climate projections for each scenario; development of quantile-based climate change factors; and application of quantile-based climate change factors to an observed historical climate dataset. Each of these primary steps involves several interim steps as summarized below.

4.1.1 Selection of Climate Projection Subsets

Each HDe future climate scenario is developed based on a subset of downscaled and bias-corrected climate projections from the LOCA ensemble (see Section 3.1). The projections in each subset are determined based on the range of projected changes in basin-average annual mean precipitation and temperature over the ARBS study area between an historical reference period and a selected future period.

The subset selection process was repeated three times, once for each of the selected future time periods (2040-2069, 2055-2084, and 2070-2099). The subset of LOCA projections used in a given scenario may differ between time periods—i.e., the subset of projections used in the CT scenario for 2040-2069 may differ from the subset used in the CT scenario for 2070-2099. Subset selection was based on projected changes in basin-average annual precipitation and temperature over the ARBS study area. Subsequent steps in the HDe methodology were carried out for each individual grid cell based on the subset of projections identified for each scenario—i.e., the same subset of LOCA projection is used at each grid cell throughout the CalSim3 domain.

Each step of the subset selection procedure is described below:

- *Compute Basin-Average Precipitation and Temperature*

  First, timeseries of basin-average annual precipitation and temperature over the ARBS study area are computed for each of the 64 LOCA projections. Basin-averages are computed by taking the area-weighted average of gridded precipitation and temperature over the ARBS study area. This step results in 64 timeseries of basin-average precipitation and 64 timeseries of basin-average temperature (one timeseries of precipitation and temperature for each LOCA projection).

- *Compute Period-Average Precipitation and Temperature*

  Next, timeseries of basin-average annual precipitation and temperature are averaged over the selected historical reference period and future analysis periods. ARBS climate scenarios were developed using the historical reference period 1980-2009 and three future analysis periods: 2040-2069, 2055-2084, and 2070-2099. Period averages are computed as the arithmetic mean of basin-average annual precipitation and temperature over each period. This step results in 64 period averages of basin-average precipitation and temperature for each of the selected time periods.

  Figure 29 and Figure 30 show boxplots of period-averaged basin-average annual precipitation and annual mean temperature over the ARBS study area from the 64 downscaled and bias-correct climate projections in the LOCA ensemble. Figure 29 indicates that while the range of precipitation

increases across time periods from the historical reference period (1980-2009) to the end of the 21st century (2070-2099), the ensemble median annual precipitation (thick horizontal line within each box) shows little change between periods. In contrast, Figure 30 shows that both the ensemble median and the range of annual mean temperatures across the LOCA ensemble increase substantially between periods.

- *Compute Projected Changes in Precipitation and Temperature*

  Projected changes in period-average basin-average precipitation and temperature are computed for each projection for each future time period. For each LOCA projection, the projected change in temperature is computed as the simple difference between the period-average temperature over a given future period and over the historical reference period (future average minus historical average). The projected change in precipitation is computed as the percent change in period-average precipitation over a given future period and over the historical reference period. This step results in 64 projected changes in period-average basin-average precipitation and temperature for each future time period.

  Figure 31 Figure 32 show boxplots of projected changes in period-average basin-average annual precipitation and annual mean temperature over the ARBS study area from the 64 downscaled and bias-correct climate projections in the LOCA ensemble. Projected changes in temperature are computed as the difference (°F) in period-averages between each future period and the historical reference period; projected changes in precipitation are computed as the percent difference (%) between each future period and the historical reference period. Figure 31 indicates that while projected changes in basin-average precipitation range from a decrease of more than 25% to an increase of more than 25%, the ensemble-median projected change is close to zero for all future periods. Figure 32 illustrates the broad range of projected changes in temperature across the LOCA ensemble, as well as the increase in projected change over the 21st century. Projected changes range from less than 0.5°F to nearly 4°F for the future period 2040-2069 and from approximately 1°F to more 6°F for the future period 2070-2099.

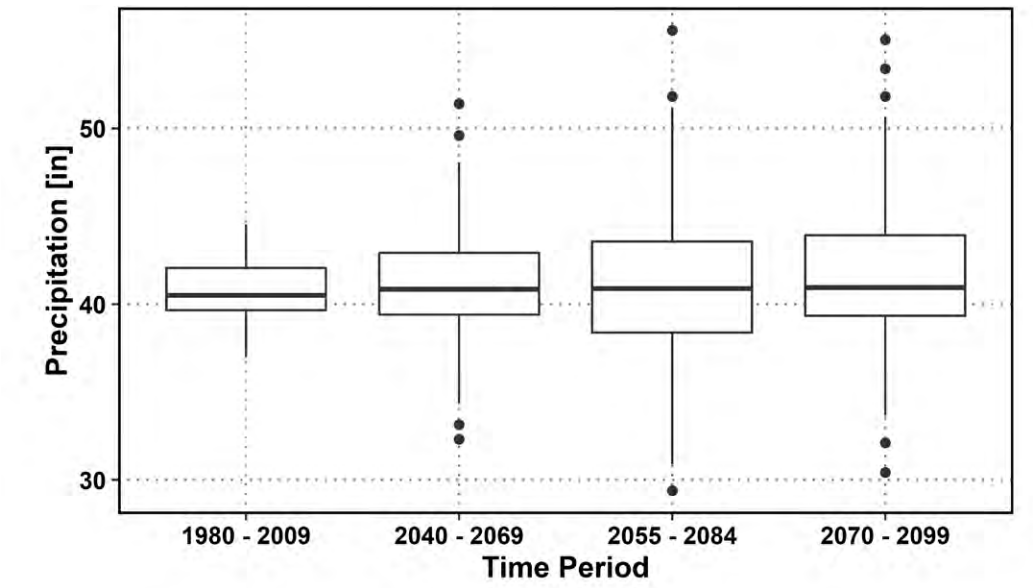

Figure 29: Boxplots of period-averaged basin-average annual precipitation (inches) over the ARBS Study Area for all 64 LOCA climate projections.

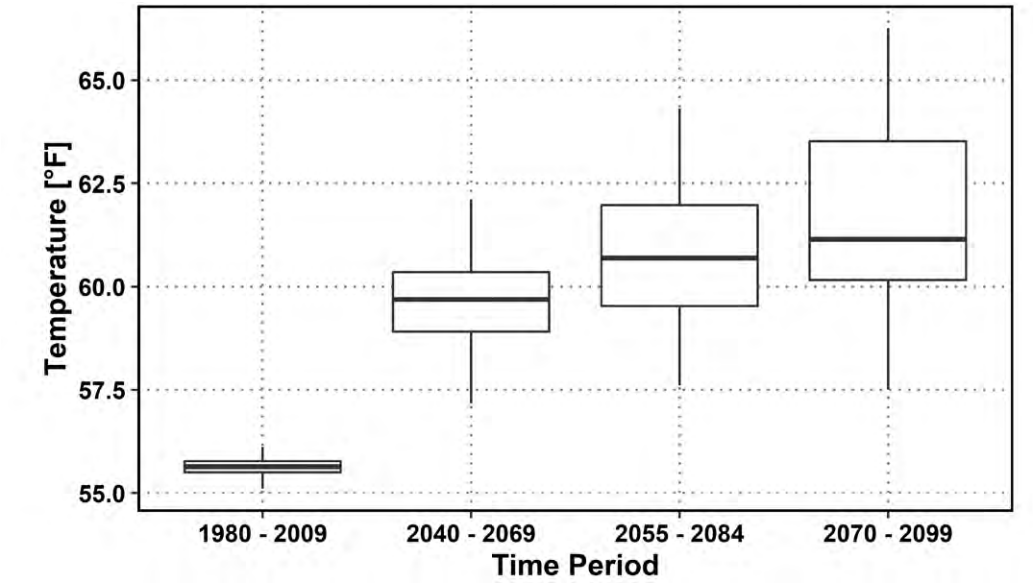

Figure 30: Boxplots of period-averaged basin-average annual mean temperature (°F) over the ARBS Study Area for all 64 LOCA climate projections.

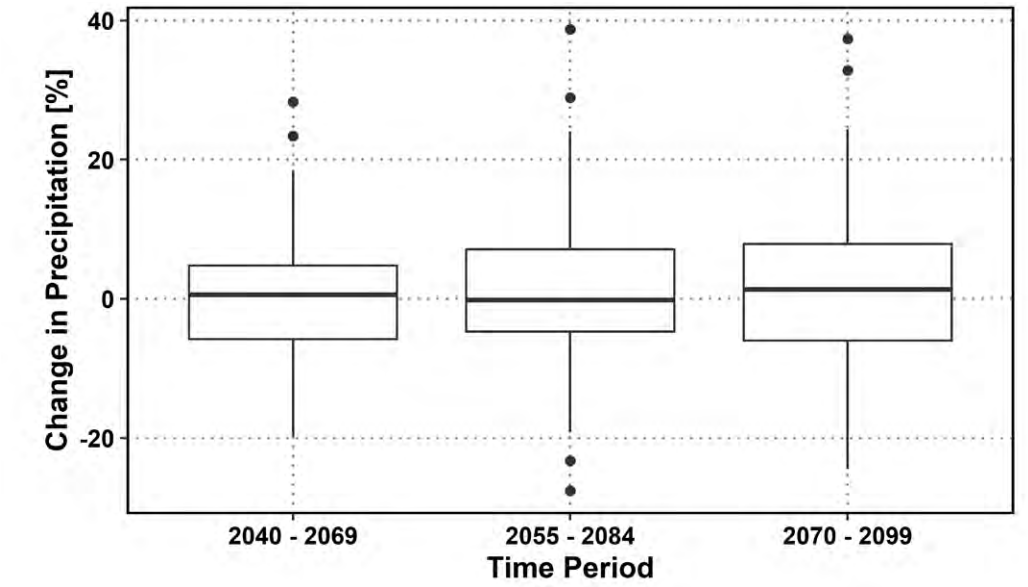

Figure 31: Boxplots of projected change (percent) in period-average basin-average annual precipitation over the ARBS Study Area between the historical reference period (1980-2009) and future time periods for all 64 LOCA climate projections.

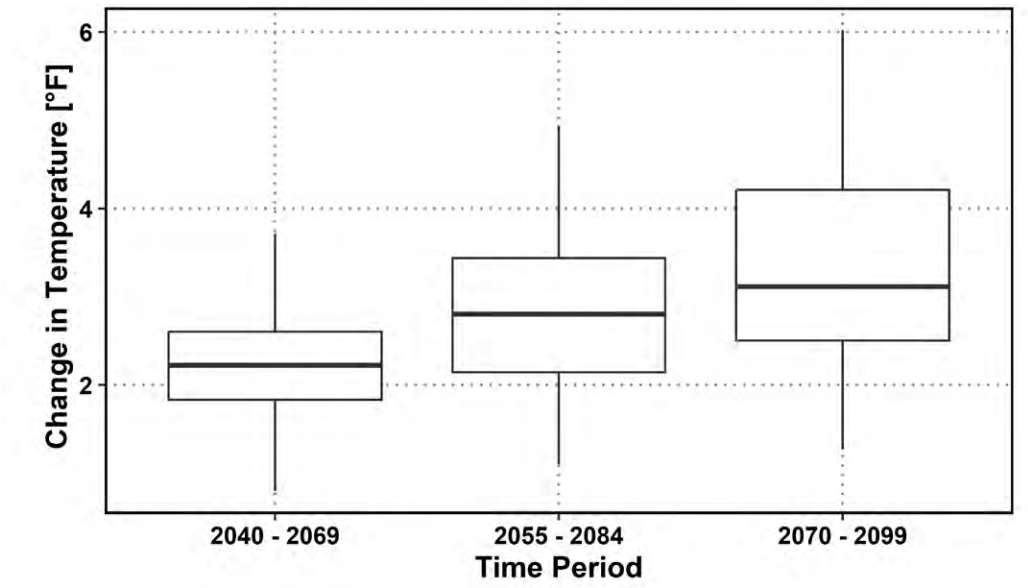

Figure 32: Boxplots of projected change (°F) in period-average basin-average annual mean temperature over the ARBS Study Area between the historical reference period (1980-2009) and future time periods for all 64 LOCA climate projections.

- *Compute Percentiles of Projected Changes in Precipitation and Temperature*

  The 10th, 50th, and 90th percentiles of projected changes in period-average basin-average precipitation and temperature are then computed from the set of 64 projected changes (as computed in the previous step). The 10th percentile value represents the lower end of the range of projected changes in basin-average precipitation and temperature; the 50th percentile (median) value represents the middle of the range of projected changes; and the 90th percentile represents the upper end of the range of projected changes. For the ARBS study area, the 10th percentile reflects a relatively small projected increase in basin-average temperature (less warming) and a relatively large projected decrease in basin-average precipitation (drier conditions) between the historical reference period and a given future period. Conversely, the 90th percentile reflects a relatively large increase in basin-average temperature (more warming) and a relatively large increase in basin-average precipitation (wetter conditions).

- *Identify Subset of Projections for Each Climate Scenario*

  Lastly, the subset of projections used each future scenario is selected based on the proximity of projected changes in precipitation and temperature to the selected percentile values computed in the previous step. The method used to select the subset of projections for each future scenario is illustrated in Figure 33.

  Figure 33 shows a scatterplot of the projected change in period-average basin-average annual temperature (abscissa or x-axis) and precipitation (ordinate or y-axis) over the ARBS study area for each of the 64 LOCA projections between the future period 2070-2099 and the historical reference period 1980-2099. Each of the 64 points in Figure 33 represents the projected change in temperature and precipitation for one projection from the LOCA ensemble.

  The horizontal dotted lines in Figure 33 represent the 10th (lower dotted line) and 90th (upper dotted line) percentiles of the range of projected changes in annual temperature computed in the previous step; the horizontal thick dashed line represents the 50th percentile (median) projected change in annual temperature. The vertical dotted lines represent the 10th (left dotted line) and 90th (right dotted line) percentiles of the range of projected changes in annual precipitation computed in the previous step; the vertical thick dashed line represents the 50th percentile (median) projected change in annual precipitation.

  A subset of six LOCA projections was selected for each of the five ARBS scenarios. Subsets were selected based on the projections nearest to the intersection of selected percentiles as follows:

- Warm-Dry Scenario (WD): 10^{th} percentile precipitation
  10^{th} percentile temperature
- Warm-Wet Scenario (WW): 90^{th} percentile precipitation
  10^{th} percentile temperature
- Central Tendency Senario (CT): 50^{th} percentile precipitation
  50^{th} percentile temperature
- Hot-Dry Scenario (HD): 10^{th} percentile precipitation
  90^{th} percentile temperature
- Hot-Wet Scenario (WW): 90^{th} percentile precipitation
  90^{th} percentile temperature

For example, projections were selected for the central tendency (CT) scenario based on the distance between each point in Figure 33 and the point represented by the intersection of the 50^{th} percentile projected change in annual temperature and the 50^{th} percentile projected change in precipitation—i.e., between each point in Figure 33 and the intersection of the two thick dashed lines. After the distance between each point and this intersection was computed, the six points nearest to the intersection were identified and selected as the basis for the CT scenario for future period 2070-2099. Subsets were similarly selected for the HD, HW, WD, and WW scenarios based on the distance between each point and the respective percentile intersections listed above.

Due to the different units of the abscissa and ordinate, the distance between points is computed as the Mahalanobis distance rather than the Euclidian distance. The Mahalanobis distance is a unitless and scale-invariant measure of distance that takes into account covariance within a dataset.

The resulting subsets for each scenario are indicated by the color of the points Figure 33 and the corresponding polygons. Projections selected for the WD scenario are represented by purple points and the purple polygon. Projections selected for the WW scenario are in blue; projections selected for the CT scenario are in green; projections selected for the HD scenario are in red; and projections selected for the HW scenario are in brown.

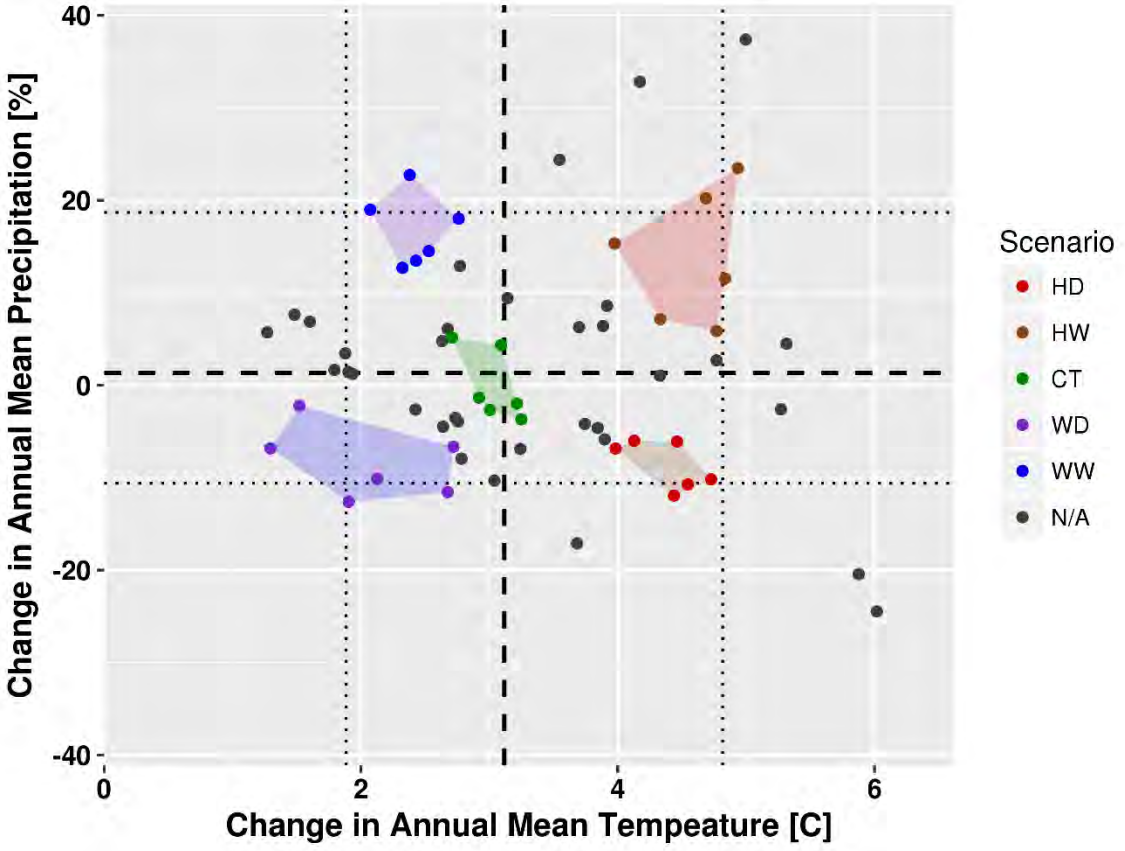

Figure 33: Scatterplot of projected changes in period-average basin-average temperature (abscissa) and precipitation (ordinate) between future period 2070-2099 and historical reference period 1980-2009. Each point represents one projection from the LOCA ensemble; the color of each point represents the scenario to which that point is assigned (red = HD; brown = HW; green = CT; purple = WD; blue = WW; black = N/A). Vertical dotted lines represent the 10th and 90th percentiles of projected changes in temperature; horizontal dotted lines represent the 10th and 90th percentiles of projected changes in precipitation. Vertical thick dashed lines represent the 50th percentile (median) projected change in temperature; horizontal thick dashed line represents the 50th percentile (median) projected change in precipitation.

4.1.2 Development of Quantile-Based Climate Change Factors

HDe climate scenarios are developed by adjusting the baseline climate scenario to reflect projected changes in precipitation and temperature between the historical reference period (1980-2009) and each selected future period (2040-2069, 2055-2084, and 2070-2099). Projected changes in precipitation and temperature are represented by quantile-based change factors, where change factors represent the projected change in the probability distributions of precipitation and temperature between historical and future periods.

Quantile-based change factors are developed for each scenario and future time period from the corresponding subset of LOCA projections (see Section 4.1.1). Change factors are computed and applied on a monthly basis to capture differences in projected climate change during different parts of the year. While

the subset of LOCA climate projections used in each future climate scenario is selected based on projected changes in basin-average, annual-mean climate over the ARBS study area, change factors are computed and applied on a grid-cell by grid-cell basis to capture spatial differences in projected climate change over the region.

The procedure used to develop quantile-based change factors is described below. The procedure is applied independently for each future time period. For each future time period, the procedure is applied independently at each 1/16° by 1/16° LOCA grid cell throughout the CalSim3 domain (see Figure 1).

- *Compute Monthly Precipitation and Temperature*

  The first step in developing quantile-based change factors is to compute monthly precipitation and temperature for each of the LOCA projections selected for use in each future climate scenario (see Section 4.1.1). Change factors are computed and applied on a monthly basis to reflect differences in projected climate change during different parts of the year. LOCA climate projections are provided on a daily timestep; projections are therefore aggregated to a monthly timescale for development of future scenarios. Monthly precipitation is computed at each grid as the total accumulated precipitation over each month at that cell. Monthly temperatures are computed separately for maximum and minimum temperatures: monthly maximum temperature is computed as the average of daily maximum temperature over each month at a given grid cell, and monthly minimum temperature is computed as the average of daily minimum temperature over each month. In addition, monthly mean diurnal temperature range (DTR) is computed as the average of daily DTR over each month, where the daily DTR is the difference between daily maximum and minimum temperatures on a given day.

  This step results in timeseries of monthly precipitation, monthly mean maximum temperature, monthly mean minimum temperature, and monthly mean DTR at each grid cell for each LOCA climate projection.

- *Partition Precipitation and Temperature by Month and Time Period*

  In order to develop monthly change factors, the timeseries of monthly precipitation and temperature values must be partitioned by month. This is achieved by converting monthly precipitation and temperature values from a timeseries (one-dimensional vector) into a two-dimensional matrix, with each row of the matrix containing monthly values over a single year and each column containing values for a single month over each year in the record (i.e., rows represent years, columns represent months).

  The resulting matrices of monthly precipitation and temperature are then partitioned into two time periods—one for the historical reference period

(1980-2009) and one for the future time period of interest (2040-2069, 2055-2084, or 2070-2099). Monthly precipitation and temperature values are partitioned between the historical and future periods as a precursor to computing projected changes between these periods.

This step results in two matrices of monthly values—one of the historical reference period and one for the selected future period—for each climate variable for each grid cell for each LOCA climate projection.

- *Pool Monthly Precipitation and Temperature over LOCA Subsets*

  Each HDe future climate scenario reflects the projected change in climate over a subset of LOCA climate projections. In order for a single HDe scenario to reflect more than one LOCA climate projections, the matrices of monthly climate values from individual LOCA projections developed in the previous step are pooled over the subset of projections selected for a given scenario.

  The subset of six LOCA projections used to develop each future climate scenario for a given period are determined based on the procedures described in Section 4.1.1 . In this step, matrices of monthly climate data from individual LOCA project are merged (pooled) over the subsets selected for each project. This results in ten matrices of monthly values (two matrices per climate scenario) for each climate variable at each grid cell: one matrix for each climate scenario for the historical reference period and one for the future climate period.

- *Develop Cumulative Distribution Functions (CDFs)*

  Matrices of pooled monthly climate values are then sorted to develop cumulative distribution functions (CDFs) of climate conditions over the historical and future time periods. Monthly values in each pooled matrix are sorted along columns from least to greatest and the cumulative exceedance probability, also referred to as quantile, of each value is estimated based on its Weibull plotting position.[9] This results in CDFs of pooled monthly climate conditions for each period.

  Example CDFs of monthly precipitation and monthly maximum temperature are illustrated in Figure 34 and Figure 35, respectively. The example CDFs show monthly precipitation and monthly maximum temperature values (ordinate or y-axis) plotted as a function of quantile

[9] The Weibull plotting position of a sample value is defined as the value's rank divided by the number of samples plus one (W = r/(n+1); W = Weibull plotting position; r = sample rank; n = number of samples).

(abscissa or x-axis).[10] The data in these figures are from the LOCA grid cell overlying Folsom Dam from the subset of six LOCA projections selected for the central tendency (CT) scenario for future time period 2070-2099. Each panel in Figure 34 and Figure 35 shows two CDFs: one for the historical reference period (1980-2009; red-orange points) and one for the future period (2070-2099; blue points). Each point in the CDFs represents one monthly value from one LOCA projection. Different shades of blue and red-orange indicate which of the six LOCA projections a given value originated. Shading is included to show that the shape of the CDF—particularly the shape near the tails—is not driven by a single LOCA projection; rather, shading demonstrates that values from each projection in the subset are generally distributed over the full range of the CDF.

Figure 34 shows that the probability distribution of monthly precipitation over the future time period (2070-2099) is generally consistent with the distribution over the historical reference period (1980-2009). The upper end of the distribution (larger precipitation amounts) is projected to increase slightly during some months (e.g., October, November, and June). However, the overall distribution is similar between periods. This is consistent with the LOCA projections selected for the central tendency (CT) climate scenario, which show little change in annual mean precipitation between periods (see Figure 33, green points and green polygon).

By contrast, Figure 35 shows a substantial shift in the probability distribution of monthly maximum temperature between periods. For most months, the shape of the CDF is similar, but values show a clear shift between periods. The shift between periods—i.e., the projected change in the probability distribution of monthly temperature—is greatest during spring and early summer (May-July) and least during late fall and early winter (November-January). The shift between periods ranges from an increase of approximately 3.5°F for December to almost 6.5°F for March.

- *Develop Climate Change Factors*

  For a given scenario and future period, climate change factors are computed from the corresponding CDFs of monthly precipitation, monthly mean maximum temperature, and monthly mean DTR. Precipitation change factors are computed as the ratio of the CDF for the future period to the CDF for the historical period. Change factors for monthly mean maximum temperature and monthly mean DTR are computed as the difference between CDF for the future period and the CDF for the historical reference period. No change factors are developed for monthly

[10] CDFs are commonly plotted such that sample values are the abscissa (x-axis) and corresponding quantiles or exceedance probabilities are the ordinate (y-axis). The transpose is used here for consistency with the procedure used to compute change factors.

mean minimum temperature; minimum temperatures under each future scenario are computed as monthly mean maximum temperature minus monthly mean DTR. This ensures that monthly mean maximum temperature, monthly mean minimum temperature, and monthly mean DTR remain consistent with each other under future scenarios.

Similar to CDFs, climate change factors are a function of quantile (cumulative probability). Climate change factors thus capture differences in projected climate change across the distribution of a given climate variable. For example, projected changes in extreme values may differ from projected changes values near the middle of the distribution.

Examples of change factors for monthly precipitation and monthly mean maximum temperature are illustrated in Figure 36 and Figure 37, respectively. Change factors in Figure 36 and Figure 37 are for the CT scenario for future time period 2070-2099, and are for the LOCA grid cell overlying Folsom Dam; change factor correspond to the CDFs illustrated in Figure 34 and Figure 35, respectively.

Figure 36 shows that change factors for monthly precipitation are close to 1.0 for most quantiles in most months. This is consistent with the relatively small difference between CDFs of monthly precipitation (Figure 34). Precipitation change factor are computed as the ratio of the CDF for the future period (2070-2099) to the CDF for the historical reference period (1980-2009); values close to 1.0 indicate little difference between CDFs at a given quantile. It should be noted that where the precipitation value is zero at a given quantile in the CDF for the historical period, the ratio of CDFs is undefined (division by zero). In these instances, the change factor is assumed to be 1.0. Figure 36 indicates that this occurs frequently during spring and summer months (March-July).

Figure 37 shows that change factors for monthly mean maximum temperature vary between months and between quantiles within a given month, consistent with the respective CDFs (Figure 35). Change factors are generally greatest during spring and early summer (May-July) and least during late fall and early winter (November-January). Change factors are largely consistent across quantiles during fall and early winter (October-December). In the months of January, February, May, and September, change factors are generally greater at higher quantiles and less at lower quantiles—i.e., relatively high temperatures are projected to increase more than relatively low temperatures. Conversely, change factors for the months of March and June are generally greater at lower quantiles and less at higher quantiles—i.e., relatively low temperatures are projected to increase more than relatively high temperatures.

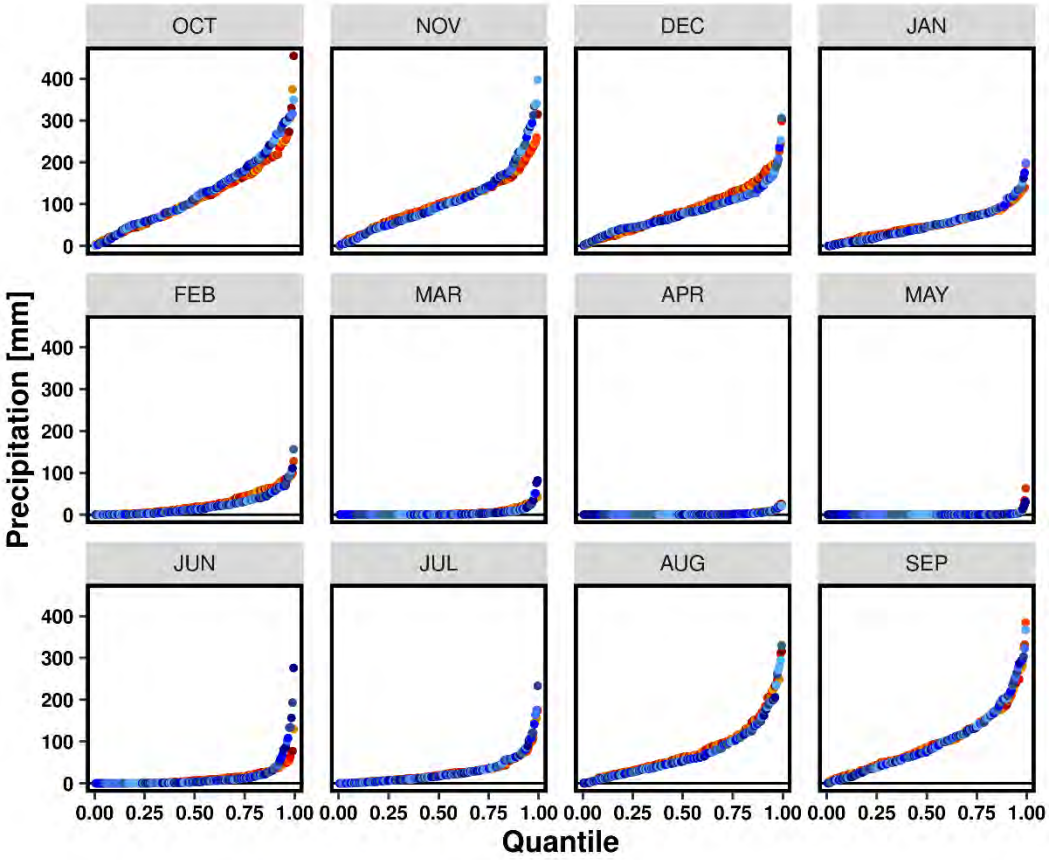

Figure 34: Cumulative distribution functions (CDFs) of monthly precipitation for the grid cell overlying Folsom Dam. CDFs are based on monthly precipitation values pooled over the six LOCA projections selected for the central tendency (CT) climate scenario for the period 2070-2099. Blue points represent monthly precipitation over the historical reference period (1980-2009); red-orange points reflect monthly precipitation over the future period (2070-2099). Different shades of blue and red-orange indicate which of the six LOCA projections from which a given value originated.

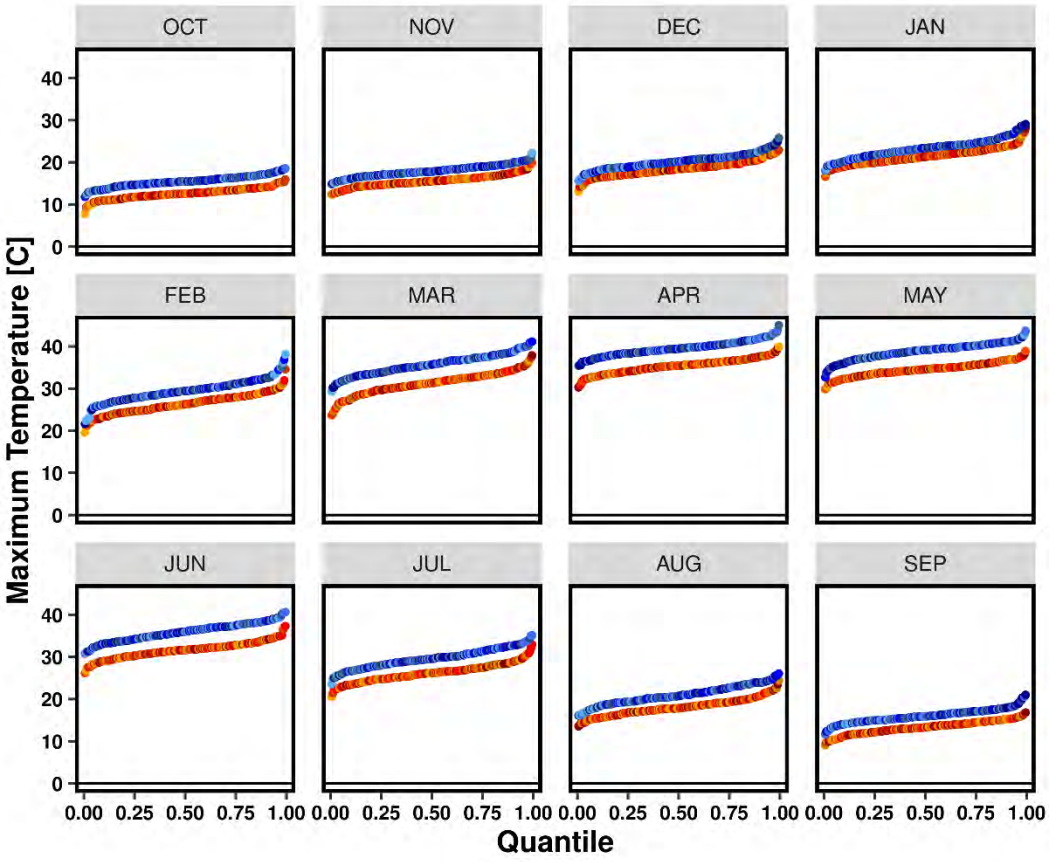

Figure 35: Cumulative distribution functions (CDFs) of monthly mean maximum temperature for the grid cell overlying Folsom Dam. CDFs are based on monthly mean maximum temperature values pooled over the six LOCA projections selected for the central tendency (CT) climate scenario for the period 2070-2099. Red-orange points represent monthly precipitation over the historical reference period (1980-2009); blue points reflect monthly precipitation over the future period (2070-2099). Different shades of red-orange and blue indicate which of the six LOCA projections from which a given value originated.

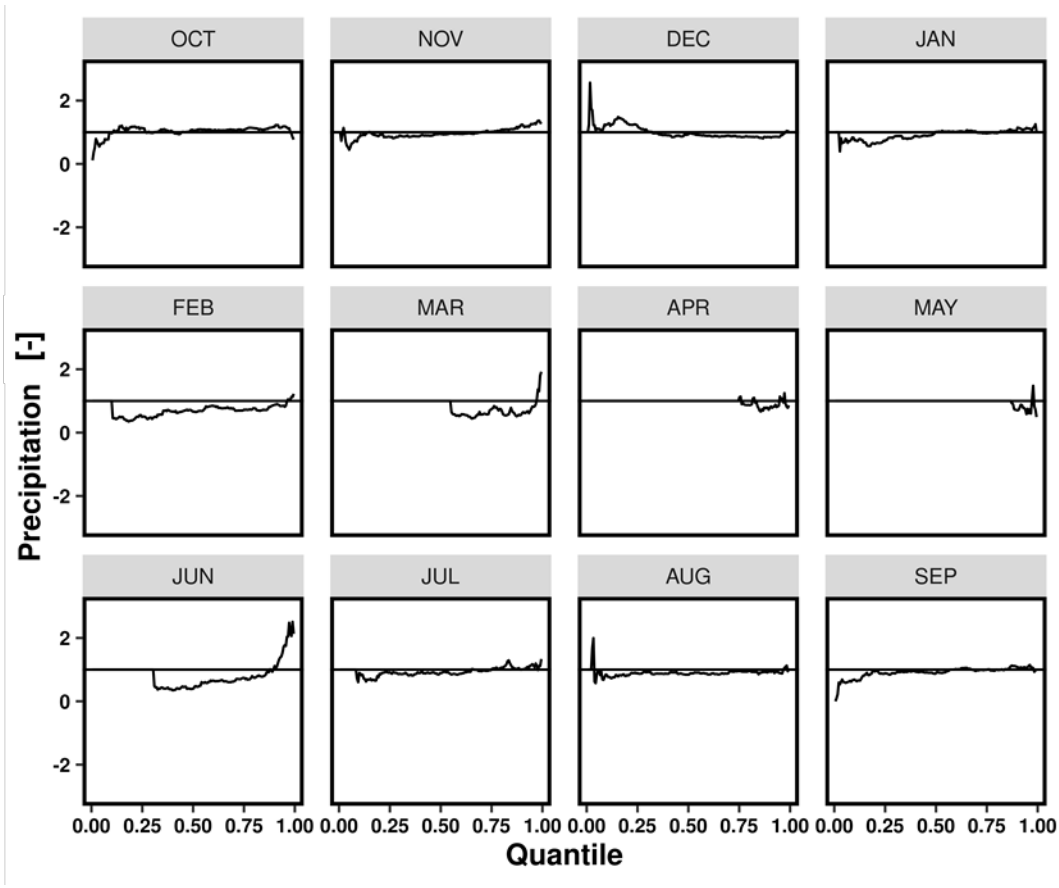

Figure 36: Quantile-based change factors [unitless] for monthly precipitation for the grid cell overlying Folsom Dam for the central tendency (CT) climate scenario for future period 2070-2099. Change factors are based on CDFs of monthly precipitation values pooled over the six LOCA projections selected for this scenario. The horizontal black line indicates a change factor value of 1.0.

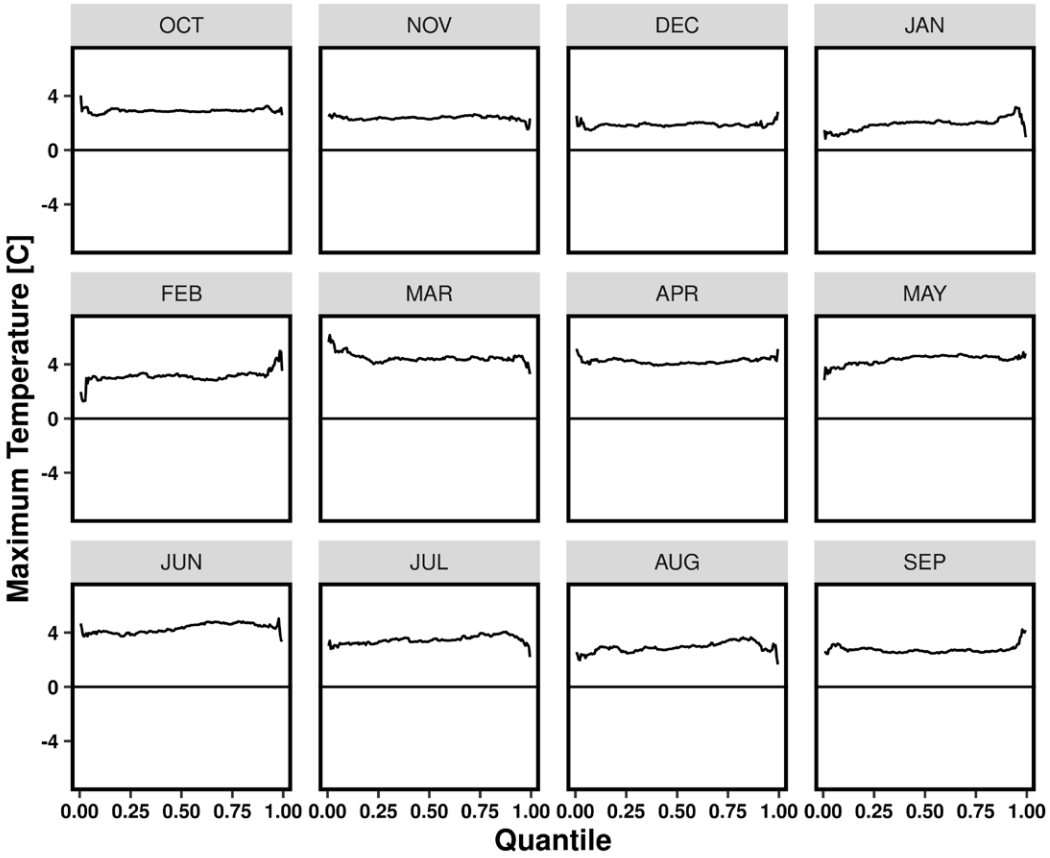

Figure 37: Quantile-based change factors [°C] for monthly mean maximum temperature for the grid cell overlying Folsom Dam for the central tendency (CT) climate scenario for future period 2070-2099. Change factors are based on CDFs of monthly mean maximum temperature values pooled over the six LOCA projections selected for this scenario. The horizontal black line indicates a change factor value of 0.0.

4.1.3 Application of Quantile-Based Change Factors

Monthly precipitation, monthly mean maximum temperature, and monthly mean DTR for each future climate scenario are computed by applying the respective quantile-based change factors to adjust the baseline climate scenario.

Precipitation change factors are applied according to Equation (1):

$$P^*_{ym} = P_{ym} \cdot \Delta^*_{Q[P_{ym}]} \quad (1)$$

Where P^*_{ym} is monthly precipitation in month *m* of year *y* under a given future scenario; P_{ym} is monthly precipitation in month *m* of year *y* under the baseline scenario (see Section 4.1); and $\Delta^*_{Q[P_{ym}]}$ is the precipitation change factor for the given scenario for the quantile (*Q*) corresponding to the baseline monthly precipitation value (P_{ym}). As described in Section 4.1.2 , precipitation change factors are based on the ratio of the precipitation CDF for a selected future period to the precipitation CDF for the historical reference period (1980-2009); precipitation under future scenarios is thus computed by multiplying the baseline precipitation value by the corresponding change factor.

Temperature change factors are applied according to Equation (2):

$$T^*_{ym} = T_{ym} + \Delta^*_{Q[T_{ym}]} \quad (2)$$

Where T^*_{ym} is monthly mean maximum temperature or monthly mean DTR for month *m* of year *y* under a given future scenario; T_{ym} is monthly mean maximum temperature or monthly mean DTR for month *m* of year *y* under the baseline scenario (see Section 4.1); and $\Delta^*_{Q[T_{ym}]}$ is the maximum temperature or DTR change factor for the given scenario for the quantile (*Q*) corresponding to the baseline monthly temperature value (T_{ym}). Temperature change factors—including change factors for monthly mean maximum temperature and monthly mean DTR—are based on the difference between temperature CDFs for a selected future period the historical reference period (1980-2009); temperature variables under future scenarios are thus computed by adding the change factor to the corresponding baseline temperature value.

The procedure used to compute monthly precipitation and monthly temperature variables under future climate scenarios from the baseline scenario and change factors is described below. The procedure is applied independently for each future time period. For each future time period, the procedure is applied independently at each 1/16° by 1/16° LOCA grid cell throughout the CalSim3 domain (see Figure 1).

- *Develop CDFs for Baseline Scenario*

  Change factors are applied to the baseline scenario on a quantile basis. To do this, CDFs must first be developed for each climate variable under the baseline scenario. CDFs are developed using the same procedure described above for developing CDFs of monthly climate conditions from the pooled LOCA projections selected for each future scenario (see Section 4.1.2). First, monthly precipitation, monthly mean maximum temperature, and monthly mean DTR from the baseline scenario are partitioned by month and by period. This is achieved by converting monthly precipitation and temperature values from a timeseries (one-dimensional vector) into a two-dimensional matrix, with each row of the matrix containing monthly values over a single year and each column containing values for a single month over each year in the record (i.e., rows represent years, columns represent months). Only the historical reference period (1980-2009) is used in developing the baseline CDFs.

  Monthly values are then sorted along columns from least to greatest and the cumulative exceedance probability, also referred to as quantile, of each value is estimated based on its Weibull plotting position. This results in set of 12 CDFs of monthly climate conditions from the baseline scenario, one for each month of the year, at each grid cell in the CalSim3 domain.

- *Apply Change Factors to Baseline Scenario*

  Change factors are applied to monthly precipitation, monthly mean maximum temperature, and monthly mean DTR from the baseline climate scenario as follows.

  First, a set of look-up functions is developed to determine the quantile (cumulative probability) of a given value with respect to the the baseline CDF. A second set of look-up functions is then developed to determine the change factor for given quantile. Each set includes 12 look-up functions, one for each month of the year.

  Look-up functions are then used to apply a change factor to each monthly value from the baseline scenario to compute the corresponding monthly value for the future climate scenario. A compute script is used to loop over all months in the baseline scenario period of record (January 1915 – December 2015). The first look-up function is used to determine the quantile of the baseline value for that month from the corresponding baseline CDF. The second look-up function is used to determine the change factor for that month and quantile. The future scenario value for that month is the computed according to Equation 1 for precipitation or Equation 2 for temperature variables.

4.1.4 Assumptions and Limitations

Several important assumptions are inherent in the HDe methodology. The HDe methodology is based on adjusting a baseline scenario to reflect projected changes in the probability distributions of precipitation and temperature between two period. As described in Section 4.1 , the baseline scenario is developed by removing long-term trends from a dataset of observed historical climate conditions. As a result, the baseline scenario and all future scenarios reflect observed historical interannual climate variability. The HDe methodology thus allows users to distinguish between natural climate variability and anthopogenic climate change, which in turn allows users to evaluate a broad range of climate variability under a given projection of future climate change. For example, the HDe method allows users to evaluate the extent to which dry conditions in a given climate scenario are driven by climate change (projected drying) versus natural climate variability (drought conditions).

However, because future climate scenarios are based on a de-trended baseline scenario, the HDe methodology does not reflect the timing of projected changes in climate. HDe scenarios therefore cannot be used to assess when future climate conditions are likely to cross a given threshold that may be relevant to planners and resource managers. For example, HDe scenarios cannot be used to assess when annual mean snowpack is projected to decrease by a certain percentage or when annual mean temperatures are projected to exceed a given threshold. The HDe methodology is consistent with to planning approaches that rely on projected build-out conditions to evaluate future water supplies, without explicit consideration of when build-out conditions will be reached. Moreover, limitations of the HDe method with respect to assessing trends or timing of certain thresholds are mitigated in this study by evaluating HDe scenarios for multiple future time periods.

In addition to limitations regarding analysis of trends and projected timing of threshold conditions, HDe scenarios do not reflect potential changes in climate variability, including the frequency, intensity, duration of weather extremes such as extreme heat events and extreme precipitation events as well as climate extremes such as drought events. Previous analyses of historical observations and GCM-based projections of future climate suggests that climate change may affect the frequency and duration of weather and climate extremes. However, the characteristics of such change remain uncertain due to limitations of GCMs in simulating these extremes. While the HDe method does not reflect projected changes in the frequency, intensity, and duration of weather and climate extremes, it ensures that characteristics of weather and climate variability on daily to inter-decadal timescales is realistic and is not affected by limitations of GCMs.

4.2 Future Climate Scenarios

The baseline climate scenario represents observed historical climate variability over the period 1915-2015, de-trended such that monthly and annual mean climate conditions over the full 101-year record are consistent with the historical reference period 1980-2009. Future climate scenarios were developed by adjusting the baseline scenario to represent a plausible range of future climate conditions over the ARBS study area and the extent of the CVP-SWP system. The ARBS climate scenarios were evaluated to characterize the range of future climate conditions represented in the Basin Study. Similar to observed historical climate and LOCA projections, future climate scenarios were evaluated on a $1/16^{th}$ degree grid and averaged over the ARBS study area, the CalSim3 domain, and selected basins. Selected basins considered in evaluating and characterizing the ARBS climate scenarios are illustrated in Figure 12.

4.2.1 Future Temperature Scenarios

Consistent with individual LOCA projections (see Section 3.2), all ARBS climate scenarios indicate an increase in annual and seasonal average temperatures over the ARBS study area and the CalSim3 domain. The change in annual mean basin-average temperature over the ARBS study area under each future climate scenario compared to the Baseline scenario is given in Table 3 and the spatial distribution of change in annual average temperature is illustrated in Figure 38. The 'warm' scenarios (WD, WW) indicate an increase in annual average temperatures of approximately 3.7-4.3°F by the end of the 21st century, while the 'hot' scenarios (HD, HW) indicate an increase of approximately 7.9-8.3°F by the end of this century. Annual maximum temperatures are projected to increase more than annual minimum temperatures, with the 'warm' scenarios (WD, WW) indicating increases of 4.1°F and 4.2°F, respectively. Similarly, the 'hot' scenarios (HD, HW) indicate an annual maximum temperature increase of 8.2-8.4°F, with an increase in annual minimum temperatures of approximately 7.5-8.3°F by the end of the century.

Spatial and seasonal patterns of temperature variability in all scenarios is consistent with observed historical patterns of temperature variability across the CalSim3 domain. The spatial distribution of seasonal average temperature for the hot-wet scenario (HW) for the future time period 2070-2099 is illustrated in Figure 39; the spatial distribution of the change in seasonal average temperature between this scenario and the historical reference period is illustrated in Figure 40. Similar to observed historical temperatures, temperatures under this HD scenario are coolest in the higher elevation mountain areas and warmest in the Central Valley. Seasonal variations in temperature are also similar to observed, with summer being the warmest season and winter the coolest (Figure 40). By contrast, differences in seasonal average temperature between the scenario and the historical reference period differ by season, with the most warming occurring during summer and the least warming occurring during winter (Figure 40). However, increases in seasonal temperature are generally consistent across the

entire CalSim3 domain, with slightly larger increases in the northwest areas during summer. Spatial and seasonal patterns are similar across all future temperature scenarios and time periods, though the magnitudes of temperature changes differ between scenarios and time periods.

Timeseries of basin-average annual average temperature over the CalSim3 domain is illustrated in Figure 41. Annual average temperatures are warmer in all years under all future scenarios. The amount of warming under each scenario increases with future time horizon—i.e., warming under each scenario for the 2070-2099 future period is greater than for the 2040-2069 period. In addition, Figure 41 shows that the range of projected warming across scenarios increases with future time horizon—i.e., the difference between hot scenarios (HD, HW) and warm scenarios (WD, WW) is greater for the 2070-2099 future period compared to the 2040-2069 period. This increase in the range across scenarios is consistent with the increase in range of projected warming across LOCA projections towards the end of the 21st century.

As discussed in Section 4.1, the ensemble-informed hybrid-delta (HDe) methodology preserves the pattern of climate variability—i.e., the sequencing of relatively wet and dry years and cool and hot days, months, and years—from the observed historical baseline. As a result, interannual variability of annual average temperatures is perfectly correlated between the observed historical baseline and all future scenarios. However, the increase in temperature under future scenarios results in an increase in the occurrence of extreme temperature events. Extreme temperature events are defined here as temperatures above the 95th percentile of observed annual average temperatures over the historical reference period (1980–2009). The threshold for basin-average annual extreme temperatures over the CalSim3 domain is 57.6°F for annual average temperature, 70.5°F for annual maximum temperature, and 45.1°F for annual minimum temperature.

By definition, observed historical temperatures exhibit extreme annual temperatures in one or two years during the historical reference period (1980-2009). The number of occurrences of extreme annual temperatures during the corresponding 30-year period of each scenario are listed in Table 4. For all three future time periods (2040-2069, 2055-2084, and 2070-2099), the hot scenarios (HD, HW) experience extreme annual temperatures in all 30 years. Under the warm scenarios (WD, WW), extreme annual average temperatures occur in 27 or 28 out of 30 years for the future period 2040-2069 and in 29 or 30 years for the future period 2070-2099. Extreme annual minimum temperatures occur in all but one year. The frequency of extreme annual maximum temperatures increase the least under the warm scenarios (WD, WW), with extreme annual maximum temperatures occurring in 14-15 out of 30 years for the future period 2040-2069 and up to 26 out of 30 years for the future period 2070-2099.

While all scenarios exhibit an increase in frequency of extreme basin-average annual temperatures compared to observed historical conditions, the occurrence of

extreme seasonal temperatures varies between seasons and throughout the region. The spatial distribution of the frequency of extreme seasonal temperatures is illustrated in Figure 43 and Figure 44 for the hot-wet (HW) and warm-wet (WW) scenarios, respectively, for the future period 2070-2099. As for basin-average extreme annual temperatures, the frequency of extreme seasonal temperatures is, by definition, one or two occurrences during the 30-year historical reference period. The frequency of extreme seasonal temperatures increases throughout the region and in all seasons under the hot-wet (HW) and warm-wet (WW) scenarios. As expected, the frequency of extreme seasonal temperatures increases more under the hot-wet (HW) scenario than under the warm-wet (WW) scenario. The frequency of extreme seasonal temperatures increases the most for summer and the least for spring. Figure 44 also indicates that the frequency of extremes increases more over low-elevation areas such as the Central Valley compared to higher elevation areas of the Sierra Nevada and Cascade mountains.

Table 3. Differences in basin-average annual precipitation and temperature between baseline and future climate scenarios over the ARBS study area.

Time period	Scenario	Precip		Tavg (°F)	Tmax (°F)	Tmin (°F)
		(in)	(%)			
2040 - 2069	CT	0.1	0.1%	3.9	4.1	3.8
	HD	-2.8	-6.8%	5.2	5.4	5.0
	HW	2.1	5.0%	5.1	5.4	4.9
	WD	-2.4	-5.8%	2.9	3.2	2.7
	WW	1.9	4.5%	2.9	3.1	2.9
2055 - 2084	CT	-1.1	-2.6%	5.2	5.8	4.7
	HD	-3.4	-8.3%	6.8	7.0	6.7
	HW	2.1	5.2%	6.6	6.8	6.3
	WD	-2.9	-7.0%	3.4	3.8	3.0
	WW	3.8	9.2%	3.7	3.7	3.6
2070 - 2099	CT	-0.6	-1.6%	5.4	5.8	5.1
	HD	-4.6	-11.0%	7.9	8.4	7.5
	HW	5.3	12.7%	8.3	8.2	8.3
	WD	-4.2	-10.0%	3.7	4.1	3.3
	WW	7.0	16.9%	4.3	4.2	4.5

Notes:

- *Precip = annual precipitation, Tavg = annual mean of daily average temperature, Tmin = annual mean of daily minimum temperature, Tmax = annual mean of daily maximum temperature, CT = Central Tendency, HD = Hot-Dry, HW = Hot-Wet, WD = Warm-Dry, WW = Warm-Wet.*
- *Projected change was calculated by comparing annual mean basin-average precipitation and temperature over the ARBS study area between Baseline and future climate scenarios.*
- *Annual mean basin-average values under the Baseline scenario for the period 1915-2015 are as follows: Precip = 41.5 in; Tavg = 55.8 °F; Tmax = 20.1 °F; Tmin = 6.4 °F.*
- *Values for precipitation are given as absolute change in inches (in) and percent change (%); values for temperature are given as absolute change in degrees Fahrenheit (°F)*

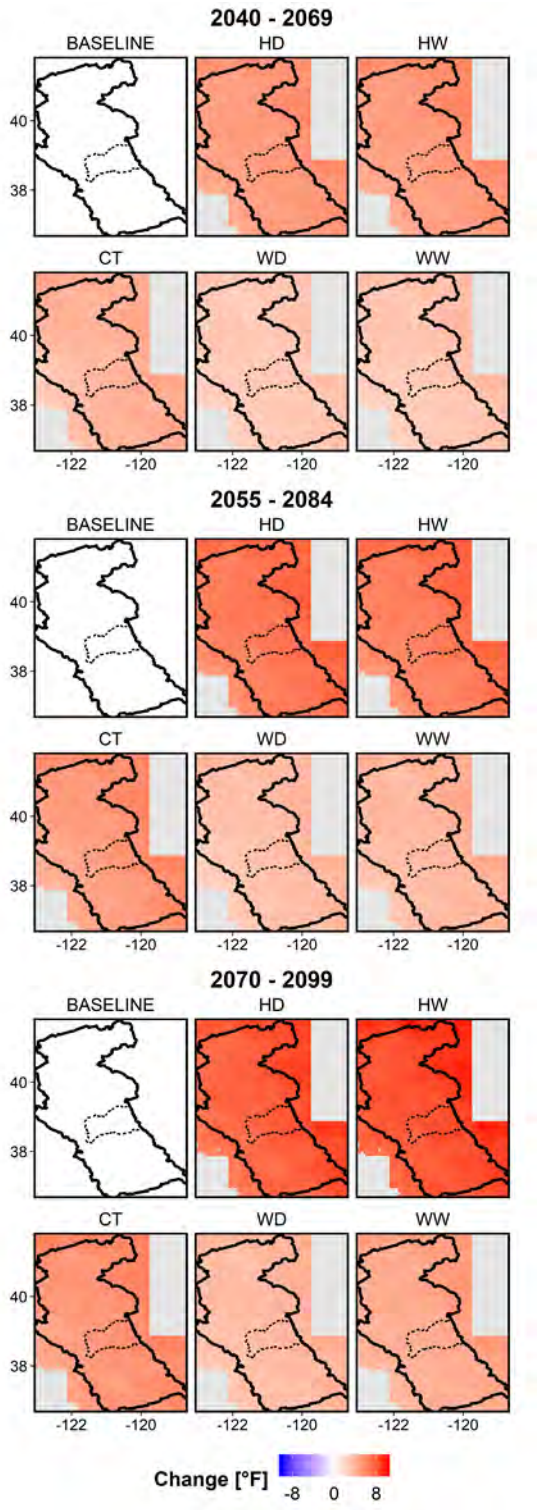

Figure 38. Spatial distribution of changes in annual average temperature under future climate scenarios compared to the Baseline. The CalSim3 domain is delineated by the black solid line and the ARBS study area is delineated by the black dashed line.

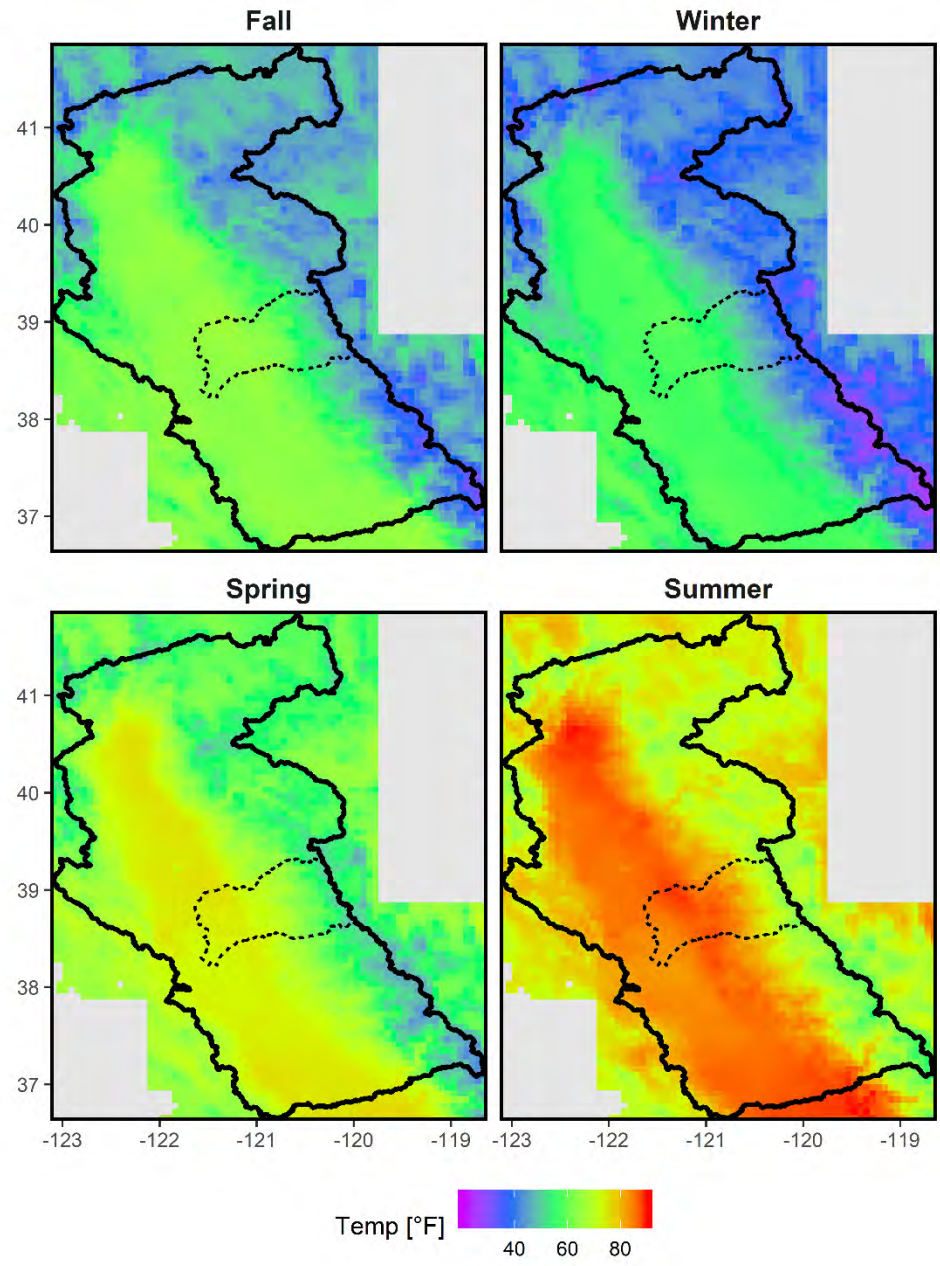

Figure 39. Spatial distribution of seasonal average temperature under the **Hot-Wet (HW)** scenario for the future period 2070–2099. The CalSim3 domain is delineated by the black solid line and the ARBS study area is delineated by the black dashed line.

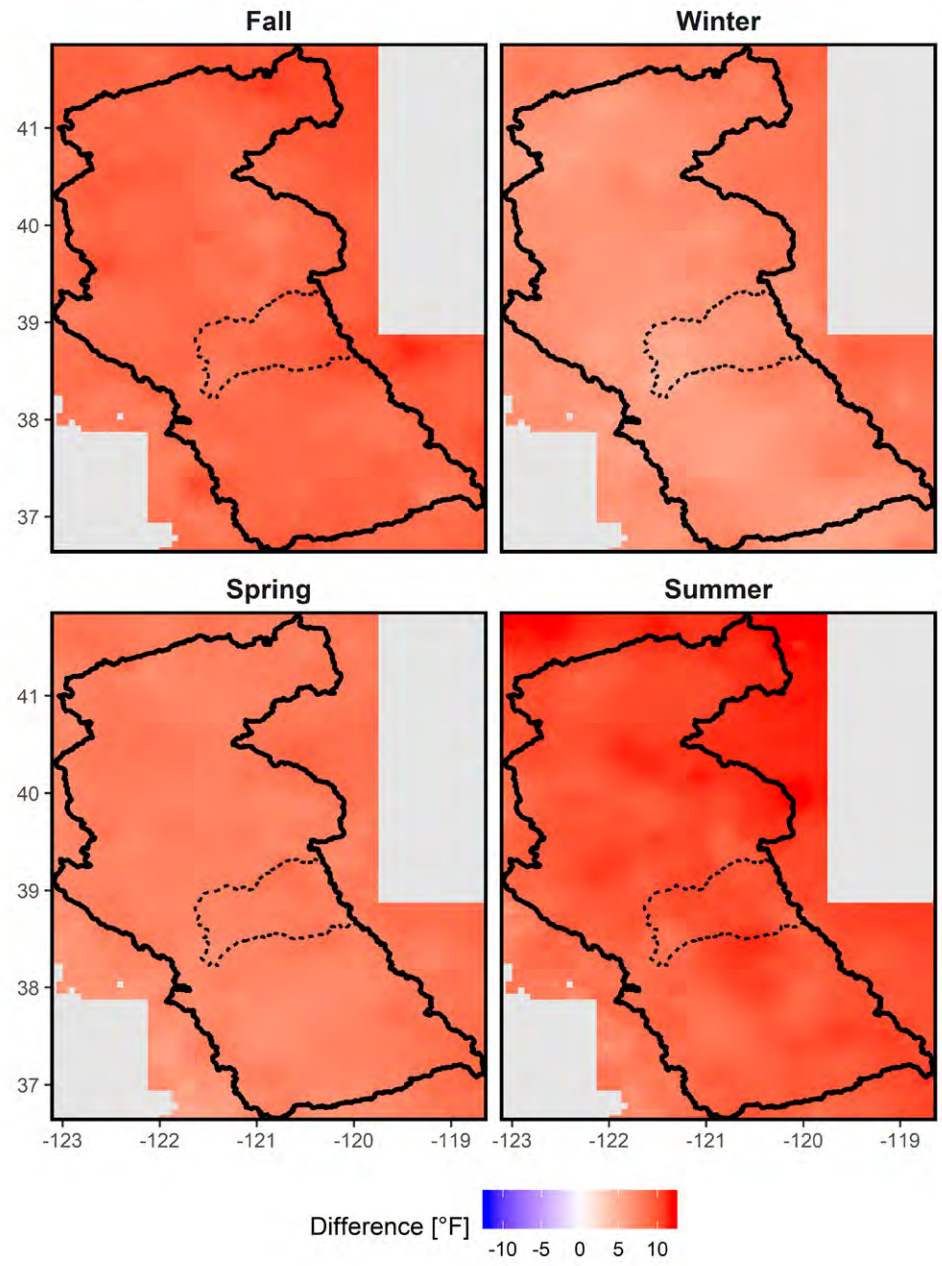

Figure 40. Spatial distribution of projected changes in seasonal average temperature under the **Hot-Wet (HW)** scenario for future period 2070-2099 compared to the Baseline. The CalSim3 domain is delineated by the black solid line and the ARBS study area is delineated by the black dashed line.

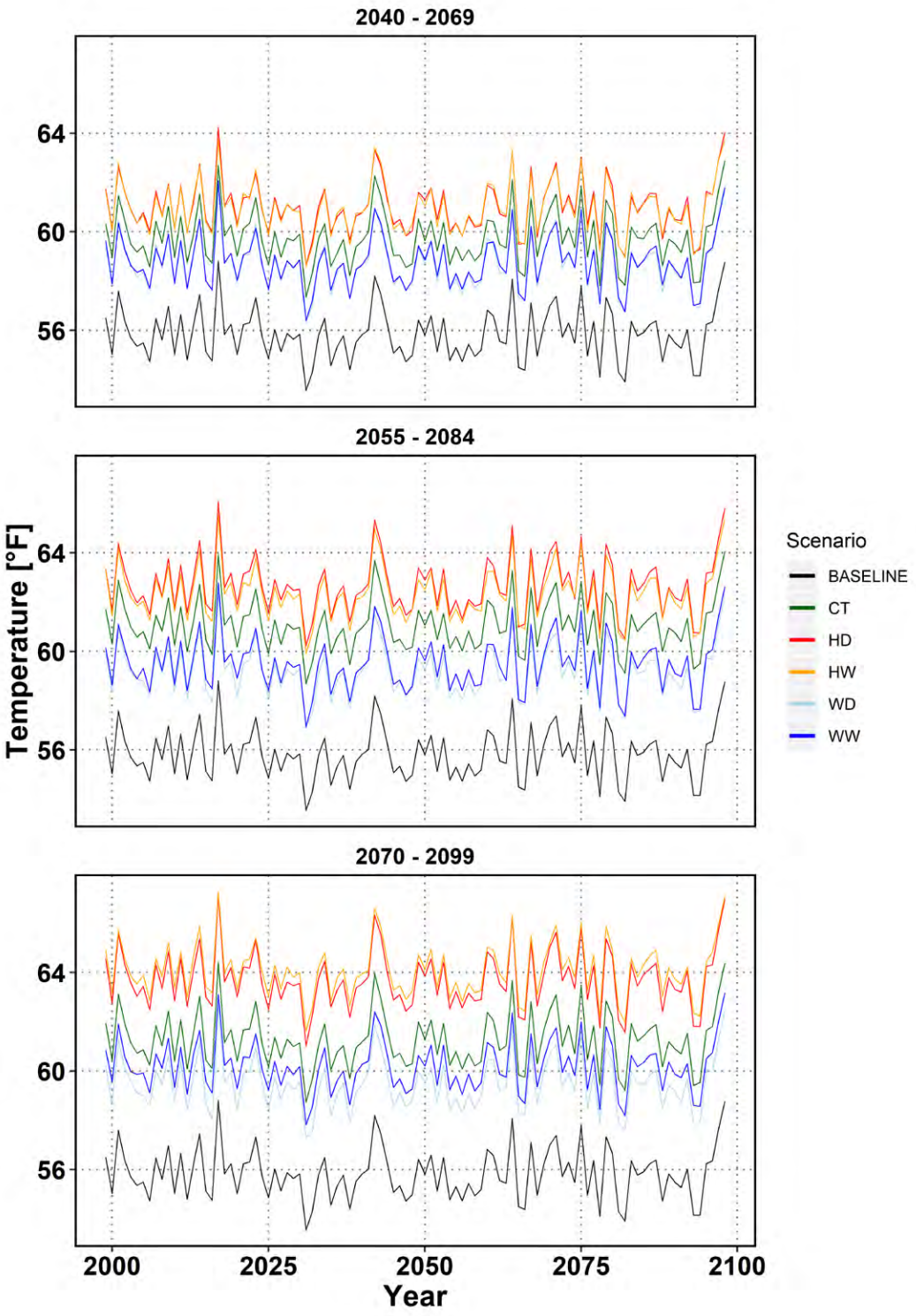

Figure 41. Timeseries of basin-average annual mean temperature over the ARBS Study Area under Baseline and future climate scenarios.

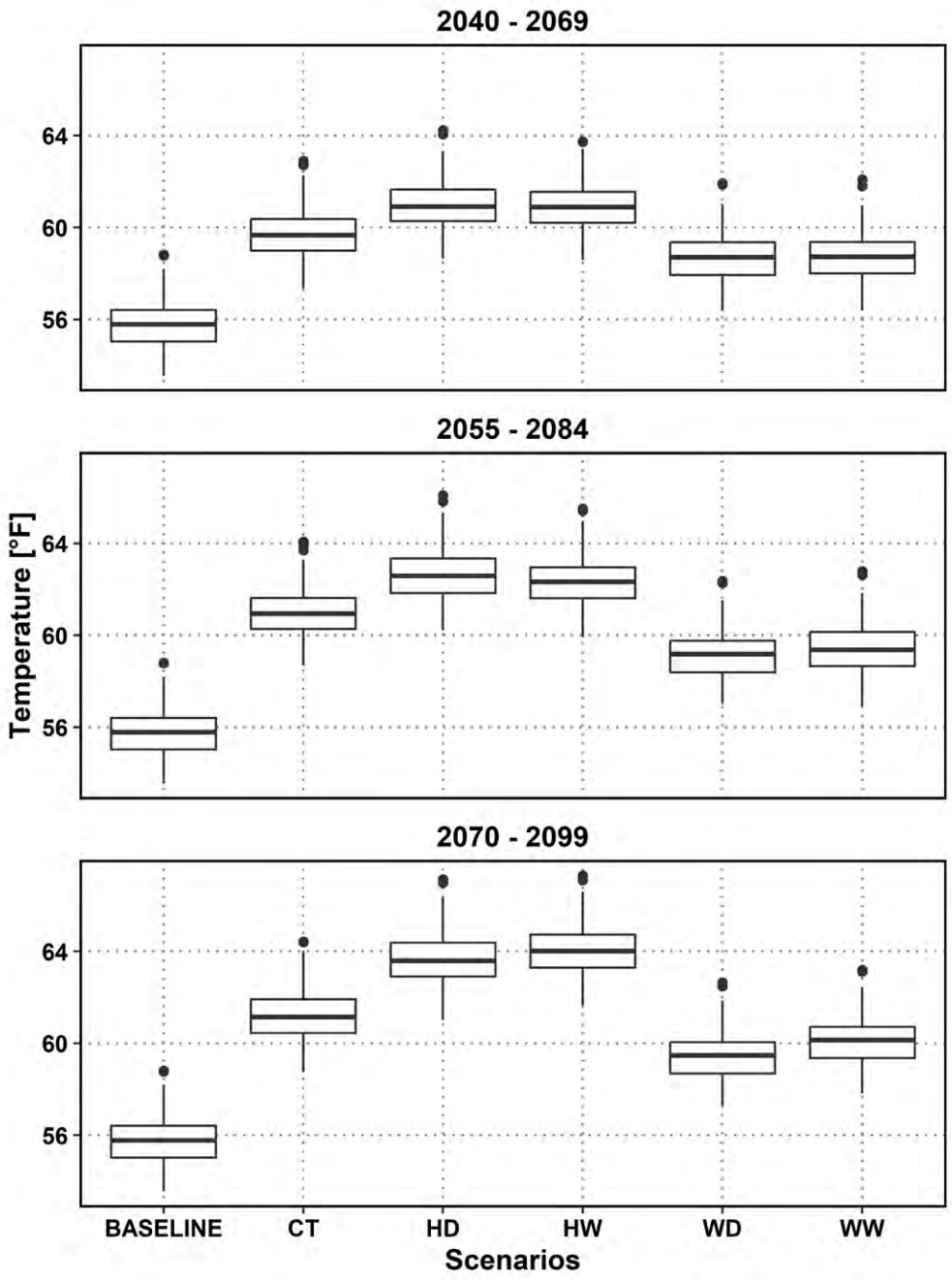

Figure 42. Boxplots of basin-average annual mean temperature under Baseline and future climate scenarios. Box limits represent the 25th and 75th quartiles; solid lines within each box represent the median; whiskers represent values extending from the 25th and 75th quartiles to values within ± 1.5*(Interquartile Range); and outliers are represented by solid black circles.

Table 4. The number of years during a 30-year period when the annual mean temperature exceeds the 95th percentile of observed annual mean temperature.

Time-period	Scenario	Frequency		
		Tavg	Tmax	Tmin
1980 - 2009	Historical	2	2	2
2040 - 2069	CT	30	26	30
	HD	30	30	30
	HW	30	30	30
	WD	27	14	29
	WW	28	15	30
2055 -2084	CT	30	30	30
	HD	30	30	30
	HW	30	30	30
	WD	28	23	29
	WW	29	22	29
2070 -2099	CT	30	30	30
	HD	30	30	30
	HW	30	30	30
	WD	29	25	29
	WW	30	26	30

Notes:

- *Tavg = annual mean of daily average temperature, Tmin = annual mean of daily minimum temperature, Tmax = annual mean of daily maximum temperature.*
- *The 95th percentile of basin-average observed annual mean Tavg is 57.8 °F; the 95th percentile of basin-average observed annual mean Tmax is 70.5 °F; the 95th percentile of basin-average observed annual mean Tmin is 45.1 °F.*

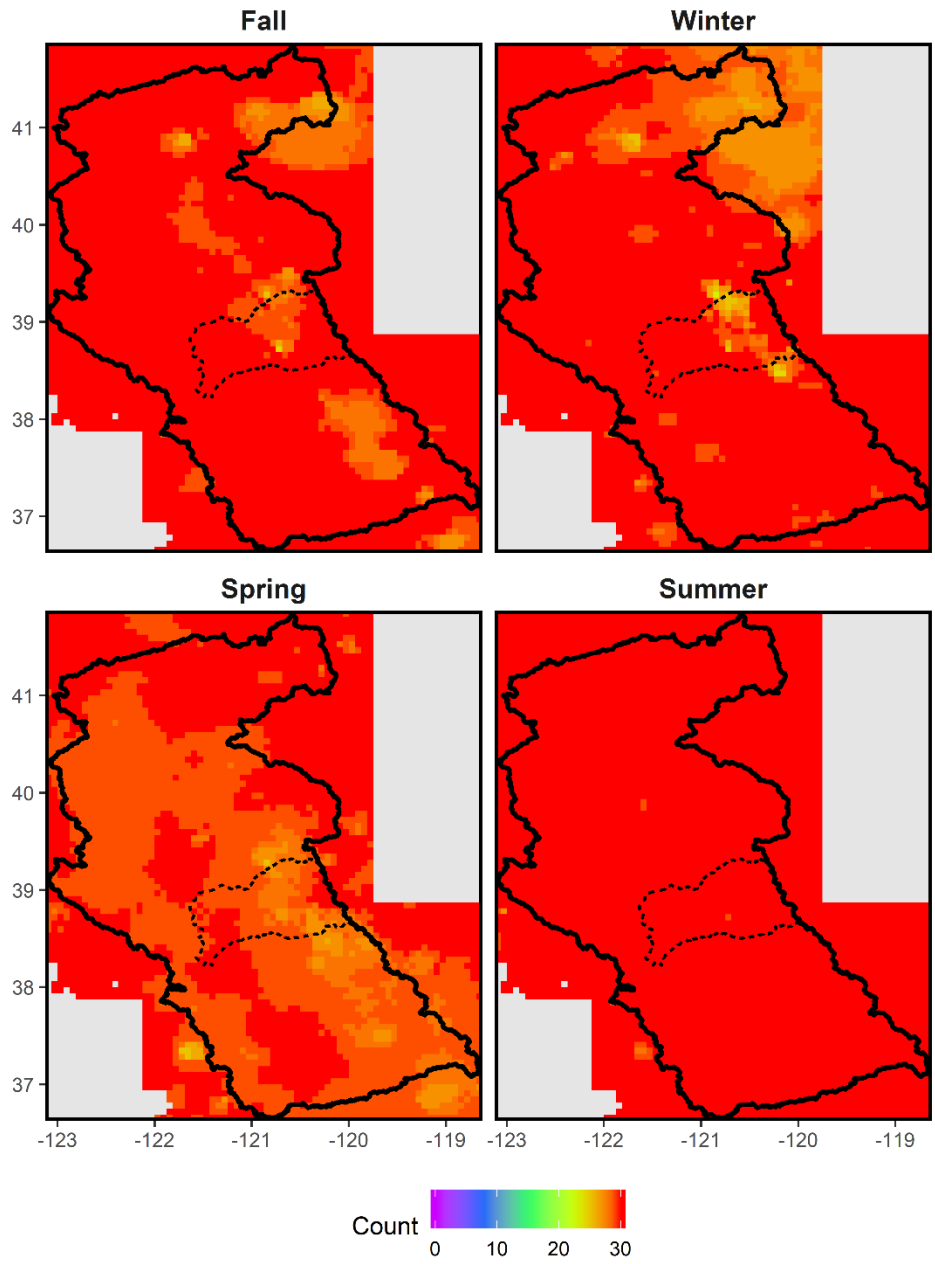

Figure 43. Spatial distribution of the frequency of extreme seasonal mean temperature over a 30-year period of under the **Hot-Wet** scenario for the future period 2070–2099. Extreme seasonal mean temperature is defined as seasonal mean temperatures exceeding the 95th percentile of observed seasonal mean temperatures during the historical reference period (1980-2009). The CalSim3 domain is delineated by the black solid line and the ARBS study area is delineated by the black dashed line.

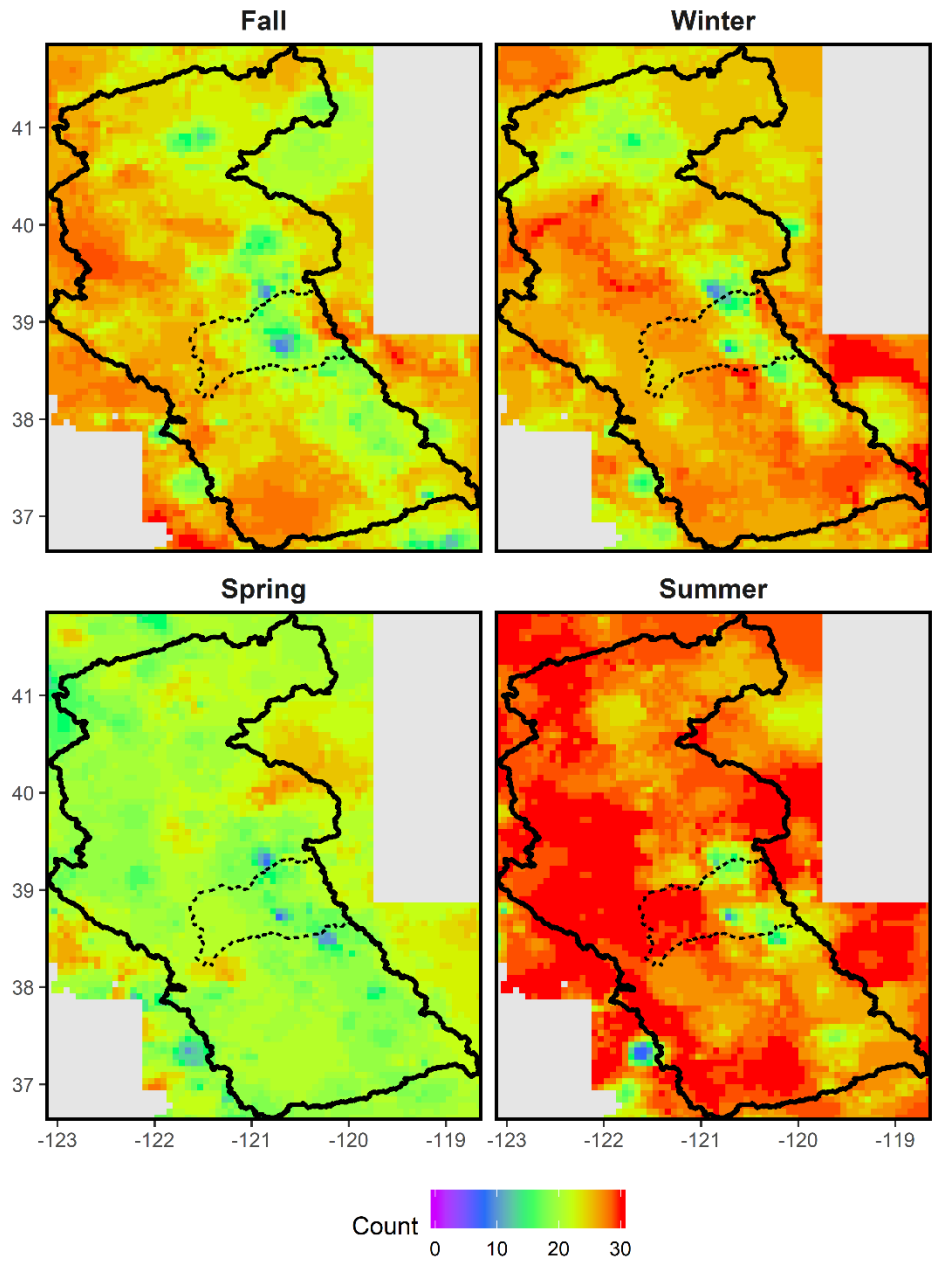

Figure 44. Spatial distribution of the frequency of extreme seasonal mean temperature over a 30-year period of under the **Warm-Wet** scenario for the future period 2070–2099. Extreme seasonal mean temperature is defined as seasonal mean temperatures exceeding the 95th percentile of observed seasonal mean temperatures during the historical reference period (1980-2009). The CalSim3 domain is delineated by the black solid line and the ARBS study area is delineated by the black dashed line.

4.2.2 Future Precipitation Scenarios

The Basin Study climate scenarios reflect a wide range of future precipitation conditions, consistent with the large uncertainty in projected precipitation changes across the ensemble of LOCA downscaled climate projections (Figure 27). Spatial distributions of the change in average annual precipitation under each scenario and future time period compared to the historical baseline are illustrated in Figure 45. The wet climate scenarios (HW, WW) indicate an increase in average annual precipitation of 10 to 20 percent over most of the region, while the dry scenarios (HD, WD) indicate a 10 percent decrease. This corresponds to an increase of approximately 5-7 inches (13-17%) in mean annual basin-average precipitation over the ARBS study area under the wet scenarios and a decrease of approximately 4 inches (10%) under the drier scenarios (Table 3). Changes in mean annual precipitation under each scenario increases with future timer horizon, with smaller changes for the 2040-2069 period and larger changes for the 2070-2099 period.

As discussed in Section 4.1, the ensemble-informed hybrid-delta (HDe) methodology preserves the pattern of climate variability—i.e., the sequencing of relatively wet and dry years and cool and hot days, months, and years—from the observed historical baseline. The spatial distribution of average seasonal precipitation under the hot-wet (HW) scenario for the future period 2070-2099 is illustrated in Figure 46. The spatial and seasonal distribution of precipitation under the hot-wet scenario is similar to the observed historical baseline (Figure 19), with more precipitation in the higher elevation mountain areas and during the fall and winter seasons and less precipitation in the Central Valley and during spring and summer seasons. This spatial and seasonal pattern is consistent across all future scenarios.

In contrast, the spatial and seasonal distributions of changes in average seasonal precipitation differ between scenarios. Spatial and seasonal distributions of the change in average seasonal precipitation under the hot-wet (HW) and hot-dry (HD) scenarios for the period 2070-2099 compared to the observed historical baseline are illustrated in Figure 47 and Figure 48, respectively. Figure 47 indicates that under the hot-wet scenario, average seasonal precipitation increases over most of the region during fall, winter, and summer. However, spring precipitation decreases slightly under this scenario compared to the observed historical baseline. Differences in seasonal precipitation are greatest over the higher elevation mountain areas and least over the Central Valley. Figure 48 indicates that under the hot-dry scenario, average seasonal precipitation decreases over most of the region during fall, winter, and spring. However, precipitation increases over some areas during fall and winter. Average seasonal precipitation under the hot-dry scenario also increases slightly over much of the region during summer.

In addition to changes in average precipitation, climate scenarios also exhibit changes in the frequency of annual and seasonal precipitation extremes. Precipitation extremes are defined here as annual or seasonal precipitation below the 5^{th} percentile (extremely dry) or above the 95^{th} percentile (extremely wet) of precipitation over the observed historical baseline period (1980-2009). For the ARBS study area, extreme wet years are defined as years with basin-average precipitation greater than 69.2 inches and extreme dry years are defined as years with basin average precipitation less than 25.0 inches. The number of extreme wet and dry years over the ARBS study area during a 30-year period is listed in Table 5 for each scenario and future time period.

The frequency of wet and dry scenarios is, by definition, one or two years out of 30 under the observed historical baseline. The frequency of extreme wet years is between one to three under all scenarios for the 2040-2069 and 2055-2084 future periods. By the 2070-2099 future period, the frequency of extreme dry years increases to three years out of 30 under the wet scenarios (HW, WW) and decreases to zero under the dry and central tendency scenarios (HD, WD, CT). By contrast, the frequency of extreme dry years increases for the future period 2040-2069 under all but the warm-wet scenario. By the 2070-2099 future period, the frequency of extreme dry years increases to more than ten out of 30 years under the dry scenarios (HD, WD), increases to three years under the central tendency scenario (CT), and decreases to zero under the warm-wet scenario (WW).

Spatial distributions of the frequency of extreme wet seasonal precipitation are illustrated in Figure 51 and Figure 52 for the hot-wet (HW) and warm-wet (WW) scenarios, respectively, for the future period 2070-2099. Spatial distributions of the frequency of extreme dry seasonal precipitation in these scenarios are illustrated in Figure 53 and Figure 54. Extreme wet seasonal precipitation is projected to occur more frequently in winter and less frequently in spring under both the hot-wet and hot-dry scenarios. In contrast, extreme dry conditions are projected to occur more often in spring and less often in winter under both scenarios. Changes in the frequency of extreme precipitation have the potential to significantly impact water management in the region.

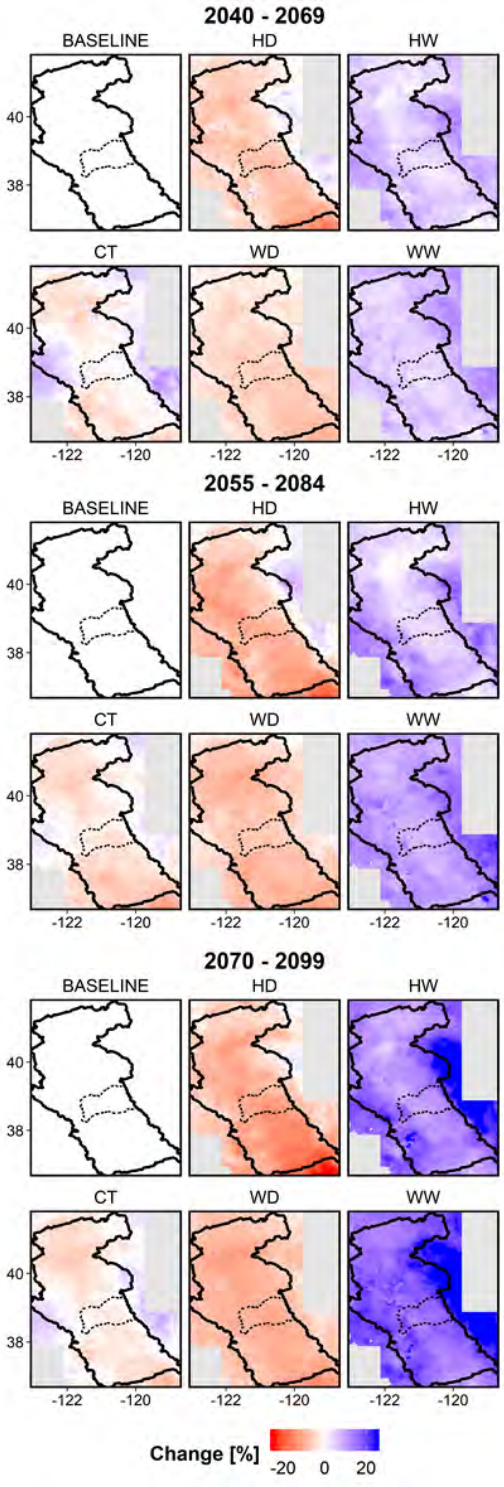

Figure 45. Spatial distribution of the change in annual mean precipitation under future climate scenarios compared to the Baseline. The CalSim3 domain is delineated by the black solid line and the ARBS study area is delineated by the black dashed line.

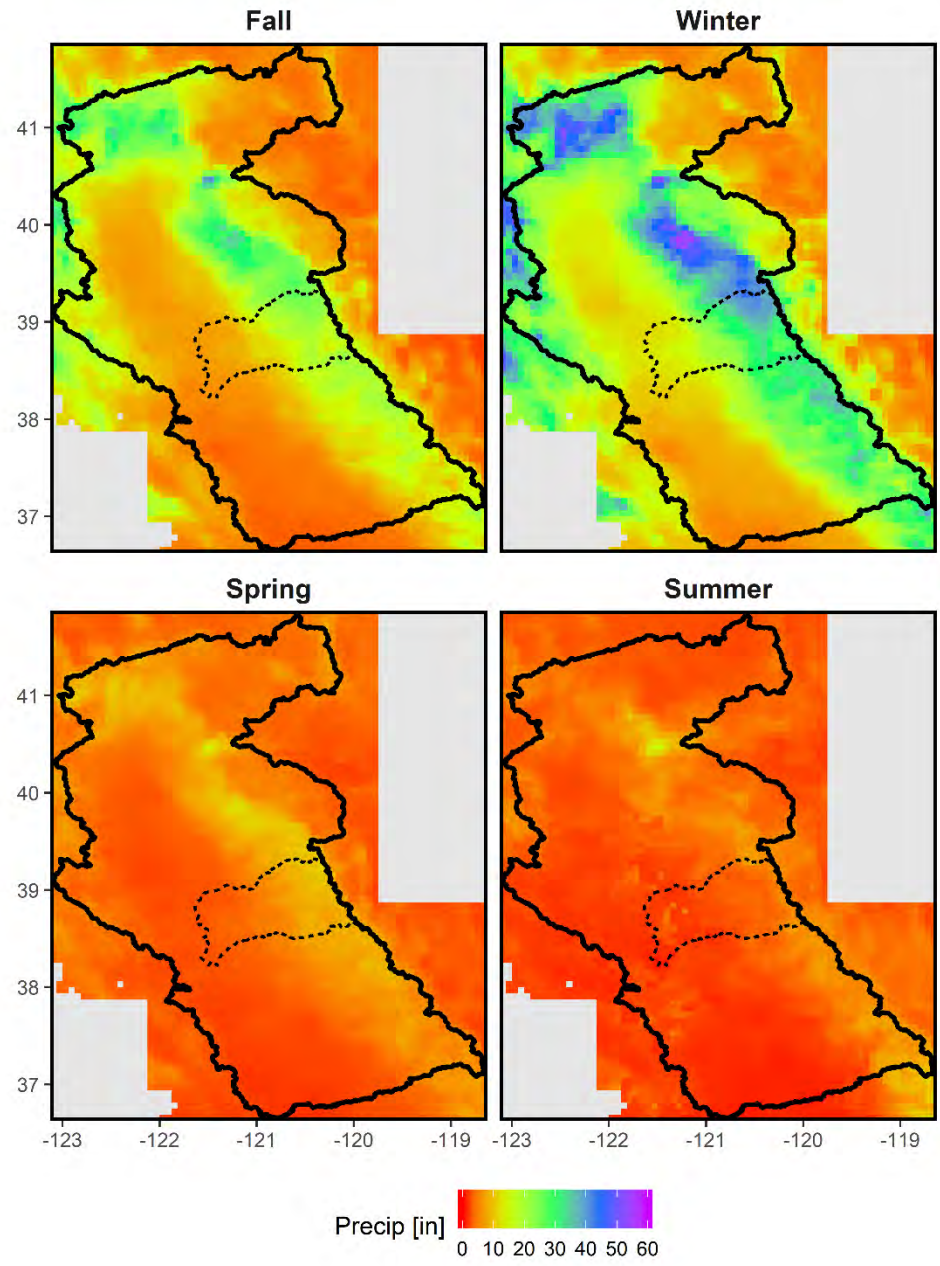

Figure 46. Spatial distribution of seasonal average seasonal precipitation under the **Hot-Wet** scenario for the future period 2070-2099. The CalSim3 domain is delineated by the black solid line and the ARBS study area is delineated by the black dashed line.

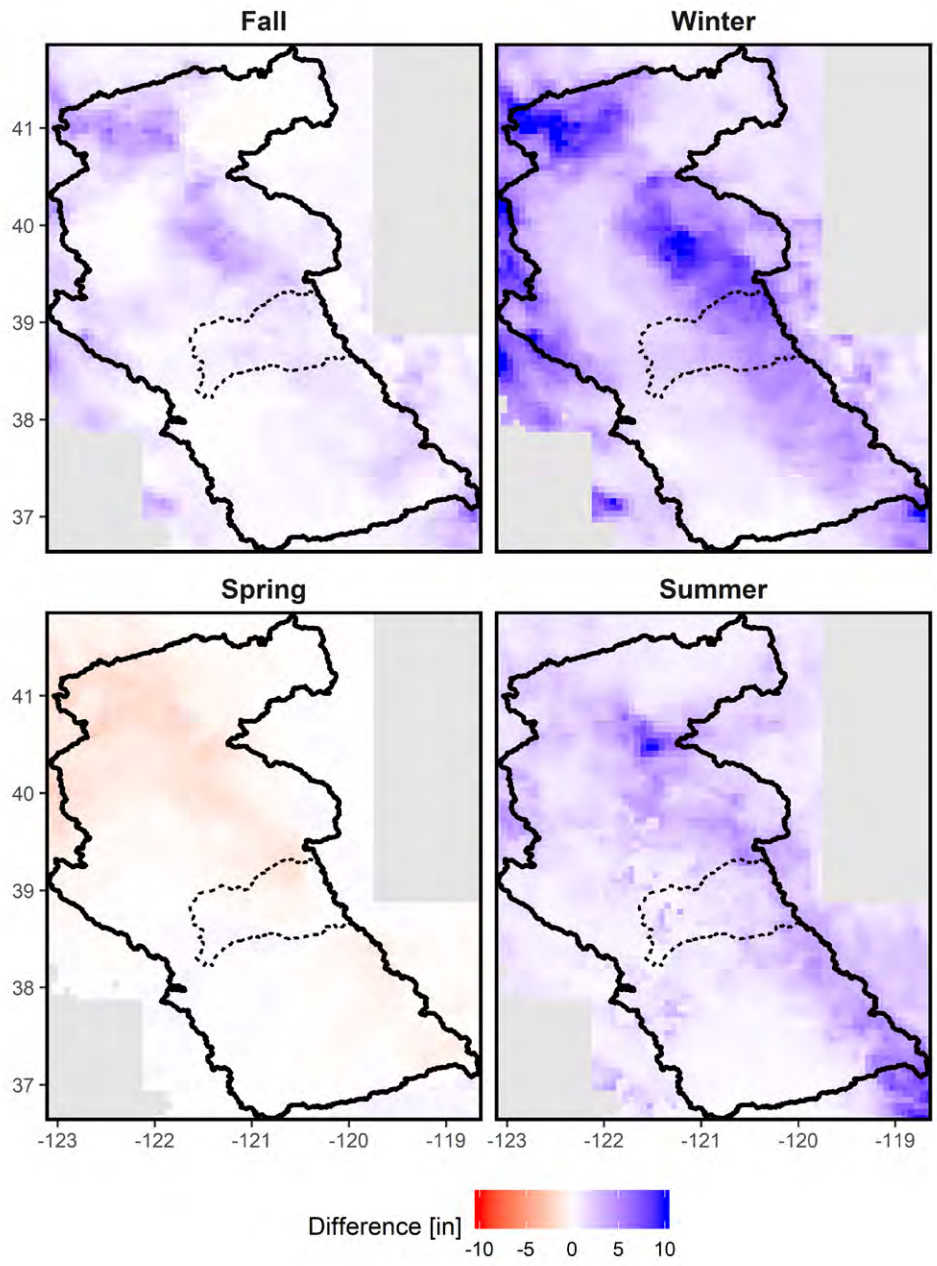

Figure 47. Spatial distribution of the difference in seasonal mean precipitation under the **Hot-Wet (HW)** scenario for the future period 2070–2099 compared to the Baseline. The CalSim3 domain is delineated by the black solid line and the ARBS study area is delineated by the black dashed line.

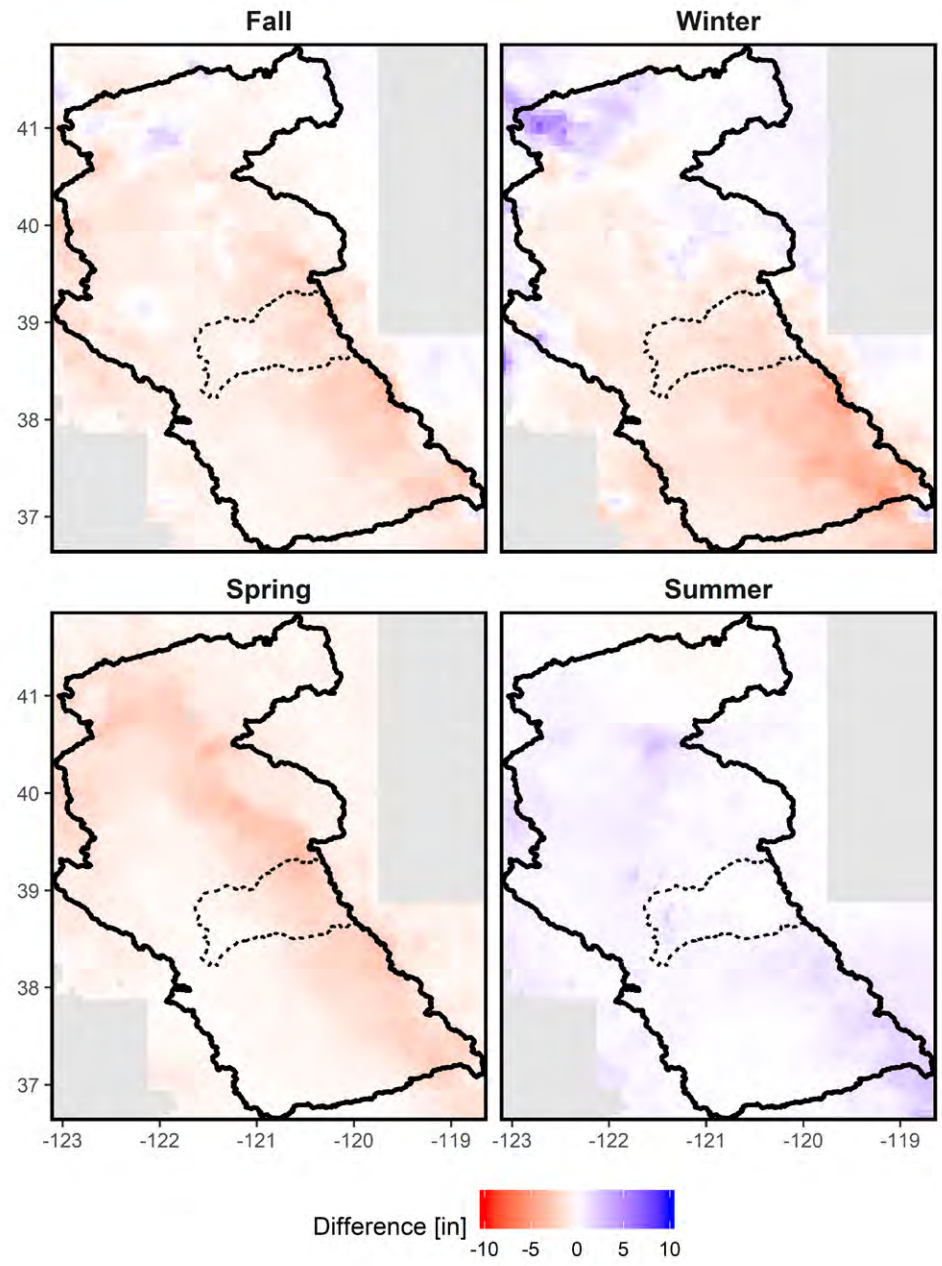

Figure 48. Spatial distribution of the difference in seasonal mean precipitation between the **Hot-Dry (HD)** scenario for the future period 2070–2099 and the Baseline. The CalSim3 domain is delineated by the black solid line and the ARBS study area is delineated by the black dashed line.

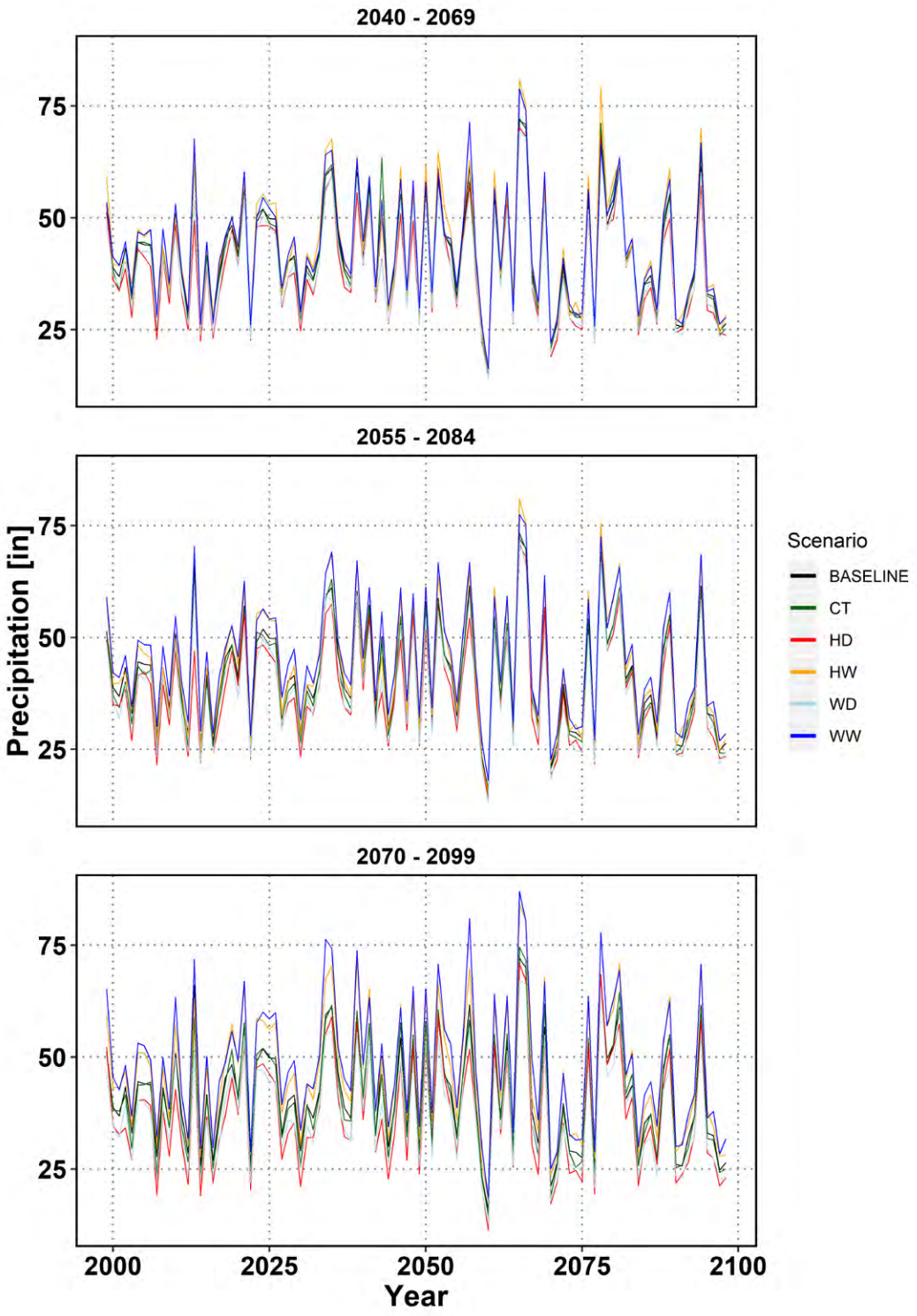

Figure 49. Timeseries of basin-average annual precipitation over the ARBS Study Area for each scenario and future time period.

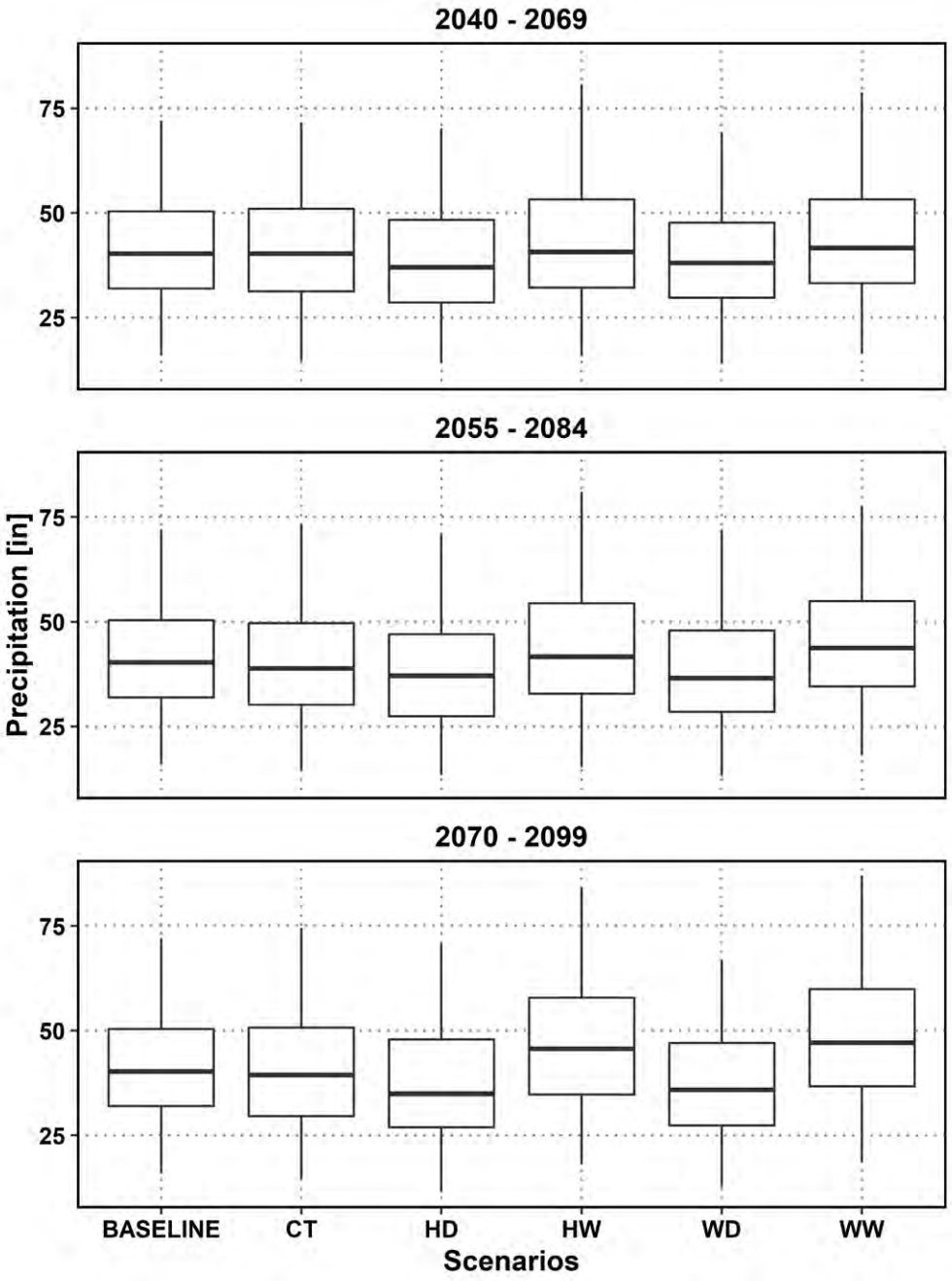

Figure 50. Boxplots of basin-average annual precipitation under the Baseline and future climate scenarios. Box limits represent the 25th and 75th quartiles; solid lines within each box represent the median; whiskers represent values extending from the 25th and 75th quartiles to values within ± 1.5*(Interquartile Range); and outliers are represented by solid black circles.

Table 5. The number of years during a 30-year when annual precipitation is below the 5th percentile or above the 95th percentile of observed annual precipitation.

Time-period	Scenario	Frequency	
		Precipitation	
1980 - 2009	Historical	2	2
2040 - 2069	CT	2	2
	HD	2	1
	HW	2	2
	WD	2	1
	WW	1	3
2055 -2084	CT	5	2
	HD	6	1
	HW	4	3
	WD	7	1
	WW	2	3
2070 -2099	CT	3	0
	HD	11	0
	HW	1	3
	WD	10	0
	WW	0	3

Notes:

- *The 5th percentile of basin-average observed annual precipitation is 25.0 inches*
- *The 95th percentile of basin-average observed annual precipitation is 69.2 inches.*

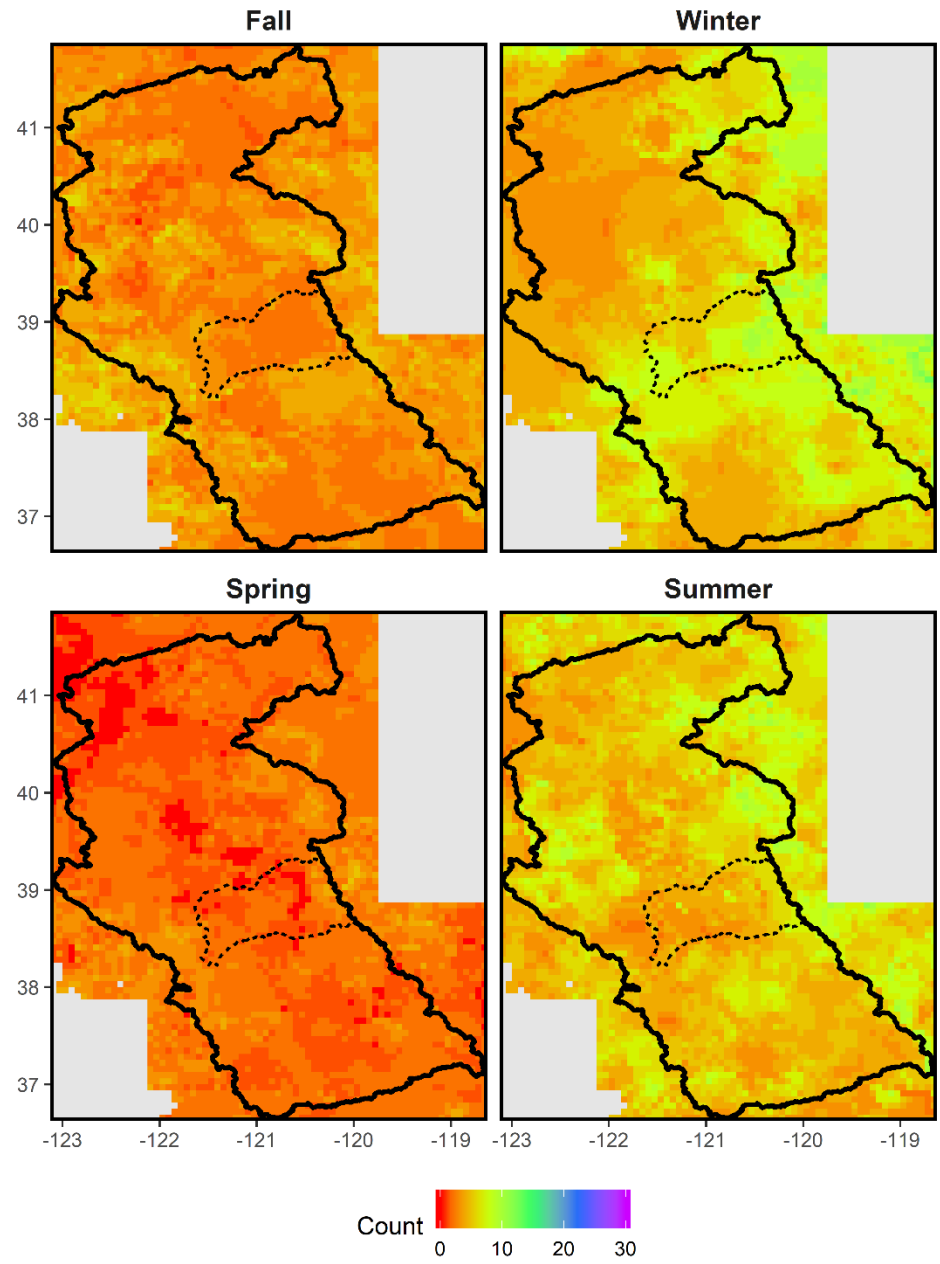

Figure 51. Spatial distribution of the frequency of extreme wet seasonal precipitation over a 30-year period under the **Hot-Wet (HW)** scenario for the future period 2070-2099. Extreme wet seasonal precipitation is defined as seasonal precipitation exceeding the 95th percentile of observed seasonal precipitation during the historical reference period (1980-2009). The CalSim3 domain is delineated by the black solid line and the ARBS study area is delineated by the black dashed line.

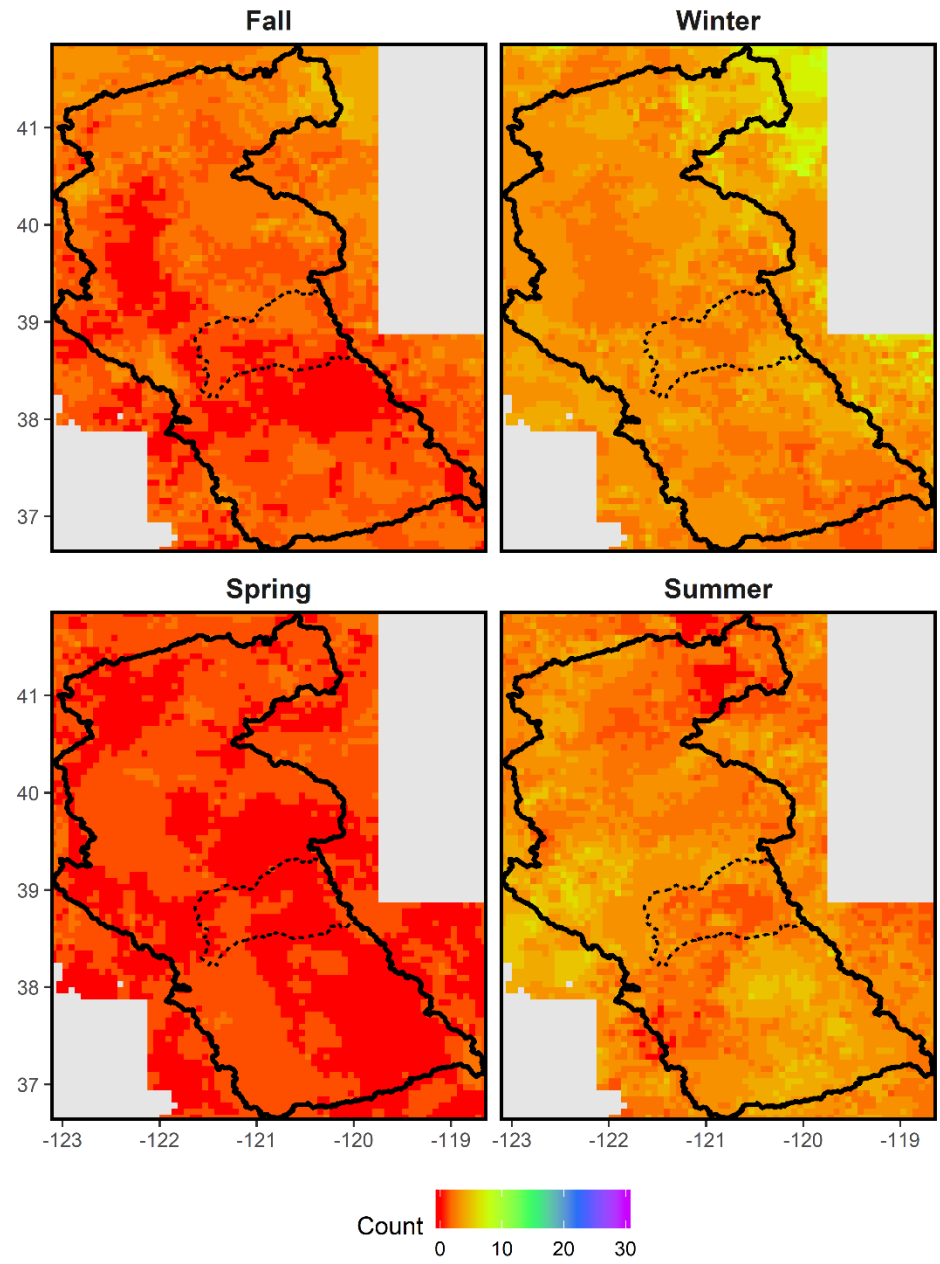

Figure 52. Spatial distribution of the frequency of extreme wet seasonal precipitation over a 30-year period under the **Hot-Dry (HD)** scenario for the future period 2070-2099. Extreme wet seasonal precipitation is defined as seasonal precipitation exceeding the 95th percentile of observed seasonal precipitation during the historical reference period (1980-2009). The CalSim3 domain is delineated by the black solid line and the ARBS study area is delineated by the black dashed line.

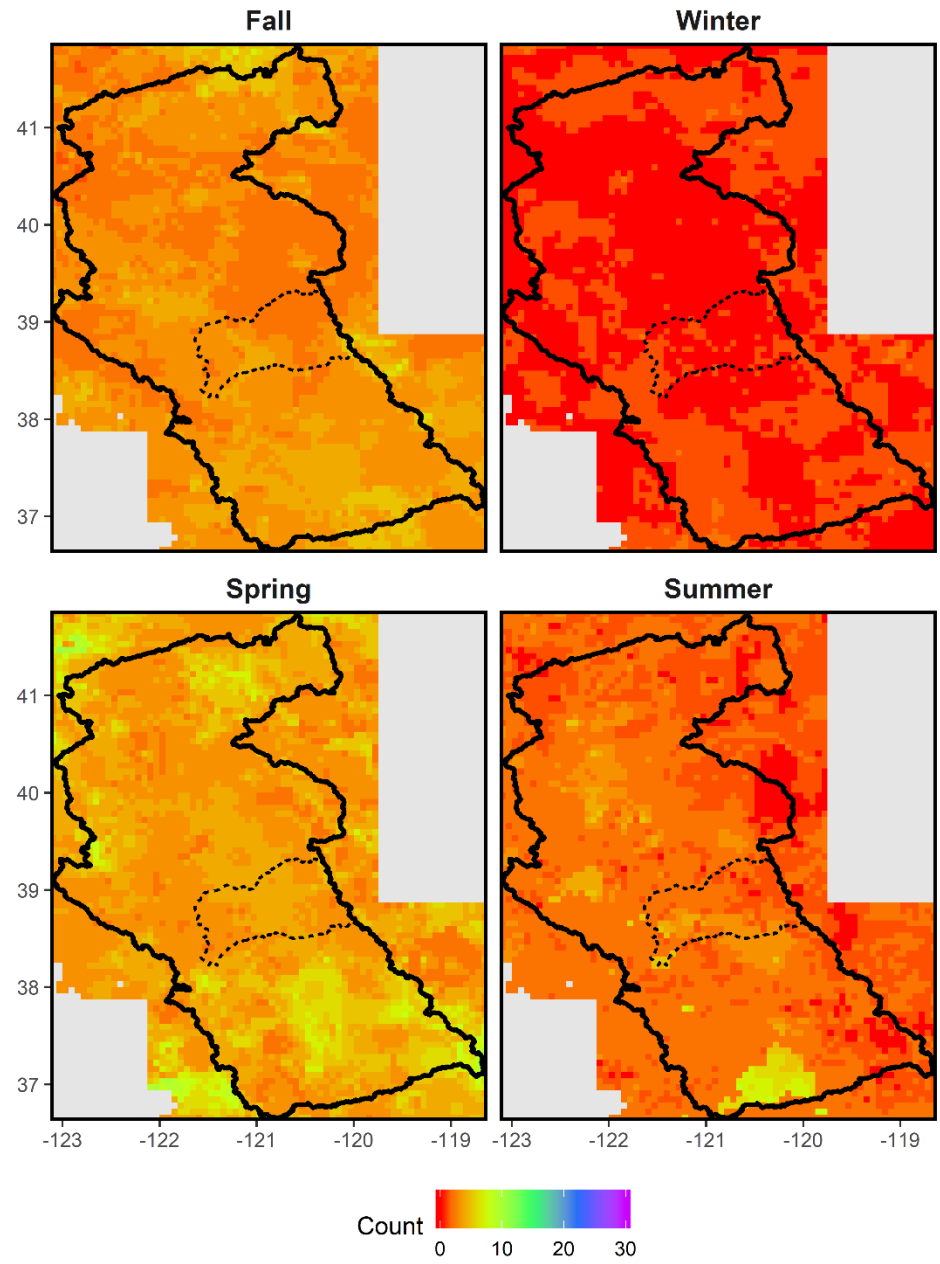

Figure 53. Spatial distribution of the frequency of extreme dry seasonal precipitation over a 30-year period under the **Hot-Wet (HW)** scenario for the future period 2070-2099. Extreme dry seasonal precipitation is defined as seasonal precipitation less than the 5th percentile of observed seasonal precipitation during the historical reference period (1980-2009). The CalSim3 domain is delineated by the black solid line and the ARBS study area is delineated by the black dashed line.

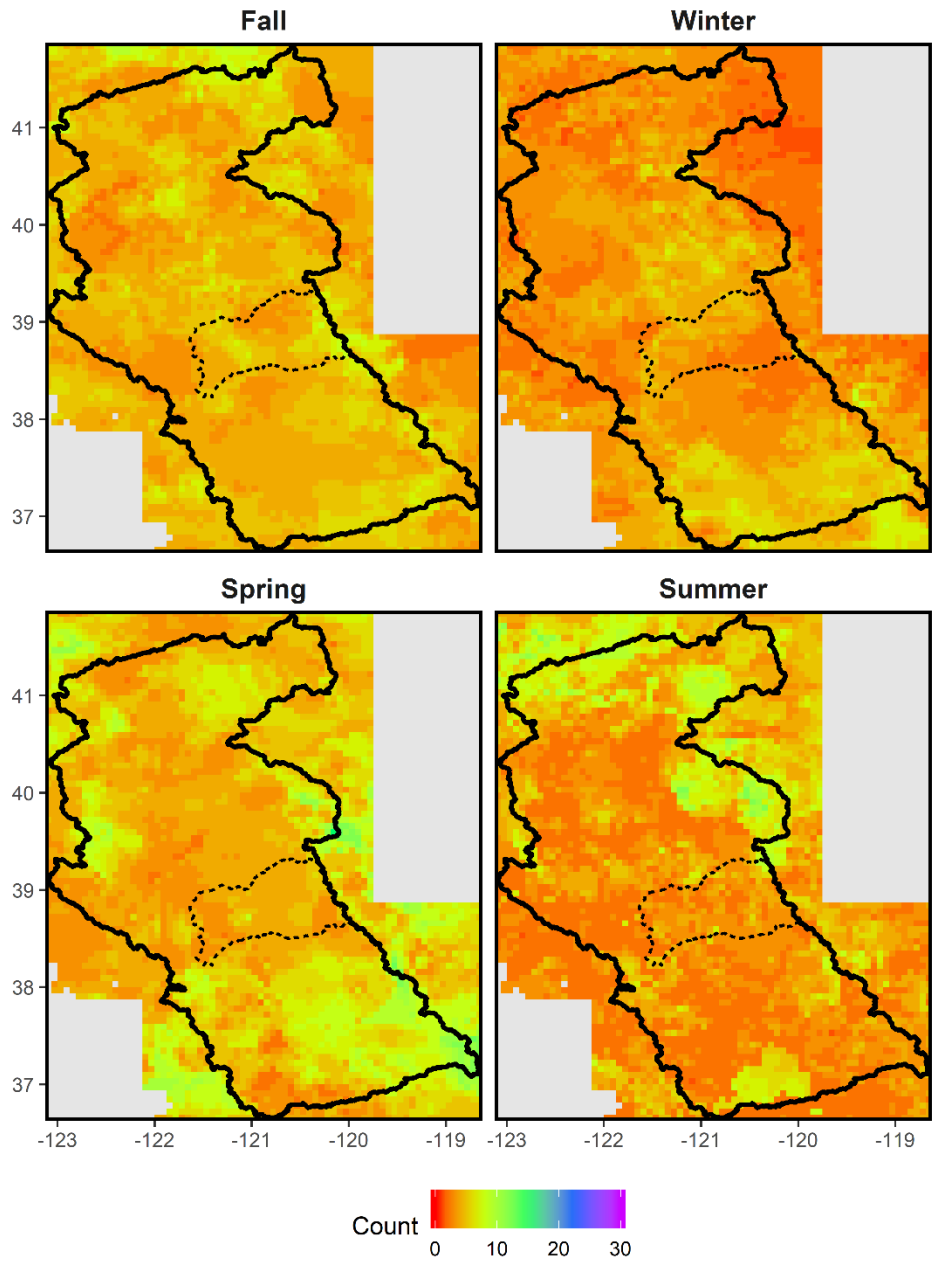

Figure 54. Spatial distribution of the frequency of extreme dry seasonal precipitation over a 30-year period under the **Hot-Dry (HD)** scenario for the future period 2070-2099. Extreme dry seasonal precipitation is defined as seasonal precipitation less than the 5th percentile of observed seasonal precipitation during the historical reference period (1980-2009). The CalSim3 domain is delineated by the black solid line and the ARBS study area is delineated by the black dashed line.

5 ARBS Hydrology Scenarios

A suite of hydrology scenarios was developed to evaluate the effects of climate change on water supplies and demands in the ARBS study area and the CalSim3 domain (Figure 1). Hydrology scenarios were developed by using the Variable Infiltration Capacity (VIC) hydrology model to simulate hydrologic conditions under each of the climate scenarios and future time periods considered in the Basin Study (see Section 4). The VIC hydrology model is a large-scale, semi-distributed hydrologic model that simulates the surface water balance at each grid cell, including infiltration and soil moisture storage, evaporation and transpiration, and surface runoff and baseflow. Hydrology scenarios were used to develop streamflow inputs to the CalSim3 water resources planning model, which was then used to evaluate changes in water supplies, demands, and management throughout the Central Valley Project and State Water Project, including the ARBS Study Area.

This section describes the hydrology scenarios used to analyze future water supplies, demands, and management in the ARBS study area and surrounding region. The VIC model and the hydrology scenario methodology area described in Section 5.1 and the resulting hydrology scenarios are characterized in Section 5.2.

5.1 Hydrology Scenario Methodology

Hydrology scenarios were developed by using the VIC hydrology model to simulate hydrologic conditions under each of the ARBS climate scenarios. The VIC model is a large-scale, semi-distributed hydrology model developed by researchers at the University of Washington and Princeton University in collaboration with researchers from around the world (Liang et al. 1994, Nijssen et al. 1997, Lohmann et al. 1998). VIC simulates the land surface water balance, including evapotranspiration and runoff, on a rectilinear grid. Streamflow can be then computed by routing surface runoff and baseflow from the VIC model grid using a routing model.

VIC has two distinguishing features compared to most other large-scale hydrologic models. First, VIC represents sub-grid variability in soil moisture storage capacity as a spatial probability distribution. Second, VIC represents baseflow as a non-linear function of soil moisture in the lowest soil layer. Spatial variability in soil properties at scales smaller than the model grid scale is therefore represented statistically, without assigning soil parameters to specific sub-grid locations. These features allow VIC to represent surface runoff and baseflow under a wide range of land surface conditions. VIC has been widely applied to analysis of large-scale hydrologic conditions, including simulation of historical hydrologic conditions (Abdulla et al. 1996, Maurer et al. 2001, Livneh et al. 2013) as well as simulation of hydrologic conditions under future climate projections or scenarios (Hamlet and Lettenmaier 1999 [Climate Change], Nijssen et al. 2001,

Beyenne et al. 2009, Cuo et al. 2009). VIC has also been used to develop seasonal hydrologic forecasts (Hamlet and Lettenmaier 1999, Hamlet and Lettenmaier 2000, Wood et al. 2002, Wood et al. 2005, Wood and Lettenmaier 2007).

Static model inputs represent physical properties at each grid cell, including land surface elevation, soil properties, land cover and vegetation properties, and parameters related to surface runoff and baseflow. Time-varying model inputs include timeseries of daily precipitation, daily maximum temperature, daily minimum temperature, and daily average wind speed at each model grid cell.

The ARBS hydrology scenarios were developed using the VIC model version 4.2.b. The VIC model was configured on the same 1/16 degree (approximately 6 km) grid as the Livneh observed historical climate dataset and the LOCA bias corrected and downscaled climate projections. Static model inputs were obtained from an existing VIC model for the state of California that was developed by the California Water Commission in support of the Water Storage Investment Program (CWC 2016). Static model inputs were previously calibrated to closely match historical streamflows over the period 1970-2003 for twelve major streamgages throughout the Sacramento and San Joaquin river basins. Model parameters adjusted during calibration included parameters describing the rates of infiltration and baseflow as a function of soil property, along with the soil layer depths. Calibration was carried out by the California Water Commission; no additional calibration was carried out as part of the ARBS. It should be noted that streamflows simulated by the VIC model are considered naturalized flows as they do not include the effects of water management, including storage, diversions, imports, and other water management actions; calibration was therefore based on full natural flows rather than observed streamflows (Vano et al. 2012, Hamlet et al. 2013, CWC 2016).

Time-varying model inputs were developed from the Livneh observed historical climate dataset (see Section 2) and the ARBS baseline and future climate scenarios (see Section). ARBS climate scenarios were developed at a monthly time step using the HDe scenario methodology (see Section 4.1); however, VIC requires daily inputs of precipitation, maximum temperature, minimum temperature, and wind speed.

Daily precipitation inputs for each scenario were developed by disaggregating monthly precipitation from the scenario based on the distribution of daily precipitation during the corresponding month in the merged Livneh dataset (see Section 2.1) according to Equation 3:

$$p^*_{ymd} = P^*_{ym} \cdot \left(\frac{p_{ymd}}{P_{ym}}\right) \quad (3)$$

Where p^*_{ymd} is the daily precipitation under a given future climate scenario for year *y*, month *m,* and day *d*; P^*_{ym} is the monthly total precipitation under that future scenario for year *y* and month *m*; p_{ymd} is the daily precipitation from the

merged Livneh observational dataset for year *y*, month *m*, and day *d*; and P_{ym} is the monthly total precipitation from the merged Livneh observational dataset for year *y* and month *m*. This approach assumes that the distribution of monthly precipitation over days within that month—i.e., the fraction of monthly total precipitation that occurs on each day of the month—under all future climate scenarios is consistent with the observed distribution during that month from the merged Livneh dataset.

It should be noted that this assumption results in the same frequency of precipitation under future scenarios does not reflect potential changes in the frequency and intensity of precipitation events: precipitation frequency in all future scenarios is identical to observed historical precipitation frequency, and precipitation intensity is scaled according to the monthly change factors applied in developing each future scenario.

Similar to daily precipitation inputs, daily maximum temperature inputs for each scenario were developed by disaggregating monthly mean maximum temperatures. Monthly mean maximum temperatures were disaggregated based on the distribution of daily maximum temperature departures in the merged Livneh dataset (see Section 2.1) during a given month from the monthly mean for that month according to Equation 4:

$$tmax^{*}_{ymd} = Tmax^{*}_{ym} + \left(Tmax_{ym} - tmax_{ymd}\right) \quad (4)$$

Where $tmax^{*}_{ymd}$ is the daily maximum temperature under a given future climate scenario for year *y*, month *m*, and day *d*; $Tmax^{*}_{ym}$ is the monthly mean maximum temperature under that future scenario for year *y* and month *m*; $tmax_{ymd}$ is the daily maximum temperature from the merged Livneh observational dataset for year *y*, month *m*, and day *d*; and $Tmax_{ym}$ is the monthly mean maximum temperature from the merged Livneh observational dataset for year *y* and month *m*. Similar to the disaggregation of monthly precipitation, this approach assumes that the distribution of daily departures in daily maximum temperature from the corresponding monthly mean—i.e., the difference between the daily maximum temperature and the monthly mean maximum temperature—under all future climate scenarios is consistent with the observed distribution during that month from the merged Livneh dataset.

Lastly, daily minimum temperature inputs for each future scenario are computed as the daily maximum temperature minus the diurnal temperature range (DTR). Monthly mean DTR under future each future climate scenario was developed using the HDe methodology as described in Section. Monthly mean DTR for each scenario is then disaggregated using the same approach used to disaggregate monthly mean maximum temperature (Equation 2; see above). Daily minimum temperature was subsequently computed by subtracting the daily DTR from the corresponding daily maximum temperature.

Historical daily wind speed from the merged Livneh dataset (see Section 2.1) was used for all ARBS scenario, including the baseline scenario and all future scenarios. Downscaled projections of future wind speed are not available to inform future scenarios of windspeed.

5.2 Future Hydrology Scenarios

Future hydrology scenarios were developed to represent hydrologic conditions over the ARBS study area and the extent of the CVP-SWP system under each of the ARBS climate scenarios. The ARBS hydrology scenarios were evaluated to characterize the range of future hydrologic conditions represented in the Basin Study. Evaluation focuses on potential evapotranspiration (PET), snow water equivalent (SWE), and total runoff. PET is a as an key indicator of landscape water demands, including consumptive use by evaporation and transpiration from bare soil, water surfaces, native vegetation, and crops. SWE is a key indicator of water supplies in the region, where runoff from many watersheds is dominated by snowmelt. Lastly, runoff is a direct indicator of the water supply available to the CVP-SWP system. Similar to observed historical climate, LOCA projections, and future climate scenarios, future hydrology scenarios were evaluated on a $1/16^{th}$ degree grid and averaged over the ARBS study area, the CalSim3 domain, and selected basins. Selected basins considered in evaluating and characterizing the ARBS climate scenarios are illustrated in Figure 12.

5.2.1 Potential Evapotranspiration

Potential evapotranspiration (PET) is the estimated amount of evapotranspiration that would occur if a sufficient water source were available—i.e., in the absence of limitations from soil moisture, vapor pressure deficit, temperature, or solar insolation. VIC computes PET as the area-weighted sum of potential transpiration and potential soil evaporation from each model grid cell. PET is commonly used to evaluate the impacts of climate change on consumptive use of water from the landscape, including evaporation from bare soil and water surfaces, evapotranspiration from native vegetation, and evapotranspiration from crops.

The spatial distribution of changes in average annual PET between the observed historical baseline and the ARBS climate scenarios are illustrated in Figure 55. Average annual PET increases throughout the CalSim3 domain under all scenarios for all future time periods. PET is strongly correlated with air temperature. PET is thus expected to increase more under the hot scenarios (HD, HW) than under the warm scenarios (WD, WW). PET increases by approximately 4-6 inches per year under the hot scenarios compared to 2-3 inches per year under the warm scenarios (Table 6). Similar to changes in annual average temperature, changes in PET are relatively uniform over the region.

The spatial distribution of average seasonal PET from the baseline scenario and the hot-wet (HW) scenario for the future period 2070-2099 is illustrated in Figure

56. The difference average seasonal in PET between the historical baseline and the hot-wet scenario for the 2070-2099 future period are illustrated in Figure 57. The spatial distribution of average seasonal PET under all future scenarios is similar to the observed historical baseline, with lower PET during the fall and winter seasons and in the higher elevation mountain areas, and higher PET during supper and spring seasons and in the lower elevation Central Valley. The largest change in PET between the historical baseline and future scenarios occur during spring and summer seasons, with little change in PET during winter and fall particularly in the higher-elevation mountain areas. The spatial and seasonal distribution changes in PET are consistent across all future scenarios and time periods.

Timeseries of basin-average seasonal and annual PET over the ARBS study area are illustrated in Figure 58 and Figure 60, respectively. Similar to future climate scenarios, future hydrology scenarios preserve the interannual variability from the historical baseline (i.e., sequencing and duration of wet and dry periods and warmer and cooler periods). The interannual variability of PET is therefore similar across all scenarios, with shifts upward under all future scenarios reflecting the increase in PET under future scenarios. The upward shift in PET is greatest under the hot scenarios (HD, HW) and under the latest future time period (2070-2099), consistent with the relative change in temperature across scenarios and time periods.

Table 6. Differences in basin-average annual average potential evapotranspiration (PET), snow water equivalent (SWE), and total runoff between baseline and future hydrology scenarios over the ARBS study area.

Time-period	Scenario	PET (in)	SWE (in)	Runoff (TAF)
2040 - 2069	CT	2.7	-2.8	-2.0
	HD	3.7	-3.4	-205.8
	HW	3.4	-3.3	142.6
	WD	2.2	-2.2	-185.1
	WW	1.6	-2.3	70.7
2055 -2084	CT	4.1	-3.5	-93.1
	HD	5.0	-3.8	-184.6
	HW	4.2	-4.0	176.9
	WD	2.8	-2.6	-211.8
	WW	2.0	-2.5	199.4
2070 -2099	CT	3.9	-3.3	-54.4
	HD	6.2	-4.3	-202.8
	HW	4.5	-4.1	366.3
	WD	3.2	-2.7	-272.5
	WW	1.8	-2.9	486.0

Notes:

- *PET = annual mean potential evapotranspiration (short grass), SWE = annual maximum snow water equivalent, Runoff = annual total runoff, CT = Central Tendency, HD = Hot-Dry, HW = Hot-Wet, WD = Warm-Dry, WW = Warm-Wet.*
- *Projected change was calculated by comparing annual mean basin-average PET, SWE, and runoff over the ARBS study area between Baseline and future hydrology scenarios.*
- *Annual mean basin-average values under the Baseline scenario for the period 1915-2015 are as follows: PET = 42.8 inches; SWE = 5.7 inches; runoff = 1,458 thousand acre-feet.*

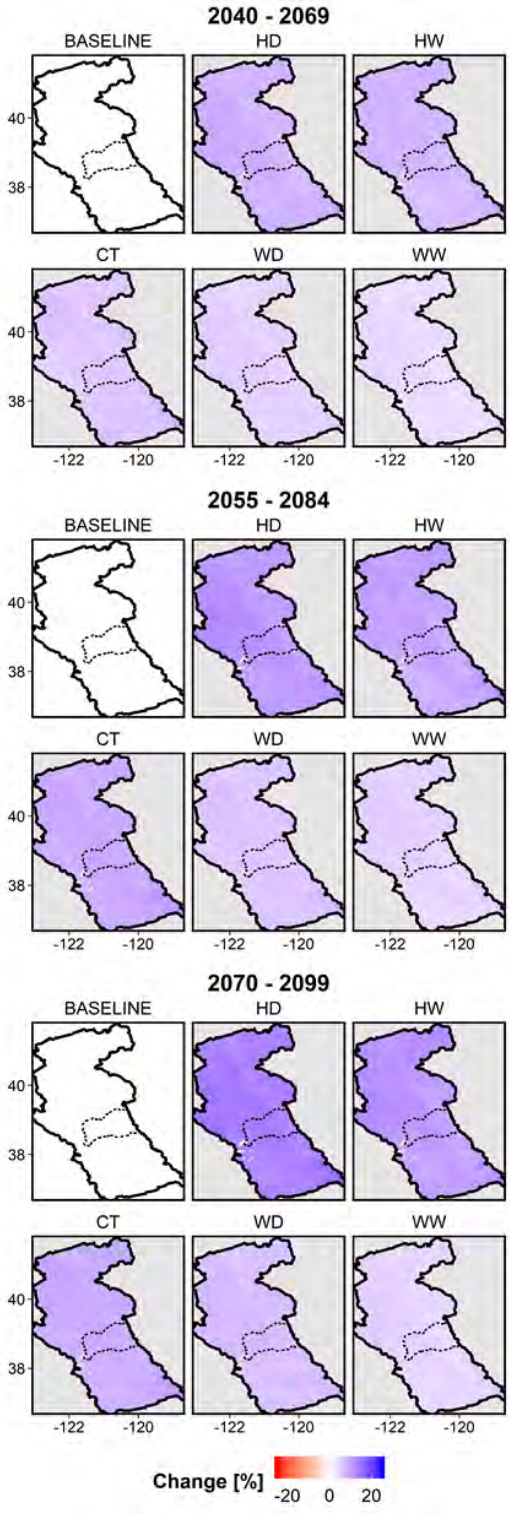

Figure 55. Spatial distribution of difference in average annual PET under future scenarios compared to the historical baseline. The CalSim3 domain is delineated by the black solid line and the ARBS study area is delineated by the black dashed line.

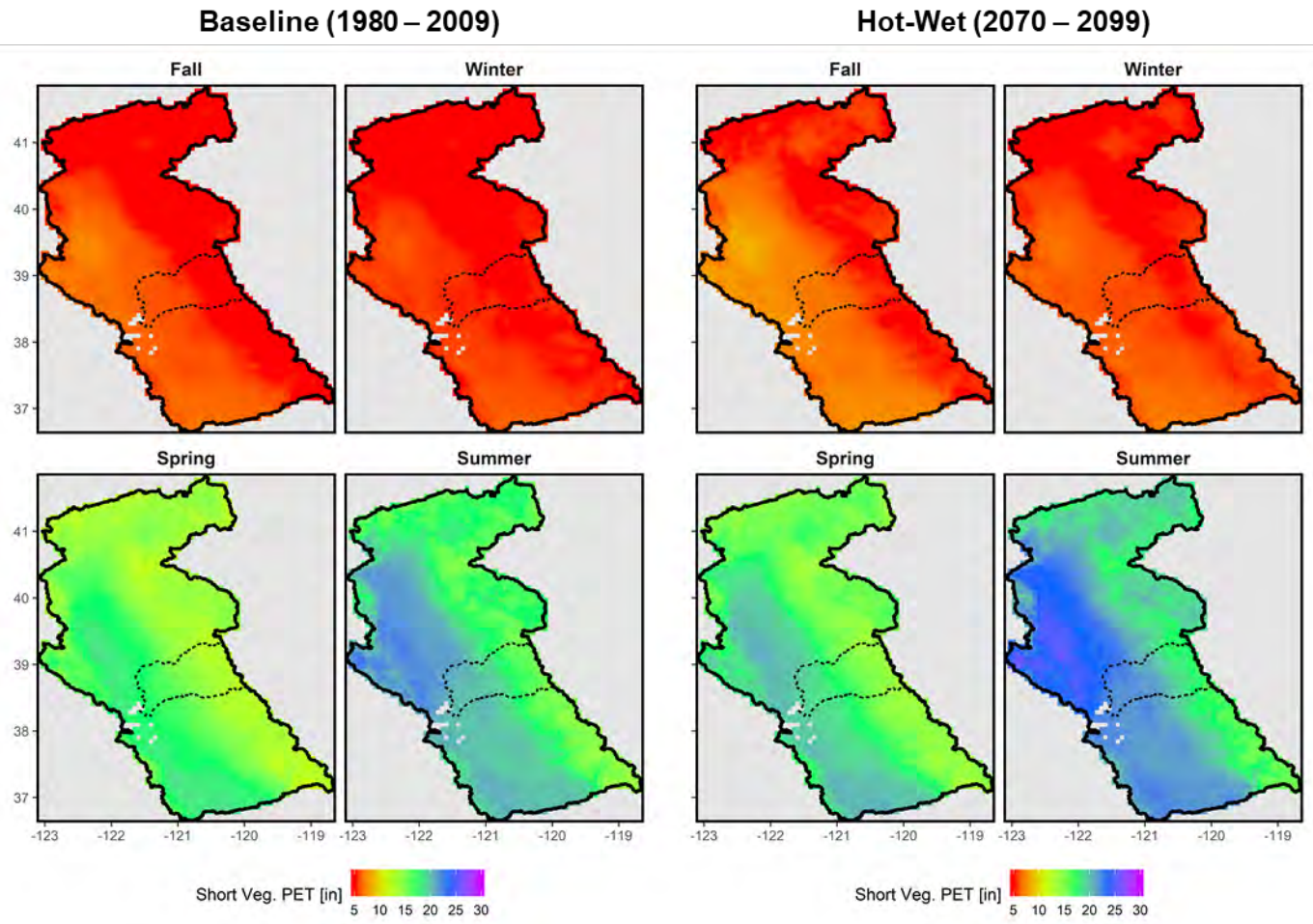

Figure 56. Spatial distribution of average seasonal PET under the historical baseline (left) and the **Hot-Wet** scenario for the future period 2070-2099 (right). The CalSim3 domain is delineated by the black solid line and the ARBS study area is delineated by the black dashed line.

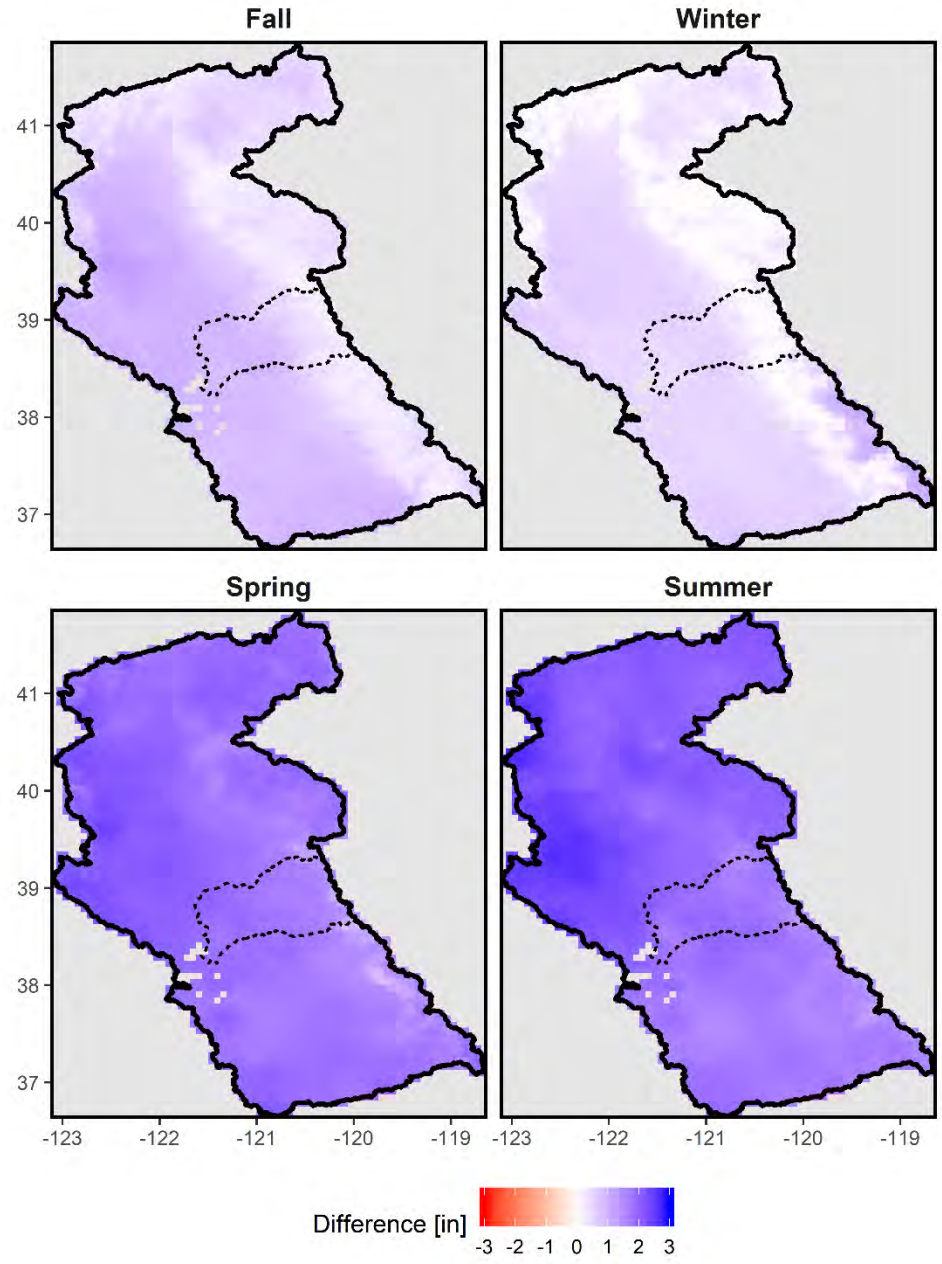

Figure 57. Spatial distribution of the difference in average seasonal PET between the historical baseline and the **Hot-Wet** scenario for the future period 2070–2099. The CalSim3 domain is delineated by the black solid line and the ARBS study area is delineated by the black dashed line.

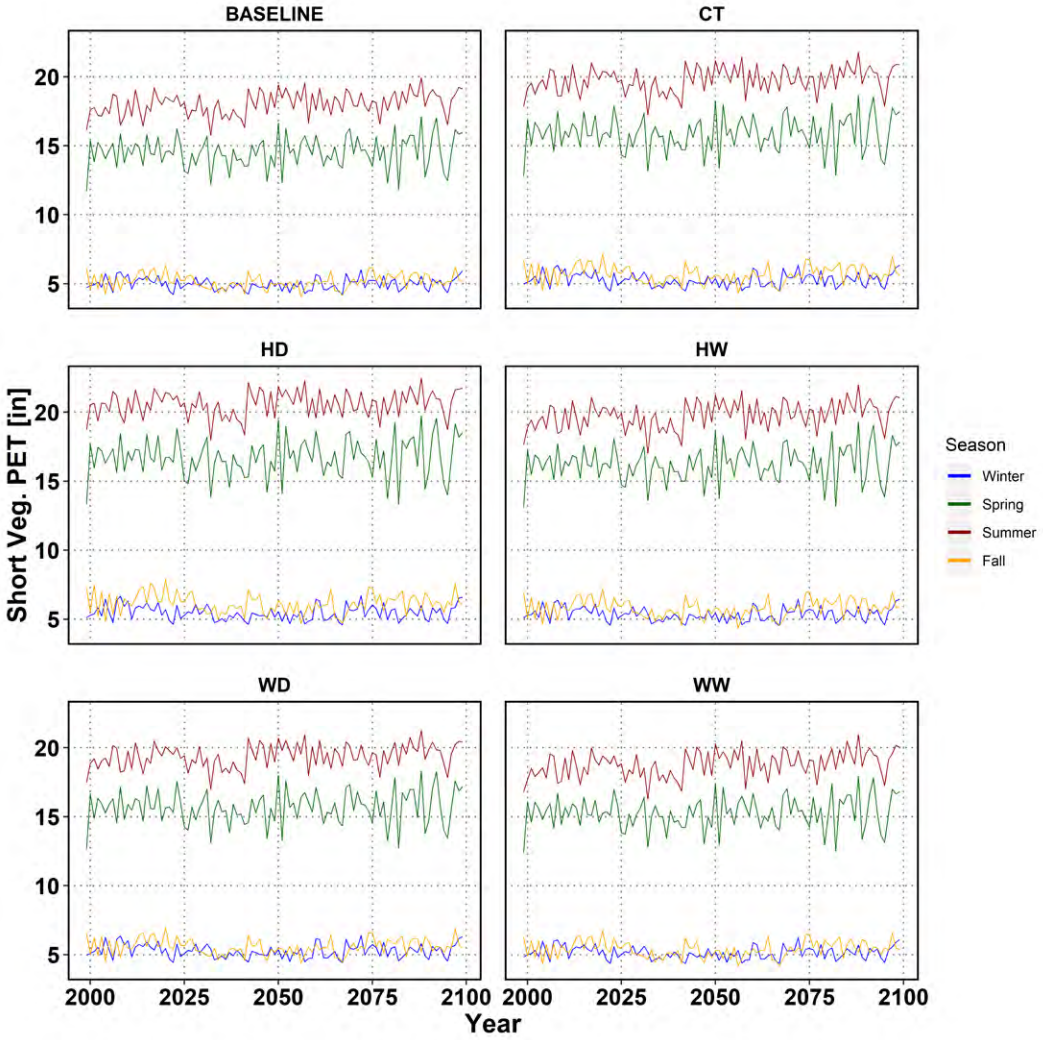

Figure 58. Timeseries of basin-average seasonal PET over the ARBS study area for the historical baseline and future scenarios for the future period 2070–2099. CT – central tendency, HD = Hot-Dry, HW = Hot-Wet, WW = Warm-Wet and WD = Warm-Dry. Color indicates season: blue = winter, green = spring, red = summer and orange = fall.

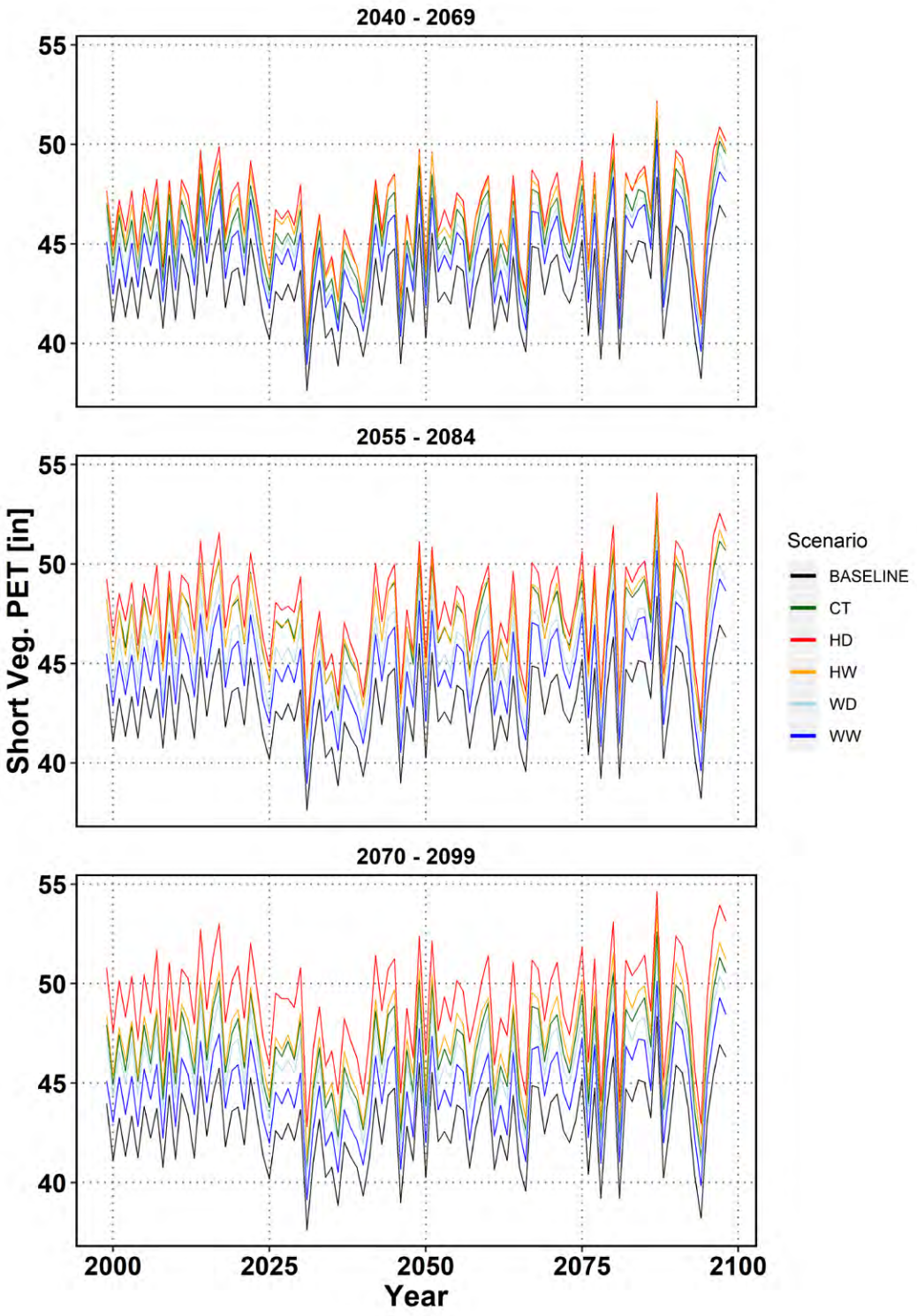

Figure 59. Timeseries of basin-average annual PET over the ARBS Study Area for the historical baseline and future scenarios for future periods 2040-2069, 2055-2084, and 2070-2099. CT – central tendency, HD = Hot-Dry, HW = Hot-Wet, WW = Warm-Wet and WD = Warm-Dry.

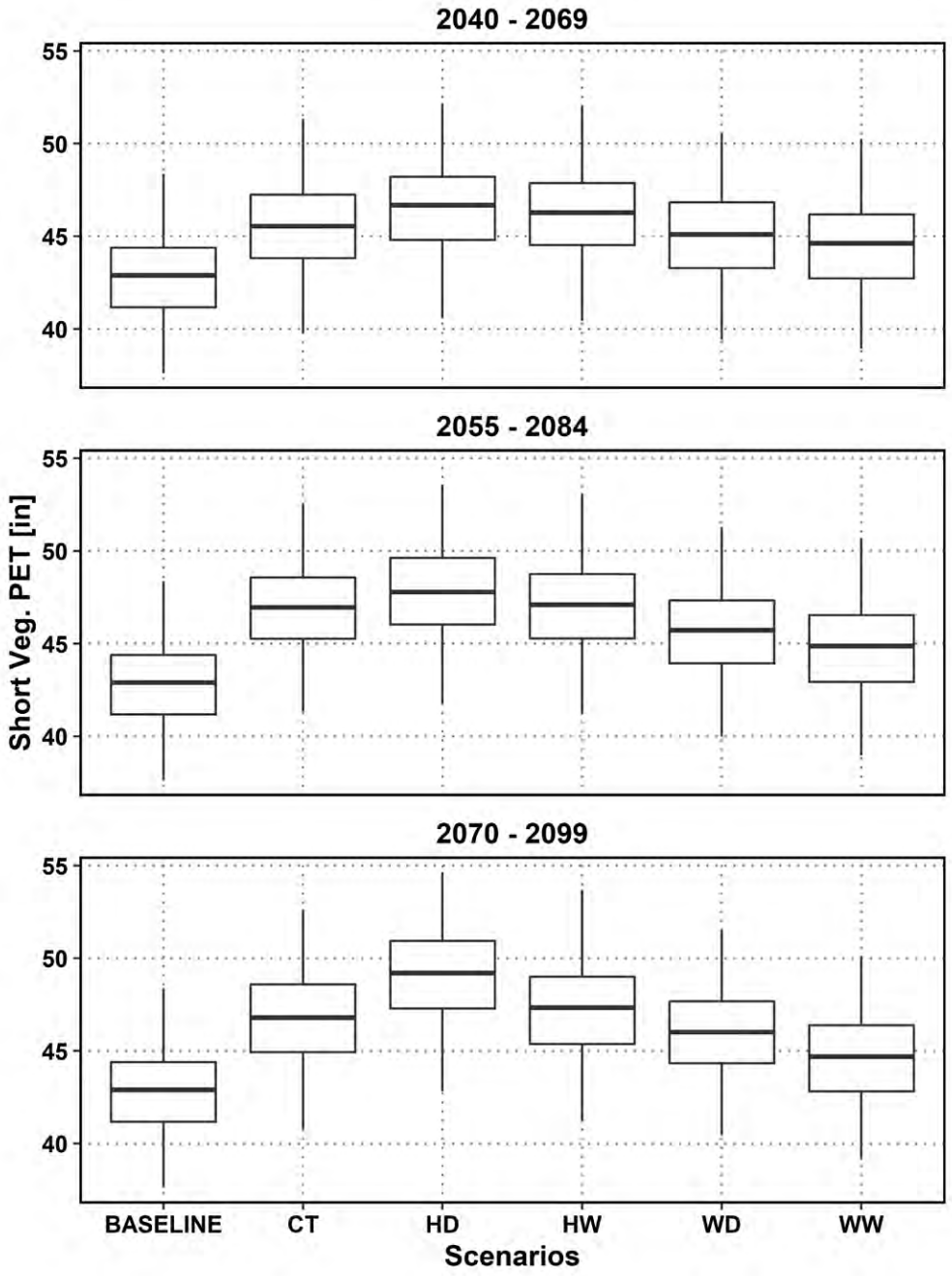

Figure 60. Boxplots of basin-average annual PET over the ARBS Study Area for the historical baseline and all future scenario for future periods 2040-2069, 2055-2084, and 2070-2099. Box limits represent the 25th and 75th quartiles; solid lines within each box represent the median; whiskers represent values extending from the 25th and 75th quartiles to values within ± 1.5*(Interquartile Range); and outliers are represented by solid black circles. CT – central tendency, HD = Hot-Dry, HW = Hot-Wet, WW = Warm-Wet and WD = Warm-Dry.

5.2.2 Future Snow Water Equivalent

Snow water equivalent (SWE) is the amount of water contained in snow and is theoretically the amount of water that would result if that snowpack was melted instantaneously. VIC estimates SWE at every timestep and grid cell by calculating the rain or snow fraction that is added to the snowpack and an energy flux balance to determine snowmelt.

SWE is projected to decrease in all future scenarios and time periods in all areas across the CalSim3 domain that received snow historically (Figure 61). Future SWE is projected to decrease by 2.7–4.3 inches on average over the ARBS study area (Table 6). This area-average change takes into account the portions of the study area located in the Central Valley and lower foothills that do not receive snow and therefore have a change of 0 inches. Areas that accumulate snow during the colder seasons are projected to have up to a 12 inch decrease in average annual SWE. Notably, snow accumulation in lower-elevation areas of the Sierra Nevada and Cascade Mountains is projected to decrease significantly. Many areas that experience relatively small or ephemeral snowpack under the baseline scenario are projected to lose all snowpack under some future scenarios. Loss of snowpack has significant implications for the amount and timing of runoff in the American River Basin and many other basins within the CalSim3 domain.

Figure 62 compares the spatial extent of baseline seasonal SWE conditions to the future hot-wet hydrology scenario during 2070 – 2099, highlighting the diminishing spatial area where snow is projected to accumulate in the future. Figure 63 shows this difference in inches, where many areas have up to a 20 inch decrease in seasonal snow averages. Areas with year-round snow are projected to have average SWE decrease by up to 50 inches during spring. Seasonality during each scenario is consistent with baseline conditions, where winter typically has the most SWE, followed by fall, spring and summer (Figure 64).

The projected interannual variability in SWE during the different hydrology scenarios is not the same as the interannual variability observed during baseline conditions (Figure 65). There is a much larger range in the baseline SWE distribution than any of the future hydrology scenarios (Figure 66). However, there are many more years with outliers, or significantly more snow than average conditions, during the projected future hydrology scenarios.

Maximum Snow Water Equivalent

Projected future trends in maximum SWE, or maximum snowpack, are very similar to those described above for SWE. All scenarios project a decrease in maximum SWE, with the largest decreases occurring in March and April (Figure 67 and Table 7). In the areas that receive snow, projected decreases in maximum SWE are up to 40 inches in March, April and May.

The 30-year average reduction in snowpack is projected to reach close to 79% by the end of the 21st century when comparing the hot-wet scenario to historic snow amounts in the Sacramento River Basin (Table 8). In contrast, the San Joaquin River Basin, which receives approximately four times the amount of snow as the Sacramento River Basin, is projected to have only a 33% reduction in snowpack when comparing the hot-wet scenario to historic snow levels. Overall, all basins are projected to experience reductions in annual snowpack levels ranging from 14 to 79% depending on location, future time period and future scenario. Higher elevation areas that receive snow are projected to have smaller reductions in snowpack than lower, warmer elevations that have historically received snow during the colder months.

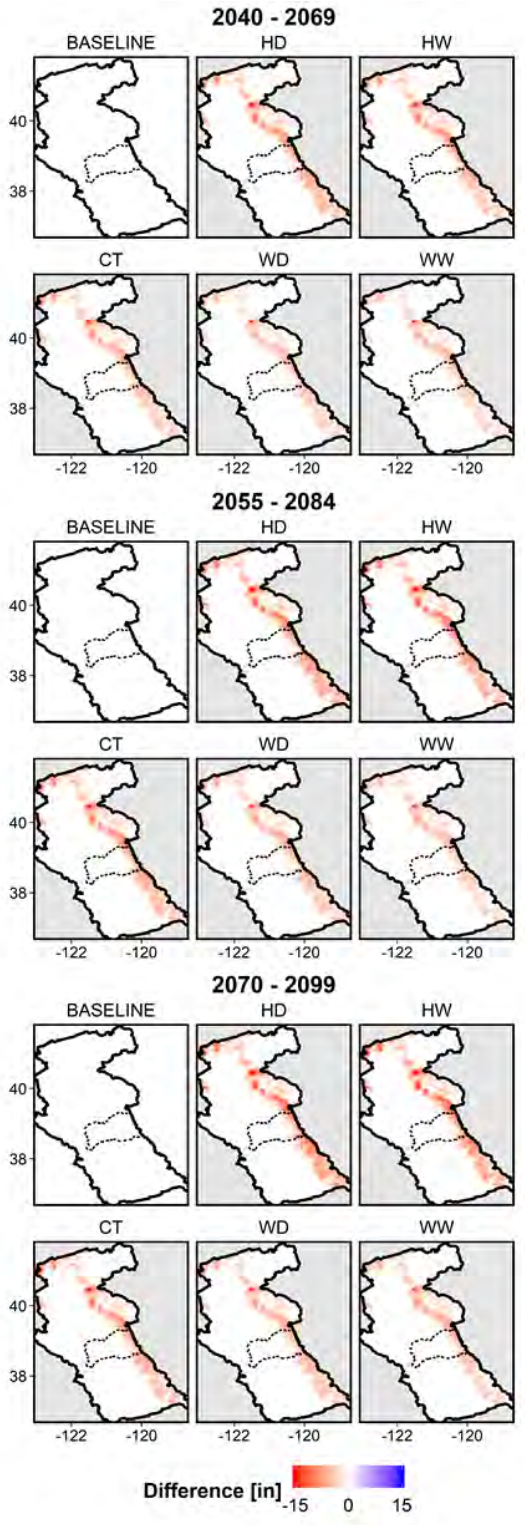

Figure 61. Projected change in 30-year average SWE from 1980-2009 (baseline) to the indicated future period for each climate scenario. CT – central tendency, HD = Hot-Dry, HW = Hot-Wet, WW = Warm-Wet and WD = Warm-Dry. The color scale indicates the difference in inches. Axes are longitudinal and latitudinal coordinates. The CalSim3 domain is delineated by the black solid line and the ARBS study area is delineated by the black dashed line.

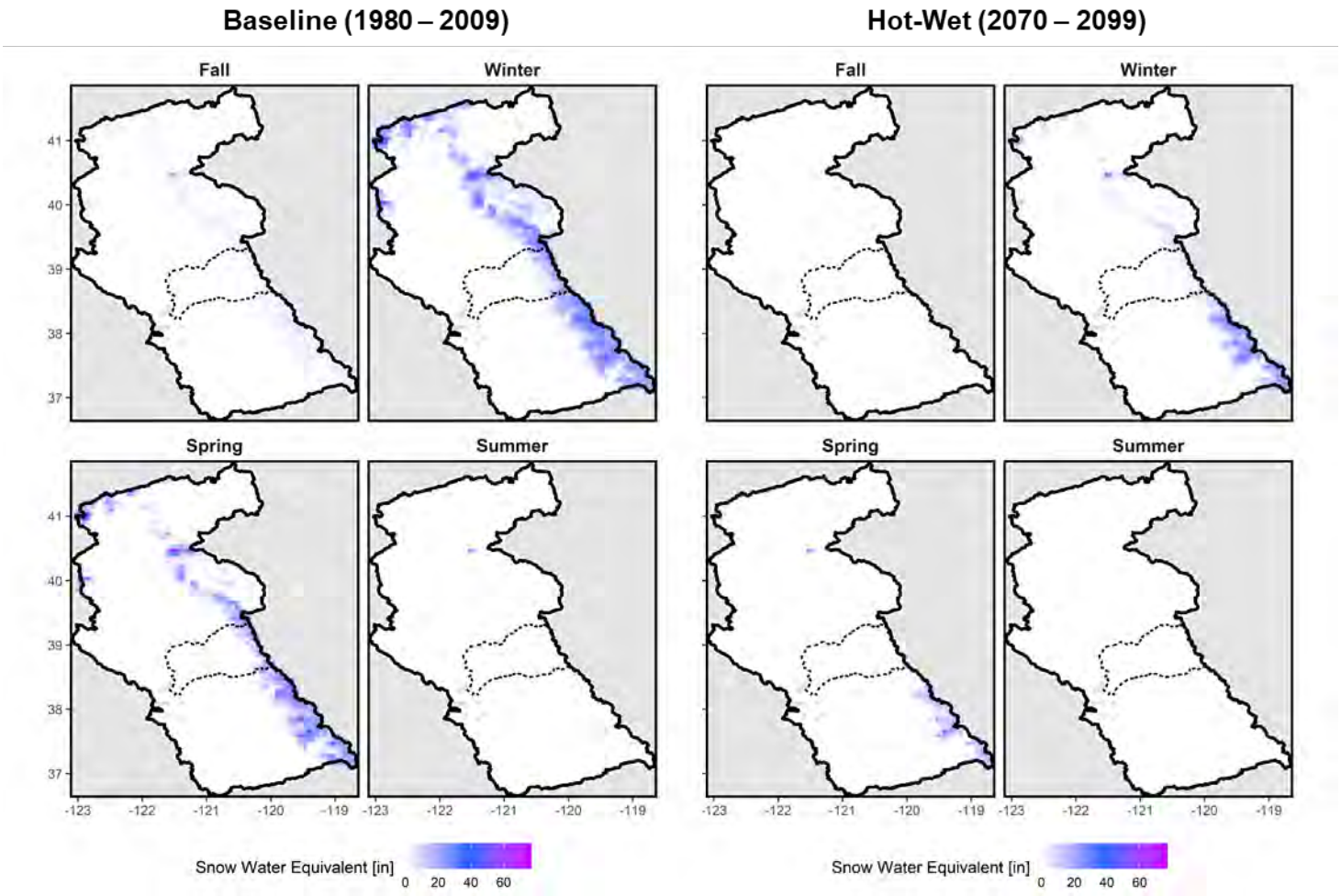

Figure 62. Spatial patterns of average seasonal SWE during baseline conditions (left) and the future hot-wet scenario (right) over the ARBS Study Area and CalSim3 domain. Axes are latitudinal and longitudinal coordinates. The color scale indicates the amount of SWE. The outline of the CalSim3 domain is delineated by the black solid line and the ARBS study area is delineated by the black dashed line.

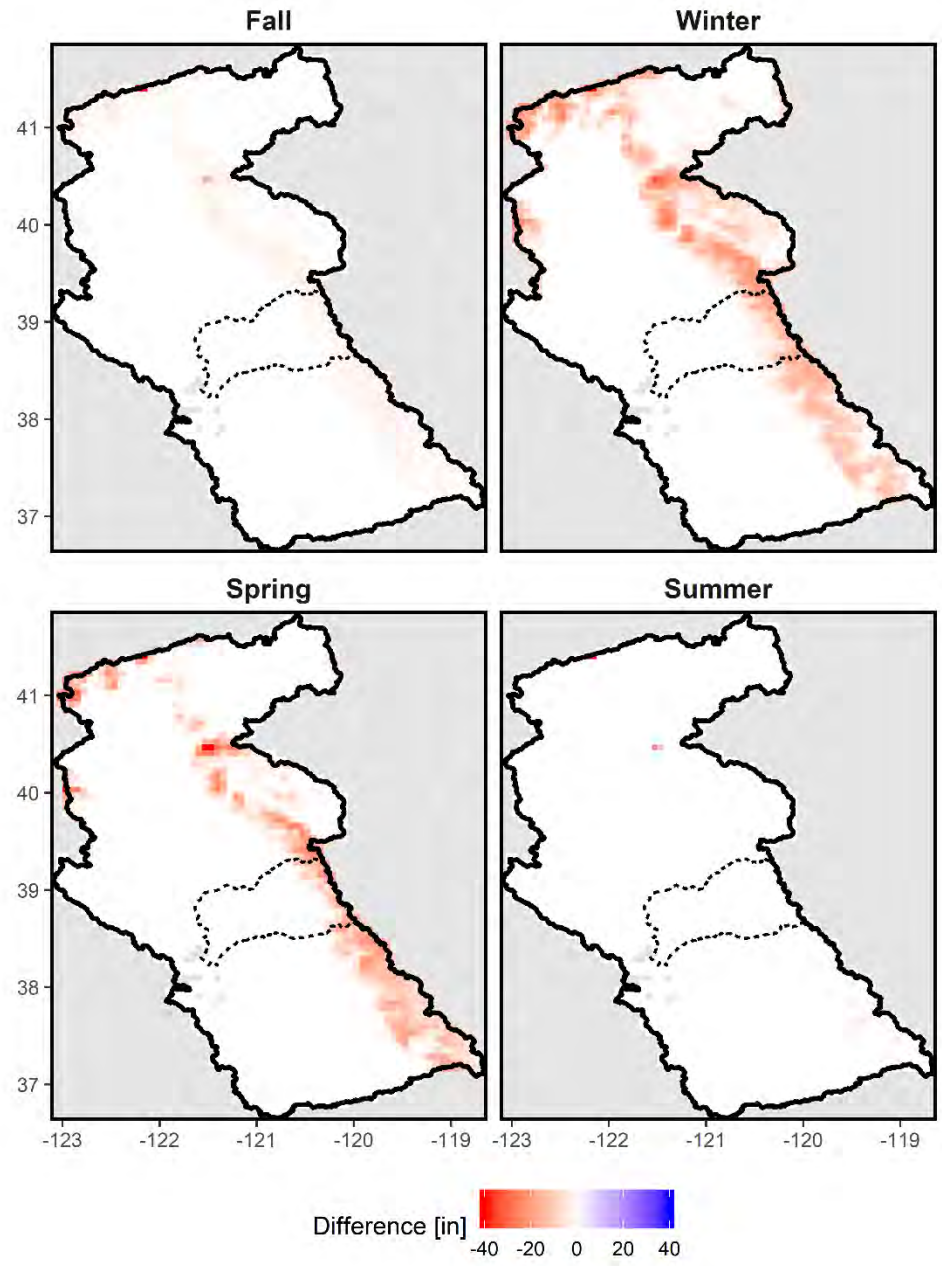

Figure 63. Spatial patterns of the difference in average seasonal SWE between the baseline period and the **Hot-Wet** scenario of 2070 – 2099 over the ARBS Study Area and CalSim3 domain. Axes are latitudinal and longitudinal coordinates. The color scale indicates the change in SWE between periods. The CalSim3 domain is delineated by the black solid line and the ARBS study area is delineated by the black dashed line.

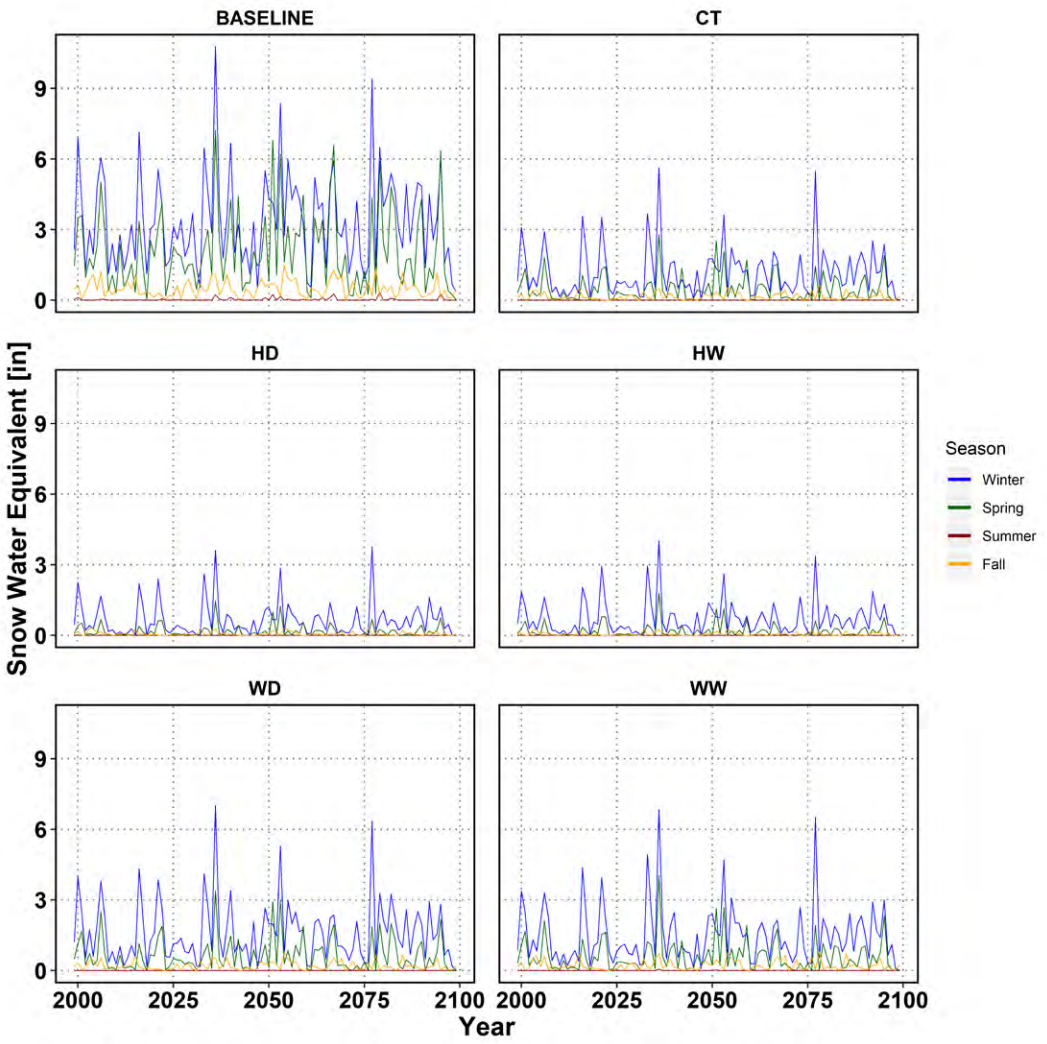

Figure 64. Projected future seasonal SWE in the ARBS study area for each scenario and the 2070 – 2099 time period. CT – central tendency, HD = Hot-Dry, HW = Hot-Wet, WW = Warm-Wet and WD = Warm-Dry. Color indicates season: blue = winter, green = spring, red = summer and orange = fall.

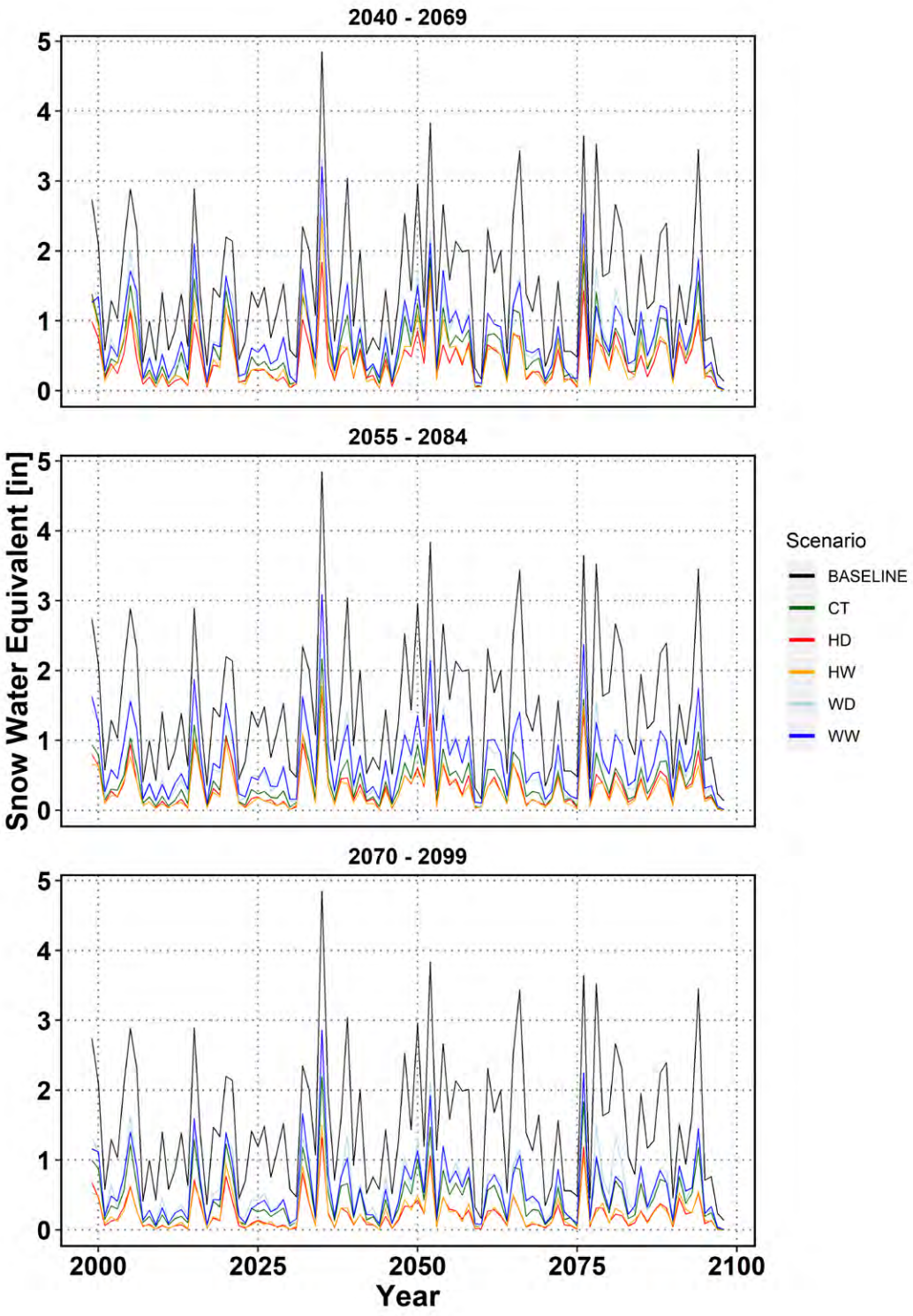

Figure 65. Projected future annual SWE in the ARBS Study Area for each scenario and future time period. CT – central tendency, HD = Hot-Dry, HW = Hot-Wet, WW = Warm-Wet and WD = Warm-Dry.

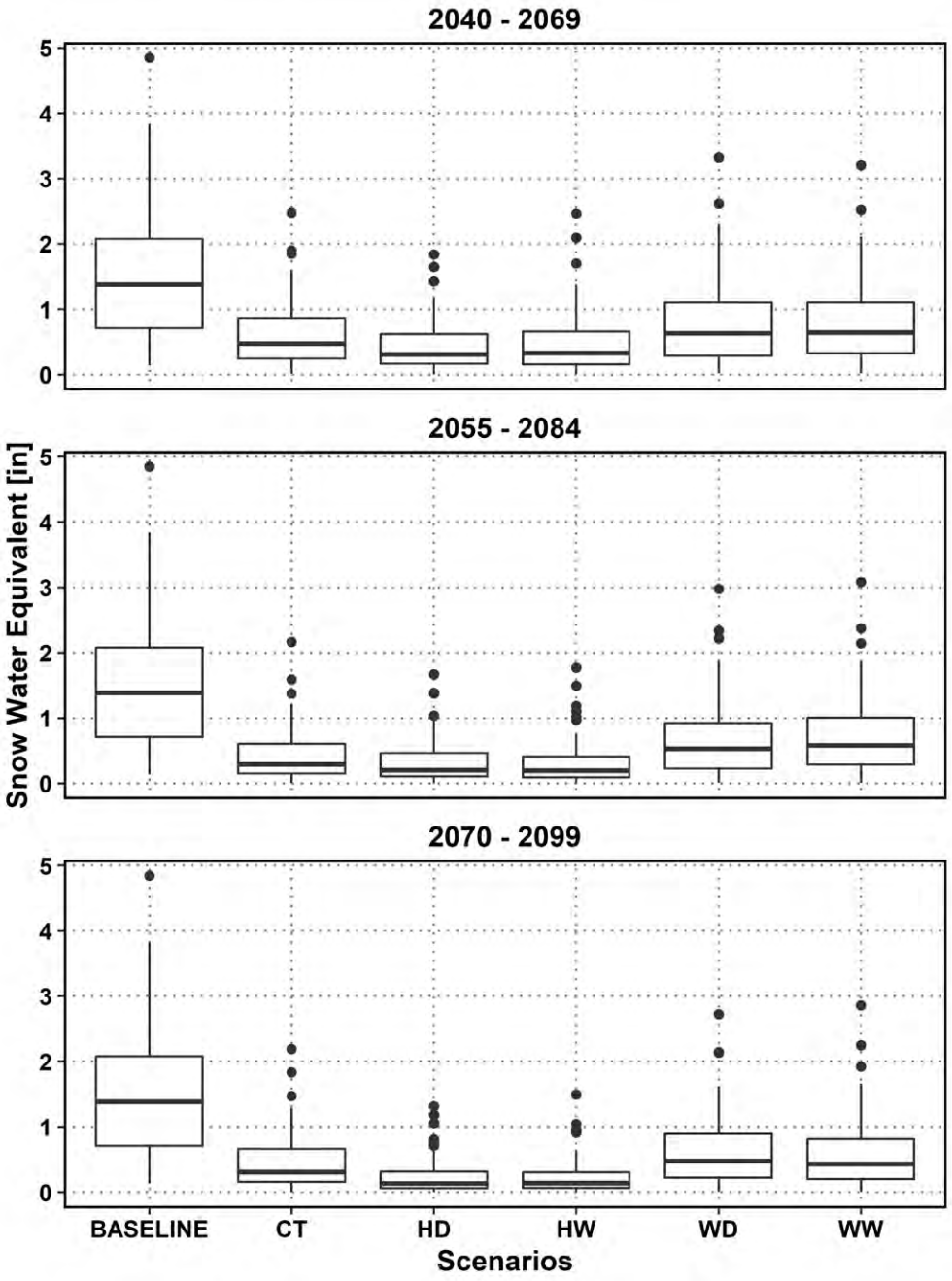

Figure 66. Distribution of baseline and scenario annual SWE during three future periods. Box limits represent the 25th and 75th quartiles; solid lines within each box represent the median; whiskers represent values extending from the 25th and 75th quartiles to values within ± 1.5*(Interquartile Range); and outliers are represented by solid black circles. CT – central tendency, HD = Hot-Dry, HW = Hot-Wet, WW = Warm-Wet and WD = Warm-Dry.

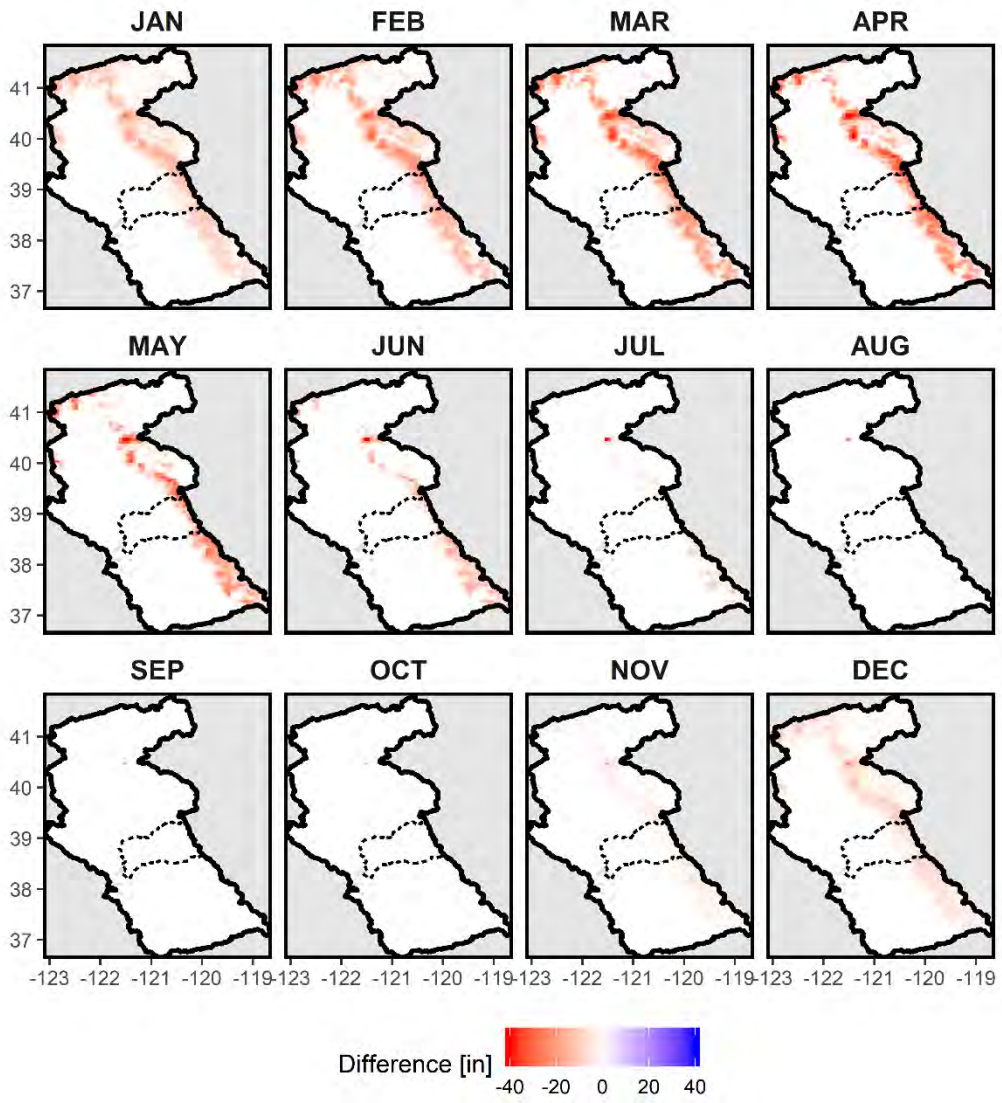

Figure 67. Spatial patterns of the difference in average monthly maximum SWE between the baseline period and the **Hot-Wet** scenario of 2070 – 2099 over the ARBS Study Area and CalSim3 domain. Axes are latitudinal and longitudinal coordinates. The color scale indicates the change in maximum SWE between periods. The CalSim3 domain is delineated by the black solid line and the ARBS study area is delineated by the black dashed line.

Table 7. Projected change in monthly maximum basin-average maximum SWE (inches) over the ARBS study area between baseline and future climate scenarios.

Time-period	Scenario	OCT	NOV	DEC	JAN	FEB	MAR	APR	MAY
2040 - 2069	CT	-0.1	-0.4	-1.0	-1.6	-2.2	-2.6	-2.6	-2.0
	HD	-0.1	-0.5	-1.5	-2.1	-2.6	-3.1	-3.0	-2.3
	HW	-0.1	-0.5	-1.1	-1.9	-2.6	-3.1	-3.0	-2.2
	WD	0.0	-0.3	-0.9	-1.4	-1.7	-2.0	-2.0	-1.6
	WW	0.0	-0.3	-0.7	-1.2	-1.7	-2.1	-2.2	-1.8
2055 - 2084	CT	-0.1	-0.5	-1.3	-2.1	-2.8	-3.1	-3.1	-2.3
	HD	-0.1	-0.6	-1.5	-2.2	-2.9	-3.5	-3.4	-2.5
	HW	-0.1	-0.5	-1.4	-2.3	-3.1	-3.6	-3.5	-2.6
	WD	0.0	-0.3	-0.8	-1.4	-2.0	-2.5	-2.5	-1.9
	WW	0.0	-0.3	-0.9	-1.4	-1.9	-2.3	-2.3	-1.8
2070 - 2099	CT	-0.1	-0.5	-1.2	-2.0	-2.6	-3.1	-3.0	-2.2
	HD	-0.1	-0.6	-1.6	-2.4	-3.3	-4.0	-3.8	-2.7
	HW	-0.1	-0.6	-1.6	-2.5	-3.1	-3.8	-3.7	-2.7
	WD	-0.1	-0.4	-1.1	-1.7	-2.0	-2.4	-2.5	-2.0
	WW	-0.1	-0.4	-1.0	-1.8	-2.2	-2.6	-2.7	-2.1

Notes:

- *CT = Central Tendency, HD = Hot-Dry, HW = Hot-Wet, WD = Warm-Dry, WW = Warm-Wet.*
- *Projected change was calculated by comparing monthly maximum basin-average SWE over the ARBS study area between Baseline and future hydrology scenarios.*
- *Red shading indicates the magnitude of change, with lighter shades indicating less change and darker shades indicating greater change.*

Table 8. Projected change in annual maximum basin-average SWE over the San Joaquin and Sacramento River Basins between baseline and future scenarios.

Time - Period	Scenario	San Joaquin River		Sacramento River	
		MAX SWE (inches)	Percent Change	MAX SWE (inches)	Percent Change
1980 - 2009	Baseline	19.2	-	7.4	-
2040 - 2069	CT	15.5	-19.2%	3.3	-55.9%
	HD	13.1	-31.9%	2.6	-65.4%
	HW	14.8	-23.0%	2.8	-62.5%
	WD	14.9	-22.5%	4.3	-42.1%
	WW	16.2	-15.5%	4.2	-43.3%
2055 -2084	CT	13.2	-31.2%	2.5	-65.6%
	HD	11.9	-38.1%	2.1	-71.8%
	HW	13.9	-27.6%	2.0	-72.9%
	WD	13.9	-27.7%	3.7	-50.3%
	WW	17.2	-10.3%	3.9	-46.8%
2070 -2099	CT	14.0	-27.0%	2.5	-66.1%
	HD	10.4	-46.0%	1.6	-78.6%
	HW	13.3	-30.8%	1.5	-80.1%
	WD	13.8	-28.2%	3.7	-50.5%
	WW	17.0	-11.6%	3.6	-51.6%

Notes:

- *CT = Central Tendency, HD = Hot-Dry, HW = Hot-Wet, WD = Warm-Dry, WW = Warm-Wet.*
- *Projected change was calculated by comparing annual maximum basin-average SWE over the San Joaquin and Sacramento River Basins between baseline and future hydrology scenarios.*

5.2.3 Future Runoff

Runoff occurs during precipitation events when the precipitation rate exceeds the infiltration capacity of the soil and surface runoff results. VIC calculates runoff for each timestep and grid cell and often a subsequent routing model is then used to determine routing of the runoff to streamflow locations.

Similar to the precipitation scenarios, there is a lot of uncertainty in projected runoff where the 'wet' scenarios suggest an increase in annual runoff and the 'dry' scenarios suggest a decrease in annual runoff (Table 6). The projected changes in runoff range from an increase of approximately 486,000 acre-feet under the warm-wet scenario to a decrease of approximately 272,500 acre-feet under the warm-dry scenario by the end of the century.

Seasonality in runoff magnitude and timing is very spatially dependent, where the colder, wetter areas in the mountains typically see the most runoff during spring (Figure 68), while the warmer, drier areas see the most runoff during the season with the most precipitation, which is normally winter (Figure 69). Seasonality is projected to shift in the mountainous areas by the second half of the 21st century, where most years will see more runoff occurring in the winter and less in the spring and summer (Figure 70 and Figure 71). For example, the Feather River and Yuba River basins are primarily snow-covered during the winter and are projected to have a shift in runoff timing where runoff occurs earlier due to warmer temperatures and early snowmelt. In contrast, the areas that are not snow-covered during the winter, such as the two groundwater bulletin 118 subbasins in the central valley, will see similar seasonal runoff patterns as were observed historically. In these areas, the seasons with the highest precipitation generally generate the most runoff.

Not only is spring runoff projected to decline substantially in most mountainous areas across all scenarios and time periods, but the total area it originates from is projected to decline. By the end of the century, the 'hot' scenarios project that the majority of spring runoff will occur only in the south east mountains within the CalSim3 domain. This trend is similar for the 'warm' scenarios, where the amount of runoff diminishes in the northern part of the CalSim3 domain and the majority originates from the more southern latitudes, although there is still some runoff originating from the central latitudes.

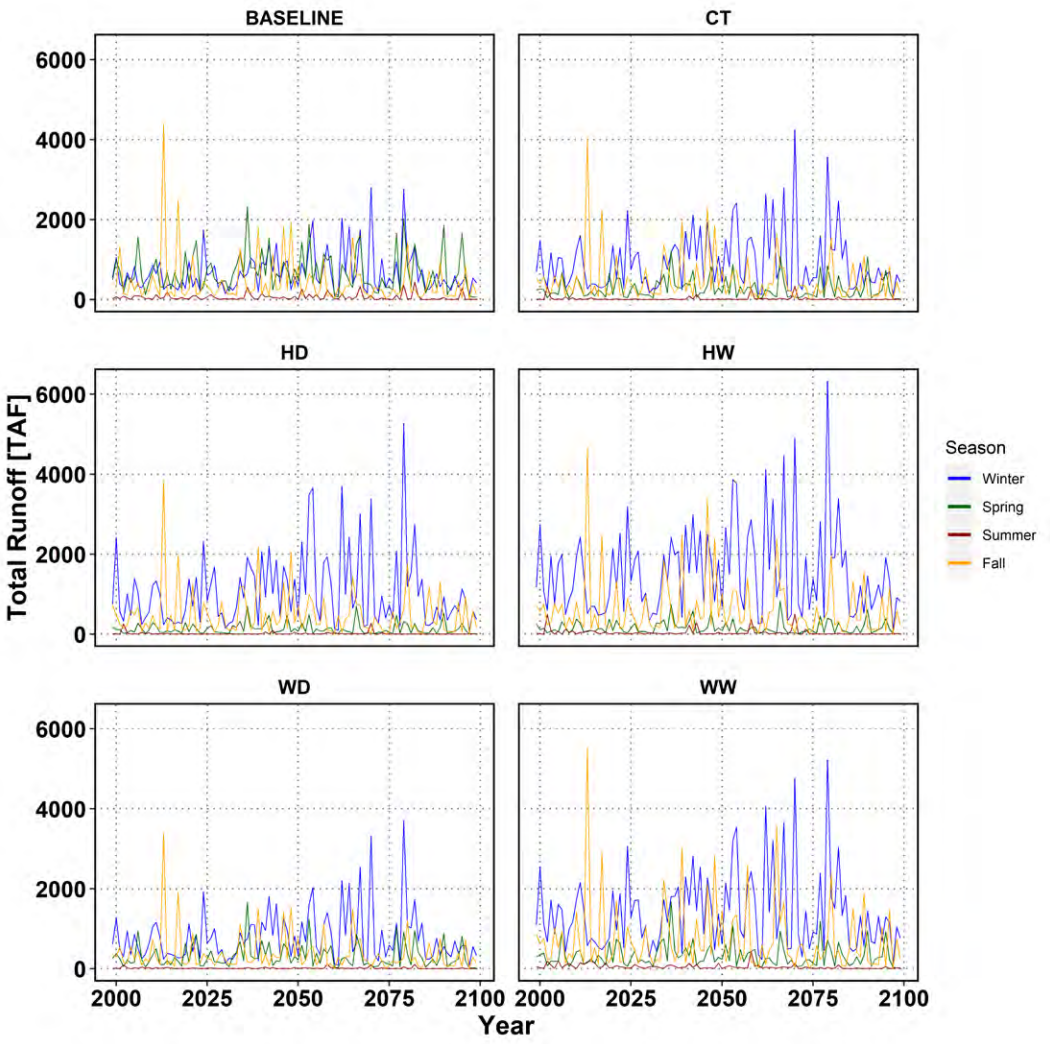

Figure 68. Projected future seasonal runoff (in thousand acre-feet) in the FTHR subarea for each scenario and the 2070 – 2099 time period. CT – central tendency, HD = Hot-Dry, HW = Hot-Wet, WW = Warm-Wet and WD = Warm-Dry. Color indicates season: blue = winter, green = spring, red = summer and orange = fall.

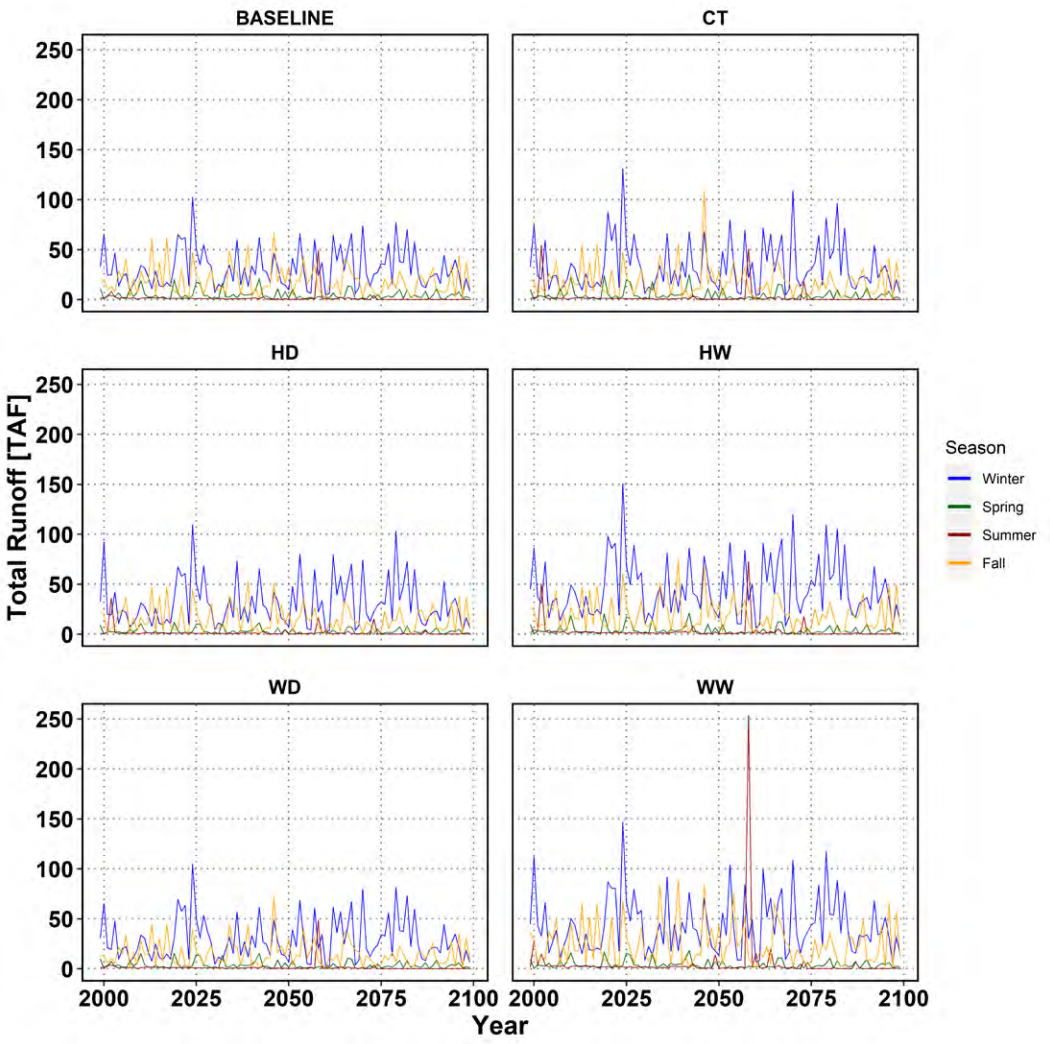

Figure 69. Projected future seasonal runoff (in thousand acre-feet) in the Bulletin 118 5.021.64 subbasin for each scenario and the 2070 – 2099 time period. CT – central tendency, HD = Hot-Dry, HW = Hot-Wet, WW = Warm-Wet and WD = Warm-Dry. Color indicates season: blue = winter, green = spring, red = summer and orange = fall.

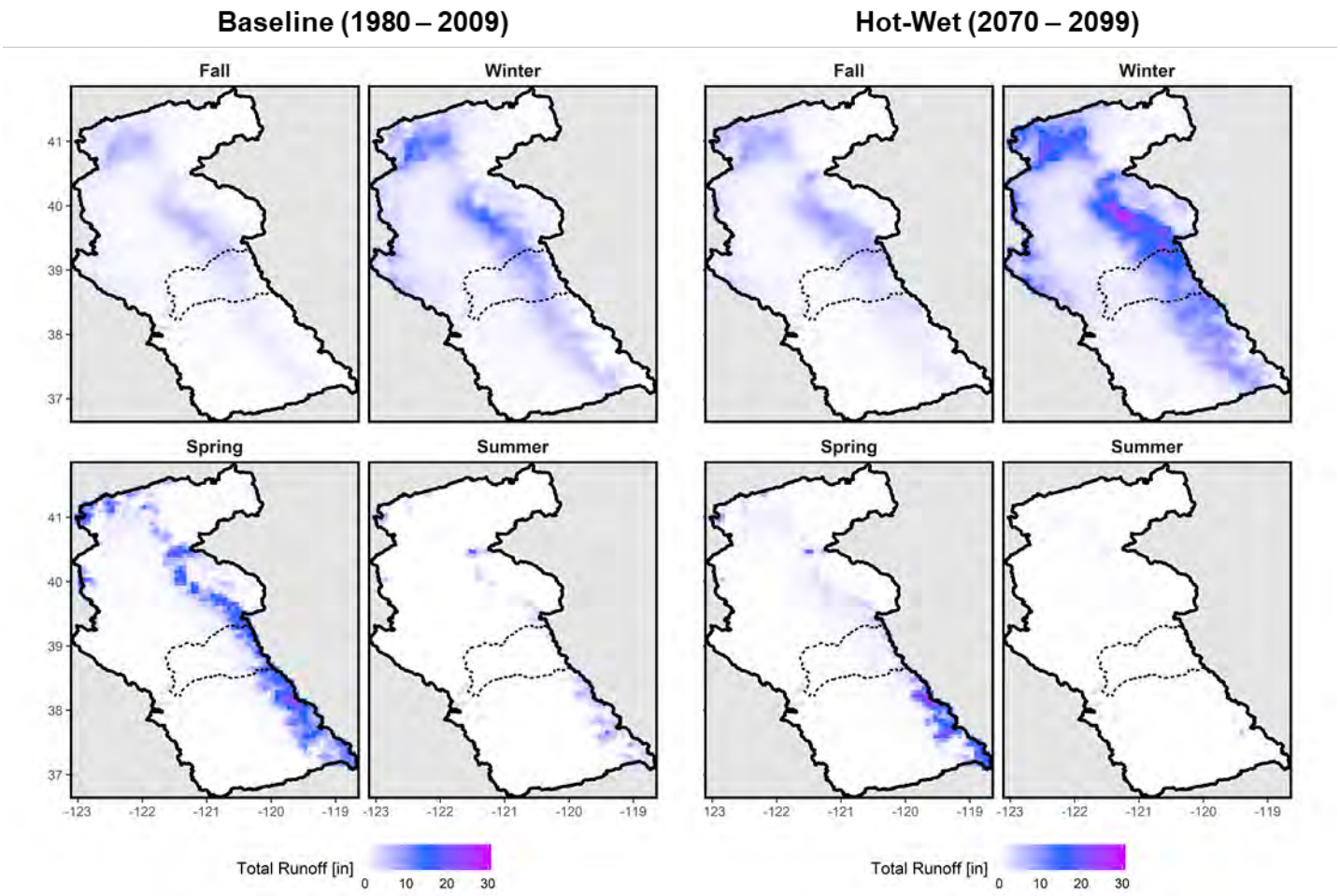

Figure 70. Spatial patterns of average seasonal runoff during baseline conditions (left) and the future hot-wet scenario (right) over the ARBS Study Area and CalSim3 domain. Axes are latitudinal and longitudinal coordinates. The color scale indicates the magnitude of runoff. The CalSim3 domain is delineated by the black solid line and the ARBS study area is delineated by the black dashed line.

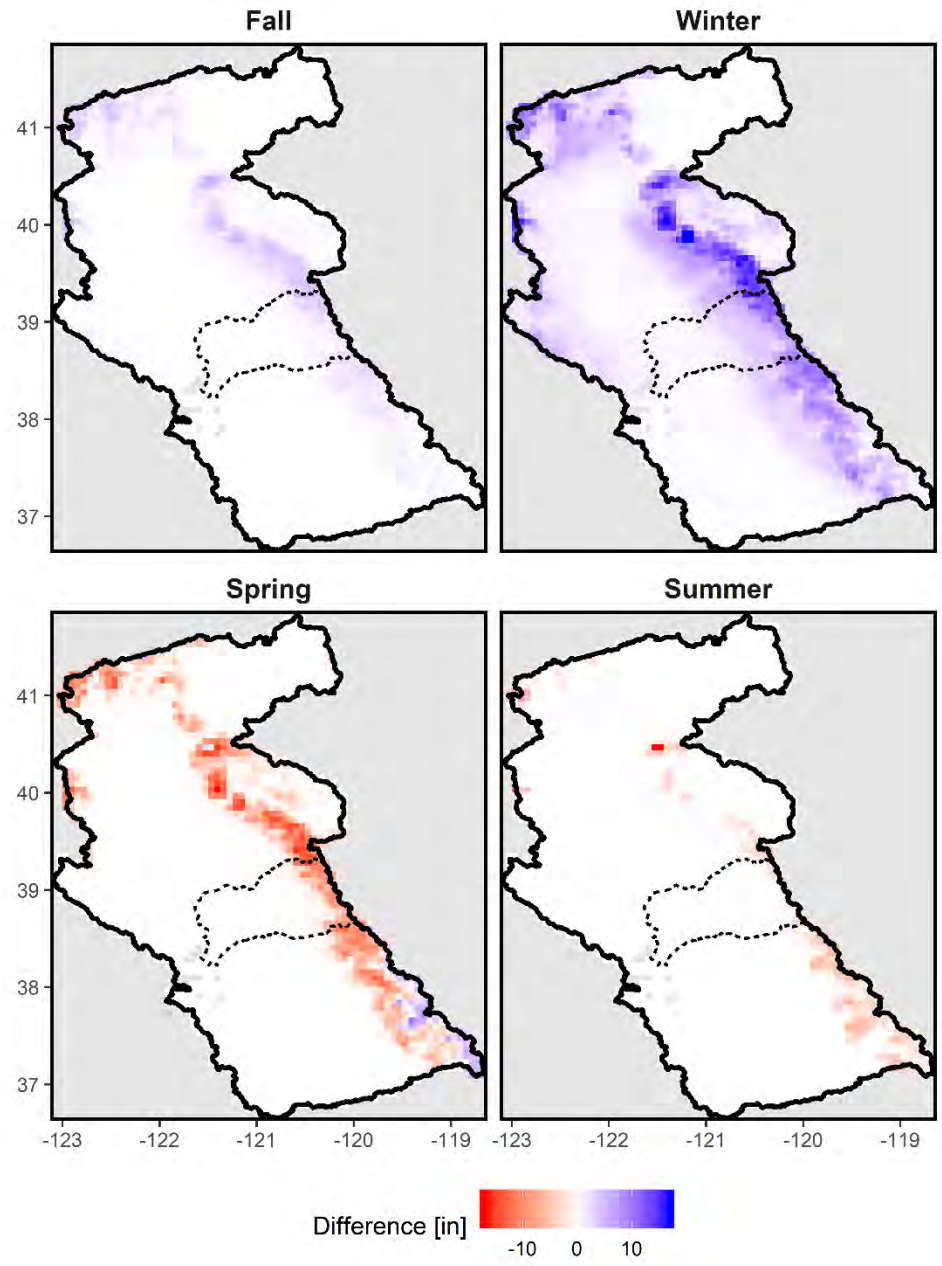

Figure 71. Spatial patterns of the difference in average seasonal runoff between the baseline period and the **Hot-Wet** scenario of 2070 – 2099 over the ARBS Study Area and CalSim3 domain. Axes are latitudinal and longitudinal coordinates. The color scale indicates the change in runoff between periods. The CalSim3 domain is delineated by the black solid line and the ARBS study area is delineated by the black dashed line.

6 References

Abdulla et al. 1996	Abdulla FA, DP Lettenmaier, EF Wood and JA Smith 1996. Application of a Macroscale Hydrologic Model to Estimate the Water Balance of the Arkansas-Red River Basin. Journal of Geophysical Research 101(D3): 7449-7459.
Bedsworth et al. 2018	Bedsworth L, D Cayan, G Franco, L Fisher, S Ziaja. (California Governor's Office of Planning and Research, Scripps Institution of Oceanography, California Energy Commission, California Public Utilities Commission) 2018. Statewide Summary Report. California's Fourth Climate Change Assessment. Publication number: SUMCCCA4-2018-013.
CPC 2015	CPC (National Oceanic and Atmospheric Administration, National Weather Service, Climate Prediction Center) 2015. Climate Glossary. URL: http://www.cpc.ncep.noaa.gov/products/outreach/glossary.shtml. Accessed September 19, 2015.
CWC 2016	CWC (California Water Commission) 2016. Water Storage Investment Program Technical Reference. URL: https://data.cnra.ca.gov/dataset/climate-change-projections-wsip-2030-2070/resource/ca0740b9-b538-4056-a8d8-2b32bdaf11a7. Accessed August 2, 2019.
DWR 2015 [CCTAG]	DWR (California Department of Water Resources) Climate Change Technical Advisory Group 2015. Perspectives and Guidance for Climate Change Analysis, in: Lynn E, A Schwarz, J Anderson, M Correa (Eds.), 140 pp. URL: https://water.ca.gov/-/media/DWR-Website/Web-Pages/Programs/All-Programs/Climate-Change-Program/Climate-Program-Activities/Files/Reports/Perspectives-Guidance-Climate-Change-Analysis.pdf. Accessed July 13, 2020.
DWR 2019 [Climate Change Basics]	DWR (California Department of Water Resources) 2019. Climate Change Basics. URL: https://water.ca.gov/Water-Basics/Climate-Change-Basics. Accessed August 2, 2019.
DWR 2019 [CalSim3]	DWR (California Department of Water Resources) 2019. CalSim3. URL: https://water.ca.gov/Library/Modeling-and-

	Analysis/Central-Valley-models-and-tools/CalSim-3. Accessed August 2, 2019.
Hamlet and Lettenmaier 1999	Hamlet AF and DP Lettenmaier 1999. Columbia River Streamflow Forecasting Based on ENSO and PDO Climate Signals. American Water Resources Association 35(6): 333-341.
Hamlet and Lettenmaier 2000	Hamlet AF and DP Lettenmaier 2000. Long-Range Climate Forecasting and its Use for Water Management in the Pacific Northwest Region of North America. Journal of Hydroinformatics 02(3): 163-182.
Hamlet et al. 2013	Hamlet AF, M McGuire Elsner, GS Mauger, SY Lee, I Tohver, and RA Norheim 2013. An Overview of the Columbia Basin Climate Change Scenarios Project: Approach, Methods, and Summary of Key Results. Atmosphere-Ocean 41(5): 392-415.
IPCC 2013 [Physical Basis]	IPCC (Intergovernmental Panel on Climate Change) 2013. Climate Change 2013: The Physical Science Basis. Contribution of Working Group I to the Fifth Assessment Report of the Intergovernmental Panel on Climate Change. (TF Stocker, D Qin, G-K Plattner, M Tignor, SK Allen, J Boschung, A Nauels, Y Xia, V Bex, and PM Midgley [Editors]). Cambridge University Press; Cambridge, United Kingdom and New York, New York, United States; 1535 pp.
IPCC 2014 [AR5 Synthesis]	IPCC (International Panel on Climate Change) 2014. Climate Change 2014: Synthesis Report. Contribution of Working Groups I, II and III to the Fifth Assessment Report of the Intergovernmental Panel on Climate Change. (Core Writing Team, RK Pachauri, and LA Meyer [Editors]). IPCC, Geneva, Switzerland, 151 pages.
IPCC 2014 [AF5 Impacts]	IPCC (International Panel on Climate Change) 2014. Climate Change 2014: Impacts, Adaptation, and Vulnerability. Contribution of Working Group II to the Fifth Assessment Report of the Intergovernmental Panel on Climate Change. (CB Field, VR Barros, DJ Dokken, KJ Mach, MD Mastrandrea, TE Bilir, M Chatterjee, KL Ebi, YO Estrada, RC Genova, B Girma, ES Kissel, AN Levy, S MacCracken, PR Mastrandrea, and LL White [Editors]). Cambridge University Press; Cambridge, United Kingdom and New York, New York, United States; 1132 pages.

Liang et al. 1994	Liang X, DP Lettenmaier, EF Wood, and SJ Burges 1994. A Simple Hydrologically Based Model of Land Surface Water and Energy Fluxes for General irculation Models. Journal of Geophysical Research 99(D7): 14415-14428.
Lohmann et al. 1998	Lohmann D, E Raschke, B Nijssen and DP Lettenmaier 1998. Regional Scale Hydrology: I. Formulation of the VIC-2L Model Coupled to a Routing Model, Hydrologic Sciences Journal 43(1): 131-141.
Lindsey 2009	Lindsey R, 2009. NASA Earth Observatory – Climate and Earth's Energy Balance. URL: https://earthobservatory.nasa.gov/features/EnergyBalance/page1.php. Accessed September 19, 2015.
Livneh et al. 2013	Livneh B, EA Rosenberg, C Lin, B Nijssen, V Mishra, K Andreadis, EP Maurer, and DP Lettenmaier 2014. A Long-Term Hydrologically Based Dataset of Land Surface Fluxes and States for the Conterminous United States: Update and Extensions [corrigendum]. Journal of Climate 27(1): 477-486.
Livneh et al. 2015	Livneh B, TJ Bohn, DS Pierce, F Munoz-Ariola, B Nijssen, R Vose, D Cayan, and LD Brekke 2015. A Spatially Compre-hensive, Hydrometeorological Dataset for Mexico, the U.S., and Southern Canada 1950-2013. Nature Scientific Data 5:150042. doi:10.1038/sdata.2015.42.
Livneh 2016	Livneh B. 2016. Personal communication.
LLNL 2019	LLNL (Lawrence Livermore National Laboratory) 2019. Green Data Oasis. URL: https://hpc.llnl.gov/services/green-data-oasis. Accessed August 11, 2019.
Maurer et al. 2001	Maurer EP, GM O'Donnell, DP Lettenmaier, and JO Roads 2001. Evaluation of the Land Surface Water Budget in NCEP/NCAR and NCEP/DOE Reanalyses Using an Off-line Hydrologic Model. Journal of Geophysical Research 106(D16): 17841-17862.
Menne 2012	Menne MJ, I Durre, B Korzeniewski, S McNeal, K Thomas, X Yin, S Anthony, R Ray, RS Vose, BE Gleason, and TG Houston 2012. Global Historical Climatology Network – Daily (GHCN Daily), Version

	3.22. NOAA National Climatic Data Center. http://doi.org.10.7289/V5D21VHZ.
NCEI 2019	NCEI (National Oceanic and Atmospheric Administration, National Centers for Environmental Information) 2019. Global Historical Climate Network Daily – Description. URL: https://www.ncdc.noaa.gov/ghcn-daily-description. Accessed January 8, 2019.
Nijssen et al. 1998	Nijssen B, DP Lettenmaier, X Liang, SW Wetzel, and EF Wood 1997. Streamflow Simulation for Continental-Scale River Basins. Water Resources Research 33(4): 711-724.
NWS 2009	NWS (National Oceanic and Atmospheric Administration, National Weather Service) 2009. National Weather Service Glossary. URL: https://w1.weather.gov/glossary/. Accessed August 2, 2019.
NWS 2015	NWS (National Oceanic and Atmospheric Administration, National Weather Service) 2015. Glossary. URL: http://w2.weather.gov/climate/help/glossary.php. Accessed September 15, 2015.
Pierce et al. 2018	Pierce DW, JF Kalansky, and DR Cayan, (Scripps Institution of Oceanography) 2018. Climate, Drought, and Sea Level Rise Scenarios for California's Fourth Climate Change Assessment. California's Fourth Climate Change Assessment, California Energy Commission. Publication Number: CNRA-CEC-2018-006.
Reclamation 2016 [Climate Projections]	Reclamation (Bureau of Reclamation) 2015. Considerations for Selecting Climate Projections for Water Resources, Planning, and Environmental Analyses. Denver, Colorado. February 2016.
Reclamation et al. 2016 [Klamath]	Reclamation (Bureau of Reclamation), California Department of Water Resources, and Oregon Water Resources Department 2016. Klamath River Basin Study Summary Report. December 2016.
Reclamation et al. 2016 [Niabrara]	Reclamation (Bureau of Reclamation) and Nebraska Department of Natural Resources 2016. Niobrara River Basin Study Summary Report. July 2016.

Reclamation 2016 [Republican]	Reclamation (Bureau of Reclamation), Colorado Division of Water Resources, Nebraska Department of Natural Resources, Kansas Water Office, Kansas Department of Agriculture Division of Water Resources 2016. Republican River Basin Study Final Report. March 2016.
Reclamation et al. 2018	Reclamation (Bureau of Reclamation), Climate Analytics Group, Climate Central, Lawrence Livermore National Laboratory, Santa Clara University, Scripps Institution of Oceanography, US Army Corps of Engineers, US Geological Survey, National Center for Atmospheric Research, and Cooperative Institute for Research in Environmental Sciences 2018. Downscaled CMIP3 and CMIP5 Climate and Hydrology Projections. URL: https://gdo-dcp.ucllnl.org/downscaled_cmip_projections/dcpInterface.html. Accessed June 15, 2018.
Shepard 1984	Shepard DS 1984. Computer Mapping: The SYMAP Interpolation Algorithm. Spatial Statistics and Models [Gaile GL and CJ Wilmott [Editors]). D. Reidel, 133-145 (1984).
USGCRP 2018	USGCRP (US Global Change Research Program) 2018. Impacts, Risks, and Adaptation in the United States: Fourth National Climate Assessment, Volume II (Reidmiller, DR, CW Avery, DR Easterling, KE Kunkel, KLM Lewis, TK Maycock, and C Stewart [Editors]). U.S. Global Change Research Program, Washington, DC, USA, 1515 pp. doi: 10.7930/NCA4.2018.
USGS et al. 2013	USGS (United States Geological Survey) and USDA NRCS (United States Department of Agriculture, Natural Resources Conservation Service) 2013. Federal Standards and Procedures for the National Watershed Boundary Dataset (WDB) (4 ed.): USGS Techniques and Methods 11-A3, 63p. https://pubs.er.usgs.gov/publication/tm11A34
Vano et al. 2012	Vano JA, T Das, and DP Lettenmaier 2012. Hydrologic Sensitivities of Colorado River Runoff to Changes in Precipitation and Temperature. Journal of Hydrometeorology 13(3): 932-949.
Wood et al. 2002	Wood AW, EP Maurer, A Kumar, DP and Lettenmaier 2002. Long Range Experimental Hydrologic Forecasting for the Easter US. Journal of Geophysical Research

	107, 4429, doi:10.1029/2001JD000659.
Wood et al. 2005	Wood AW, A Kumar, and DP Lettenmaier 2005. A Retrospective Assessment of Climate Model-Based Ensemble Hydrologic Forecasting in the Western US. Journal of Geophysical Research 110, D04105, doi:10.1029/2004JD004508.
Wood and Lettenmaier 2006	Wood AW and DP Lettenmaier 2006. A Test Bed for New Seasonal Hydrologic Forecasting Approaches in the Western United States. Bulletin of the American Meteorological Society 87(12): 1699-1712.

7 Appendix

	Variable change per century			
HUC AREA	Precip (in)	Tmax (°F)	Tmin (°F)	Tavg (°F)
HUC08_16050101	-12.9	-0.3	0.6	0.1
HUC08_16050102	**-16.3**	**1.5**	**1.8**	**1.5**
HUC08_16050201	-11.9	1.3	-0.2	0.4
HUC08_16050301	**-31.2**	**3.7**	-0.8	**1.3**
HUC08_16050302	-5.0	**1.9**	0.8	1.1
HUC08_18010103	7.7	-0.6	**0.8**	0.0
HUC08_18010104	**15.9**	-0.2	-0.3	-0.4
HUC08_18010110	**11.1**	0.0	**2.2**	**1.0**
HUC08_18010204	3.1	0.6	**2.9**	**1.7**
HUC08_18010205	**26.5**	0.9	**4.4**	**2.6**
HUC08_18010207	**36.0**	-0.8	**4.3**	**1.6**
HUC08_18010208	-13.2	0.4	**3.3**	**1.9**
HUC08_18010210	-12.9	**1.9**	**3.2**	**2.5**
HUC08_18010211	3.5	-0.4	**3.0**	**1.5**
HUC08_18010212	**13.7**	0.7	**3.8**	**2.1**
HUC08_18020001	2.0	0.1	-1.1	-0.5
HUC08_18020002	2.1	0.2	0.5	0.1
HUC08_18020003	**18.2**	-0.4	0.5	0.0
HUC08_18020004	**42.2**	-0.4	**3.5**	**1.5**
HUC08_18020005	**37.9**	-0.9	**4.7**	**2.0**
HUC08_18020104	2.5	0.3	**1.8**	**0.9**
HUC08_18020111	2.8	**1.1**	**5.3**	**3.2**
HUC08_18020115	4.3	-0.2	0.4	0.1
HUC08_18020116	5.3	-0.1	**1.5**	0.7
HUC08_18020121	**23.3**	0.0	**1.0**	0.3
HUC08_18020122	-6.0	-1.0	**3.5**	**1.1**
HUC08_18020123	-0.1	-0.3	**4.1**	**1.9**
HUC08_18020125	10.3	-0.2	**2.5**	**1.2**
HUC08_18020126	4.1	**-1.2**	**3.4**	**1.0**
HUC08_18020128	2.2	0.7	**5.4**	**3.0**
HUC08_18020129	6.2	**1.5**	**6.8**	**4.2**
HUC08_18020151	**25.2**	-0.2	0.8	0.5

Table A.1.1. Trends in observed historical precipitation and temperature over the period 1915 – 2015 for the HUC areas within the CalSim3 domain.

	Variable change per century			
HUC AREA	Precip (in)	Tmax (°F)	Tmin (°F)	Tavg (°F)
HUC08_18020152	**13.2**	0.6	**2.8**	**1.8**
HUC08_18020153	**17.8**	0.3	-1.1	-0.2
HUC08_18020154	**20.9**	0.3	**2.3**	**1.5**
HUC08_18020155	**5.7**	0.1	0.6	0.3
HUC08_18020156	**10.8**	0.2	0.2	0.1
HUC08_18020157	**19.2**	0.5	**1.8**	**0.9**
HUC08_18020158	**15.1**	0.5	**3.2**	**1.8**
HUC08_18020159	4.3	0.8	**1.3**	**1.1**
HUC08_18020161	-0.2	0.6	**5.0**	**2.8**
HUC08_18020162	**7.5**	**1.1**	**4.8**	**2.9**
HUC08_18020163	1.7	1.1	**4.2**	**2.6**
HUC08_18030009	0.1	**-2.0**	**1.8**	-0.3
HUC08_18030010	**12.8**	-0.4	-0.8	-0.6
HUC08_18040001	-2.5	0.3	**4.3**	**2.1**
HUC08_18040002	**-3.2**	**1.6**	**6.5**	**4.1**
HUC08_18040003	-1.8	**2.4**	**3.5**	**2.9**
HUC08_18040006	5.0	-0.1	-0.3	0.0
HUC08_18040007	0.2	-0.6	**2.9**	**1.0**
HUC08_18040008	1.5	-0.4	**5.4**	**2.5**
HUC08_18040009	1.1	0.6	**3.4**	**2.0**
HUC08_18040010	6.4	-0.6	**2.3**	**0.8**
HUC08_18040011	2.8	0.0	**3.6**	**1.7**
HUC08_18040012	5.6	0.4	**3.9**	**2.2**
HUC08_18040013	**6.8**	**1.7**	**6.9**	**4.3**
HUC08_18040014	-2.0	**-2.0**	**-1.9**	**-2.1**
HUC08_18040051	-2.9	**1.8**	**3.6**	**2.6**
HUC08_18050001	-1.2	**1.1**	**4.9**	**2.9**
HUC08_18050002	**8.5**	**2.4**	**6.6**	**4.5**
HUC08_18050003	3.1	**4.9**	**14.0**	**9.5**
HUC08_18050004	2.0	**3.6**	**7.7**	**5.7**
HUC08_18060002	**-6.3**	**2.8**	**5.7**	**4.0**
HUC08_18080001	4.4	-0.3	0.0	-0.2
HUC08_18080002	-1.4	0.3	0.2	-0.1
HUC08_18080003	-2.7	-0.8	**1.4**	0.2
HUC08_18090101	**-22.2**	**3.0**	0.0	1.3
HUC08_18090102	-6.5	0.6	**-2.0**	-0.6
HUC08_18020163x	2.6	**2.1**	**2.9**	**2.6**
HUC08_18040012x	1.0	**1.8**	**3.2**	**2.4**

Table A.1.2. Trends in observed historical precipitation and temperature over the period 1915 – 2015 for the HUC areas within the CalSim3 domain.

	Variable change per century			
Basin	Precip (in)	Tmax (°F)	Tmin (°F)	Tavg (°F)
WBA02	**14.8**	0.5	**2.0**	**1.5**
WBA03	**15.5**	0.3	**1.4**	**1.0**
WBA04	3.5	-0.1	**1.9**	**0.9**
WBA05	**9.6**	0.1	**3.0**	**1.5**
WBA06	**4.4**	-0.5	**1.0**	0.2
WBA07N	3.5	0.3	**0.8**	0.5
WBA07S	3.0	-0.3	**2.2**	**1.0**
WBA08N	2.7	0.6	**1.4**	**0.9**
WBA08S	1.1	0.4	**2.0**	**1.2**
WBA09	2.6	0.8	**2.2**	**1.4**
WBA10	**13.2**	0.4	**5.0**	**2.7**
WBA11	**6.3**	0.4	**2.4**	**1.3**
WBA12	**6.9**	-0.1	0.3	0.1
WBA13	**8.7**	-0.1	-0.2	-0.2
WBA14	3.0	-0.4	**-1.2**	-0.9
WBA15N	3.9	**1.3**	**1.6**	**1.6**
WBA15S	1.2	**1.7**	**3.2**	**2.4**
WBA16	-0.1	**1.8**	**3.4**	**2.6**
WBA17N	0.7	**1.1**	**1.5**	**1.2**

Table A.2.1. Trends in observed historical precipitation and temperature over the period 1915 – 2015 for the WBA areas within the CalSim3 domain.

	Variable change per century			
Basin	Precip (in)	Tmax (°F)	Tmin (°F)	Tavg (°F)
WBA17S	0.6	**1.1**	**2.3**	**1.7**
WBA18	0.7	**1.0**	**1.9**	**1.4**
WBA19	0.5	0.7	**3.4**	**2.0**
WBA20	4.0	0.4	**4.6**	**2.5**
WBA21	2.5	0.6	**4.0**	**2.2**
WBA22	0.9	1.0	**3.7**	**2.3**
WBA23	-2.5	1.0	**4.9**	**2.9**
WBA24	0.0	0.5	**6.2**	**3.2**
WBA25	1.4	**1.1**	**5.1**	**3.1**
WBA26N	2.9	**1.2**	**4.6**	**2.9**
WBA26S	2.7	**1.9**	**3.3**	**2.7**
WBA50	**-3.2**	**2.3**	**3.5**	**2.8**
WBA60N	0.4	**1.7**	**3.2**	**2.4**
WBA60S	**-3.7**	**2.3**	**2.3**	**2.3**
WBA61	**-3.9**	**1.5**	**4.2**	**2.8**
WBA62	**-4.3**	**1.0**	**5.3**	**3.2**
WBA63	-2.2	**1.0**	**3.9**	**2.3**
WBA64	-1.2	**-0.9**	**3.3**	**1.0**
WBA71	**-4.5**	**1.5**	**4.2**	**2.8**
WBA72	**-5.1**	0.4	**5.6**	**2.9**
WBA73	**-3.9**	**-1.4**	**4.0**	**1.1**

Table A.2.2. Trends in observed historical precipitation and temperature over the period 1915 – 2015 for the WBA areas within the CalSim3 domain.

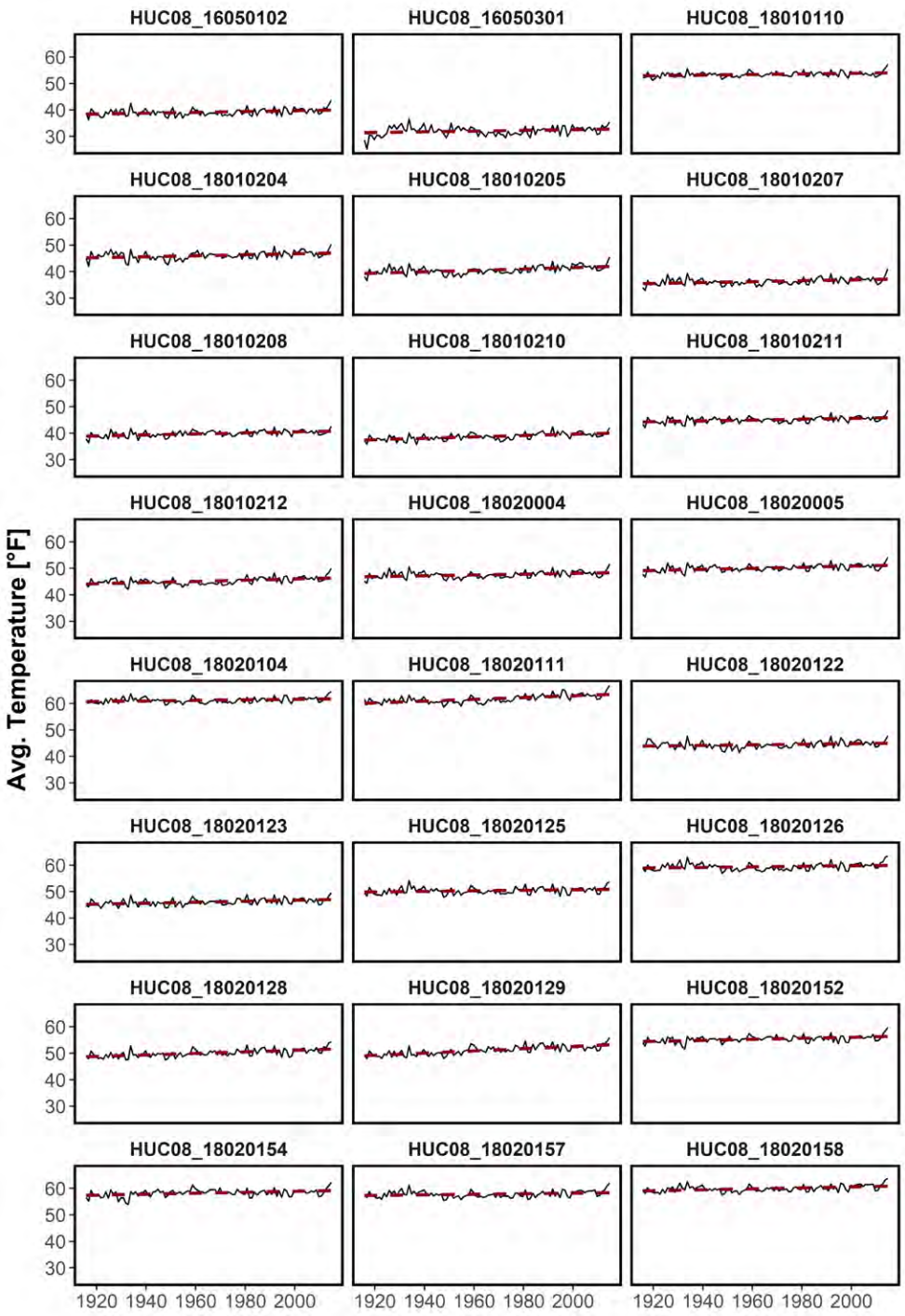

Figure A1.1 Timeseries of annual average temperature in the HUC areas with significant historical trends. The solid black line indicates Livneh water year averages while the dashed red line depicts the significant trendline.

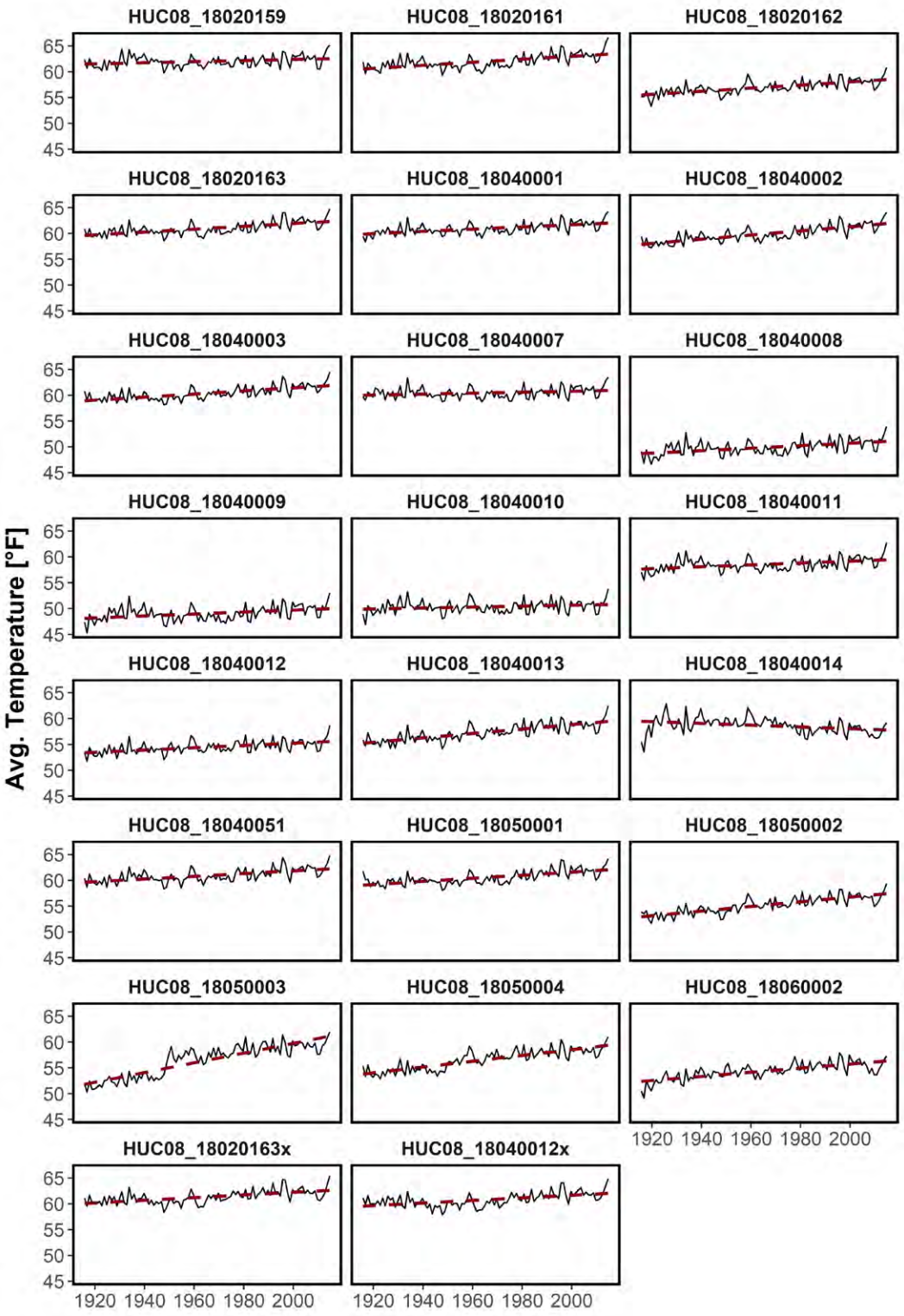

Figure A1.2 Timeseries of annual average temperature in the HUC areas with significant historical trends. The solid black line indicates Livneh water year averages while the dashed red line depicts the significant trendline.

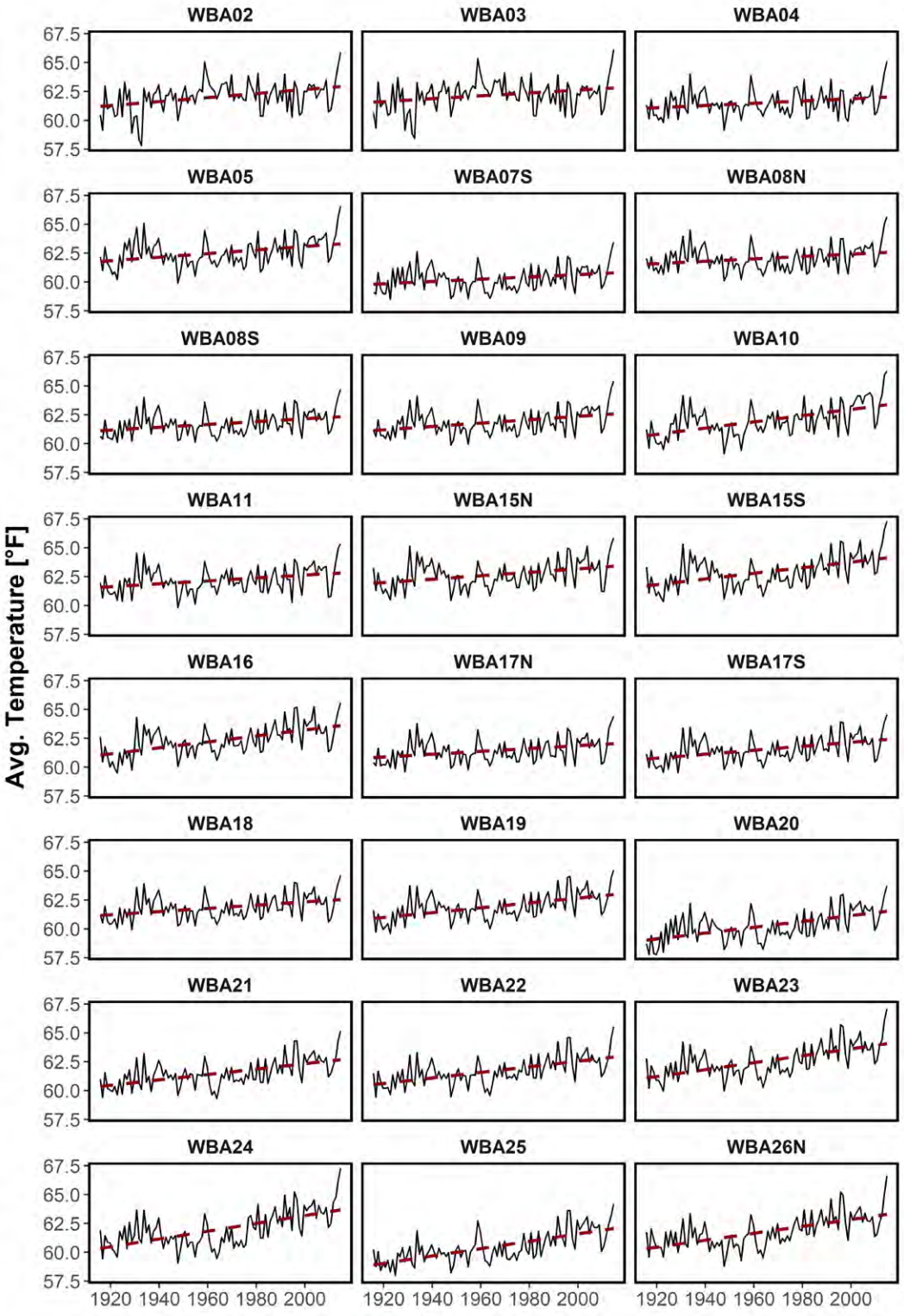

Figure A.2.1. Timeseries of annual average temperature in the WBA areas with significant historical trends. The solid black line indicates Livneh water year averages while the dashed red line depicts the significant trendline.

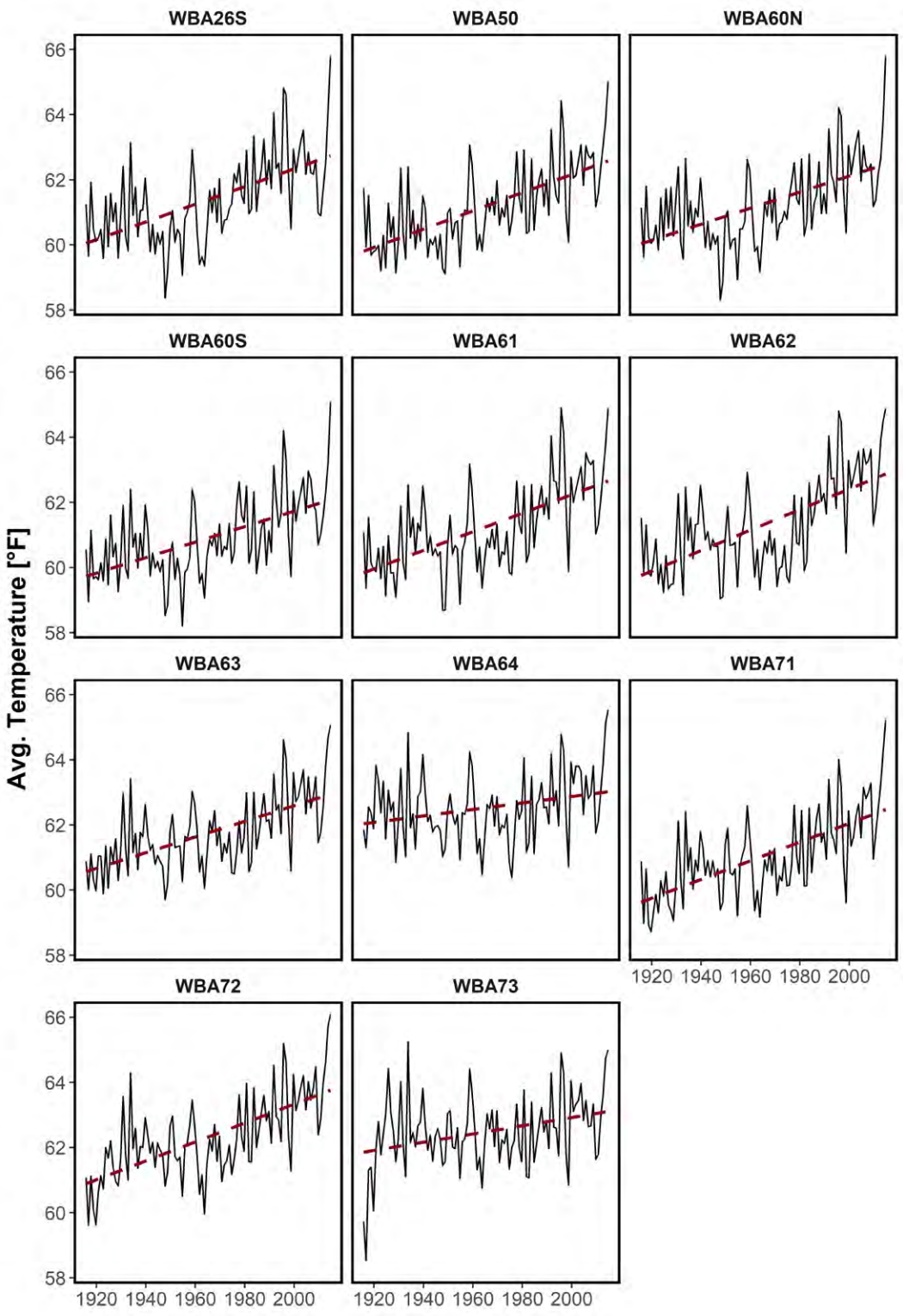

Figure A.2.2. Timeseries of annual average temperature in the WBA areas with significant historical trends. The solid black line indicates Livneh water year averages while the dashed red line depicts the significant trendline.

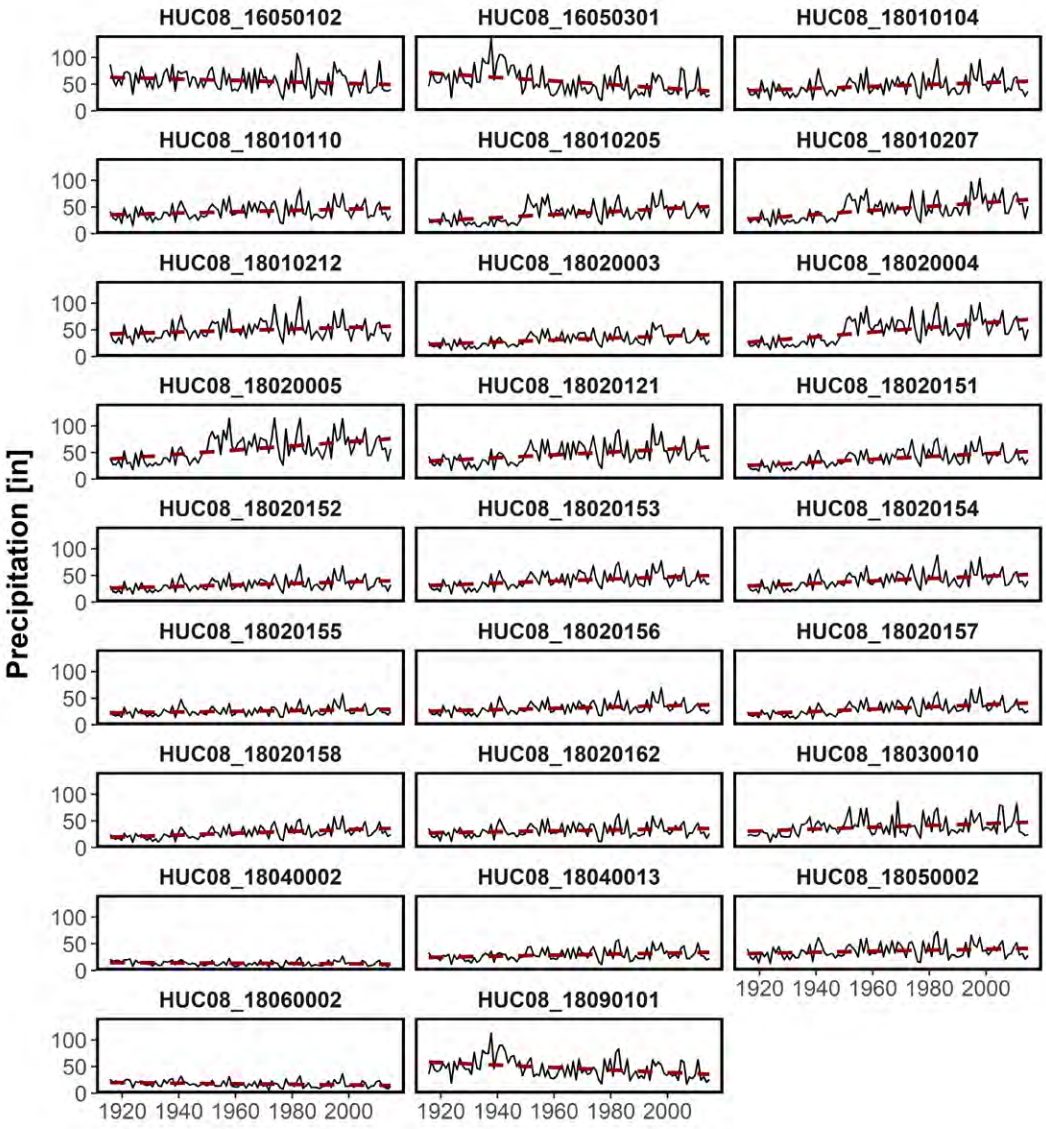

Figure A.3. Timeseries of annual precipitation in the HUC areas with significant historical trends. The solid black line indicates Livneh water year averages while the dashed red line depicts the significant trendline.

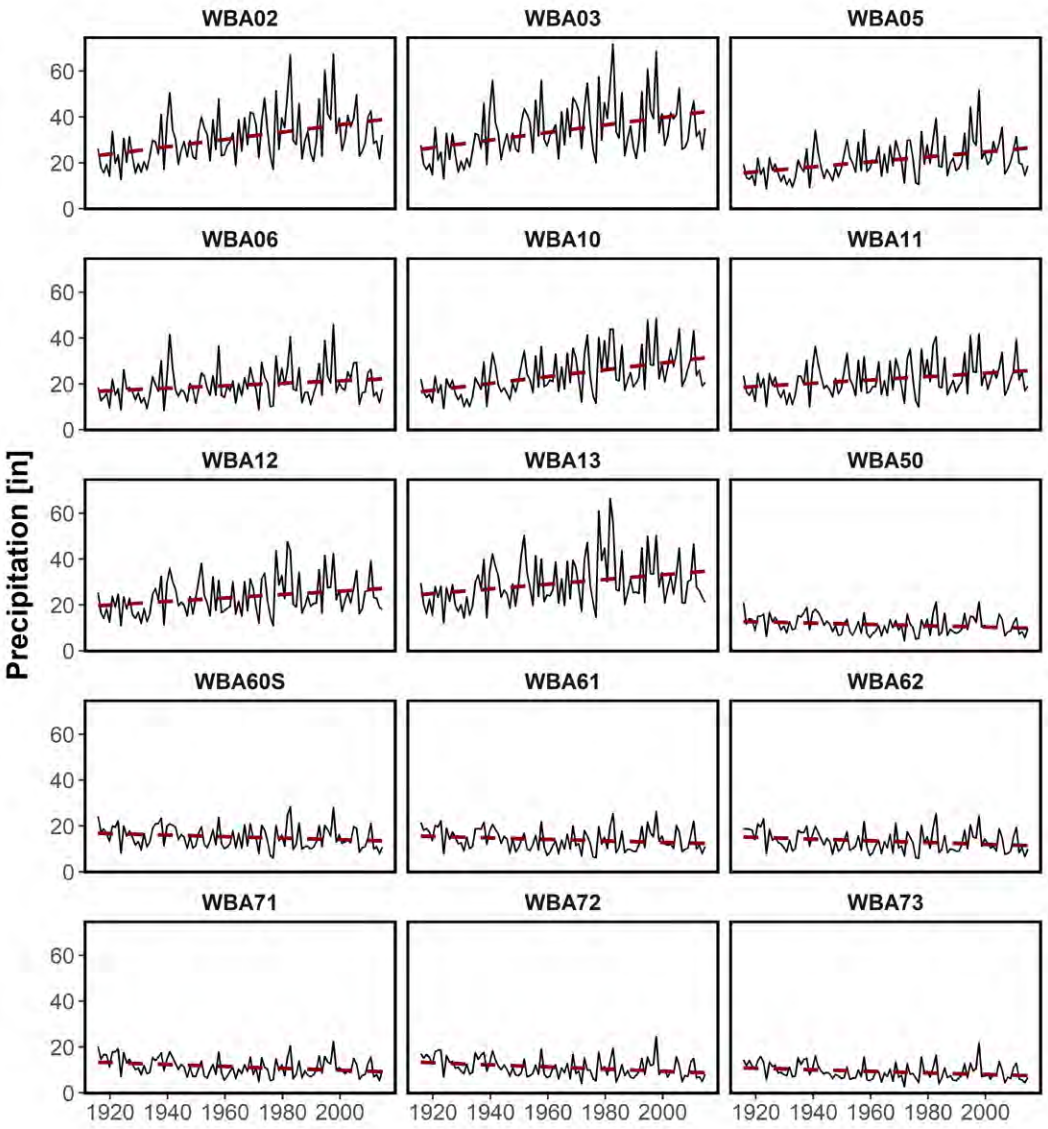

Figure A.4. Timeseries of annual precipitation in WBA areas with significant historical trends. The solid black line indicates Livneh water year averages while the dashed red line depicts the significant trendline.

LOCA Climate Projections							
access1-0.1.rcp45	access1-0.1.rcp85	access1-3.1.rcp45	access1-3.1.rcp85	bcc-csm1-1.1.rcp45	bcc-csm1-1.1.rcp85	bcc-csm1-1-m.1.rcp45	bcc-csm1-1-m.1.rcp85
canesm2.1.rcp45	canesm2.1.rcp85	ccsm4.6.rcp45	ccsm4.6.rcp85	cesm1-bgc.1.rcp45	cesm1-bgc.1.rcp85	cesm1-cam5.1.rcp45	cesm1-cam5.1.rcp85
cmcc-cm.1.rcp45	cmcc-cm.1.rcp85	cmcc-cms.1.rcp45	cmcc-cms.1.rcp85	cnrm-cm5.1.rcp45	cnrm-cm5.1.rcp85	csiro-mk3-6-0.1.rcp45	csiro-mk3-6-0.1.rcp85
ec-earth.2.rcp85	ec-earth.8.rcp45	fgoals-g2.1.rcp45	fgoals-g2.1.rcp85	gfdl-cm3.1.rcp45	gfdl-cm3.1.rcp85	gfdl-esm2g.1.rcp45	gfdl-esm2g.1.rcp85
gfdl-esm2m.1.rcp45	gfdl-esm2m.1.rcp85	giss-e2-h.2.rcp85	giss-e2-h.6.rcp45	giss-e2-r.2.rcp85	giss-e2-r.6.rcp45	hadgem2-ao.1.rcp45	hadgem2-ao.1.rcp85
hadgem2-cc.1.rcp45	hadgem2-cc.1.rcp85	hadgem2-es.1.rcp45	hadgem2-es.1.rcp85	inmcm4.1.rcp45	inmcm4.1.rcp85	ipsl-cm5a-lr.1.rcp45	ipsl-cm5a-lr.1.rcp85
ipsl-cm5a-mr.1.rcp45	ipsl-cm5a-mr.1.rcp85	miroc5.1.rcp45	miroc5.1.rcp85	miroc-esm.1.rcp45	miroc-esm.1.rcp85	miroc-esm-chem.1.rcp45	miroc-esm-chem.1.rcp85
mpi-esm-lr.1.rcp45	mpi-esm-lr.1.rcp85	mpi-esm-mr.1.rcp45	mpi-esm-mr.1.rcp85	mri-cgcm3.1.rcp45	mri-cgcm3.1.rcp85	noresm1-m.1.rcp45	noresm1-m.1.rcp85

Table A.3. The name of each of the 64 LOCA projections with their location in the table corresponding to the respective panel in Figures 26 and 28. Green shading indicates projections under RCP 4.5; red shading indicates projections under RCP 8.5.